Durham E-Theses

A Solid-state NMR Study of Formoterol Fumarate

Markwell, Andrew Fraser

A Solid-State NMR Study of Formoterol Fumarate

By

Andrew Fraser Markwell

Durham University

A Thesis submitted in partial fulfilment of the requirements for the

degree of Master of Science

Department of Chemistry

Durham University

2009

Abstract

Spectra have been obtained for each of the three formoterol fumarate solvates diethanol , diisopropanol and dibenzyl alcohol and, with the aid of solution-state data and dipolar dephasing experiments, carbon-13 spectral assignments have been made. It was shown that diethanol and diisopropanol solvates are relatively stable to magic-angle spinning but do gradually convert to anhydrate C.

The coalescence temperature of the methoxybenzene carbon atoms for diethanol, diisopropanol solvates and anhydrate C were found and an exchange rate for this ring-flip calculated.

The formoterol fumarate dihydrate, anhydrate A, anhydrate B and anhydrate C have been prepared and spectra obtained, again with the aid of solution-state data and dipolar dephasing experiments carbon-13 spectral assignments have been made where possible.

^{13}C and ^{2}H T_1 measurements suggest that the fumarate ion is mobile in the anhydrate C structure. A ^{2}H DPMAS spectrum, however does not indicate isotropic motion for the ion.

Water measurements of anhydrate A and anhydrate C indicate them to contain water. It is believed that this water is hydrogen bonded to the NH_2^+ ion and is difficult to remove by heating.

A route for preparing the solvates by bypassing the need to dry the dihydrate has been found. An ethyl acetate solvate of formoterol fumarate was produced by slurrying anhydrate C with ethyl acetate

Memorandum

The research presented in this thesis has been carried out in the Department of Chemistry, Durham University between October 2006 and October 2008. Unless otherwise stated, it is the original work of the author. None of this work has been submitted for any other degree.

Acknowledgements

Table of Contents

Chapter 1   INTRODUCTION

1.1   *Thesis overview*

The overall aim of the work described in this thesis was to understand more fully how solvent and drug molecules interact in solvates[1-3], specifically solvates of formoterol fumarate. These were characterised using solid-state Nuclear Magnetic Resonance (NMR), Thermal Gravimetric Analysis (TGA) and by moisture content.

An anhydrous crystalline solid can exhibit polymorphism[4], that is, the molecules can pack together in more than one way. Additionally, water and solvent can be involved in the structure to give hydrates and solvates.

The different states in which a molecular solid can exist are summarised in Figure 1.1

```
                         Organic Molecular Solid

        ┌──────────────────────────────────┐
    Amorphous                          Crystalline
                    ┌───────────────────┴──────────────────┐
                Polymorphs                        Solvates/ Hydrates *
            ┌───────┴───────┐                   ┌───────────┴───────────┐
        Monotropic     Enantiotropic        Reversible          Non Reversible
```
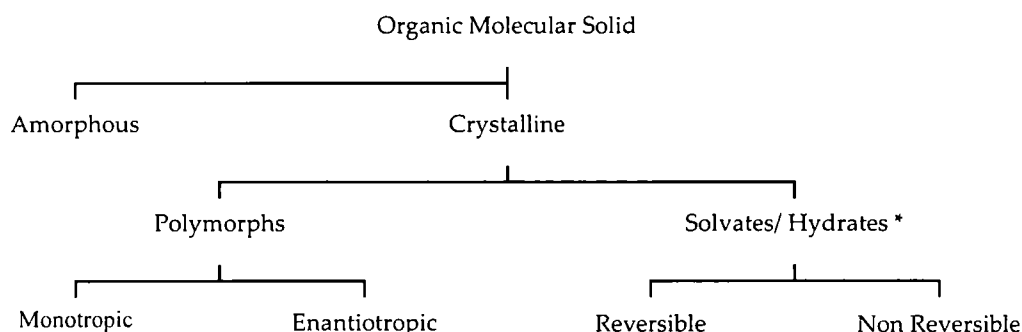
Figure 1.1 The states of a molecular solid

A solvate/hydrate which can be repeatedly desolvated and resolvated is reversible. Solvates are widely used in the pharmaceutical industry when the anhydrous forms of the active pharmaceutical ingredients (API) are unsuitable (e.g. due to a change in form with time, it may be poorly soluble and have poor processing characteristics). Solvates are often important from a processing point of view as many large-scale manufacturing processes actually involve solvates as intermediates. The reason for

---

* can also exhibit polymorphism

this is that they work very well for purification. In the final step in the production process the solvate is then desolvated or transformed to a stable hydrate. The physical properties of solvates vary widely. Some are very stable, others tend to lose solvent and stay crystalline and some lose solvent and become amorphous. Being better able to understand the behaviour of the solvates will greatly help the pharmaceutical industry, as they try to predict the suitability of different solid forms.

1.2 Polymorphs and solvates

During the investigation of formoterol fumarate three anhydrates (polymorphs) were prepared and characterised. The pharmaceutical industry recognises the importance of polymorphism and solvate formation in the crystallisation of drug compounds. Two polymorphs of the same drug compound may have different physical properties, including solubility. The different solubility of two polymorphs may affect the bioactivity of a drug which has implications for administration of the correct dosage. The conditions under which polymorphs interconvert is also important as drugs may encounter exposure to changes in temperature, pressure and relative humidity during processes such as drying, granulation, milling, compression and storage[5]. Intellectual property can also become an issue for the pharmaceutical companies who develop and market the new drugs, where challenges to patents have been made on the basis of the discovery of a new polymorph or solvate. Companies therefore deploy substantial effort and resources for the identification and characterisation of polymorphs and solvates.

Even after these tests a new polymorph may remain undetected for many years, or a sample of a new polymorph may be obtained once but never again - the phenomenon of the so called disappearing polymorph.

1.3   Disappearing polymorphs[6]

The phenomenon of disappearing polymorphs was shown in the classical case of ritonavir.[7] The new polymorphic structure of ritonavir, one which had not been used in early testing of the drug, affected how the semisolid capsule dissolved. Patients were offered the drug in liquid form until the company could reformulate the product to eliminate the wrong structure.

There are a number of parameters which can affect a process to change the polymorph produced, including temperature, rate of evaporation and purity of the starting materials. For example, there are many things which could alter the purity of the starting material. Over the years the purity of starting materials has improved due to superior processes and analytical techniques. The impurities involved in the process could have changed. This is because the starting materials could have been sourced from different manufacturers.

1.4   Amorphous forms

Amorphous materials[8] are formed when the cooling rate of a liquid is faster than the rate at which molecules can organise themselves into a more thermodynamically favourable crystalline state. Amorphous materials can also be produced by additives which interfere with the ability of the primary constituent to crystallise.

Increased solubility (between 10 and 1600 fold)[9] from crystalline to amorphous material, has been reported. This change in solubility and dissolution rate in the body make amorphous materials very important in the pharmaceutical industry. Any change in the dissolution rate can drastically change the affect of a drug. There is evidence that some of the anhydrous forms of formoterol fumarate contain a degree of disorder.[10]

1.5   Fomoterol fumarate reaction routes

Previous work performed by AstraZeneca[10] has shown how formoterol fumarate combines with water and various solvents. This work has been summarised in Figure 1.2. Formoterol fumarate dihydrate is a crystalline solid and is manufactured by

combining formoterol base with fumaric acid in a water/isopropanol environment. Once the formoterol fumarate dihydrate is produced the water in the structure is very difficult to remove. It can only be achieved by drying under vacuum at 85 ºC which produces formoterol fumarate anhydrate A[10]. This anhydrate can then be slurried with a solvent such as ethanol to produce a solvate, in this case, formoterol fumarate diethanol solvate. These solvates can form a second anhydrate, anhydrate C, by leaving to dry for several days. Anhydrates A and C can form a third anhydrate, anhydrate B, by slurrying with ethyl acetate.

Figure 1.2 Formoterol fumarate reaction routes

Chapter 1 INTRODUCTION
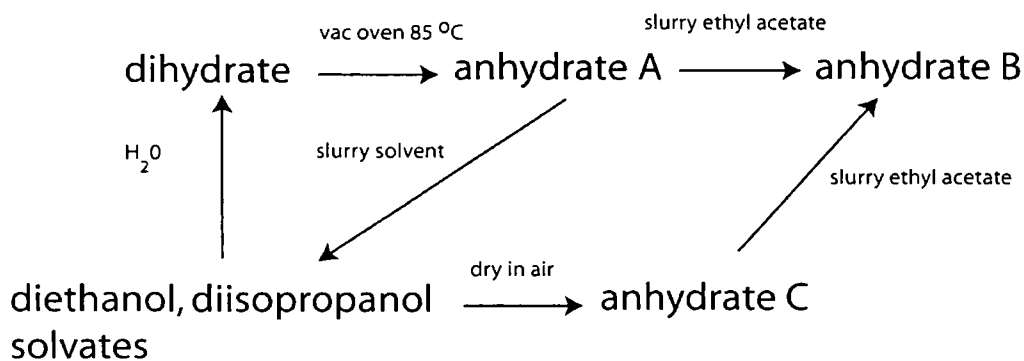
1.6 *References*

1.   Harris RK, NMR studies of organic polymorphs and solvates, *The Analyst* 2006, 131, 351-373

2.   Byrn SR, Pfeiffer RR, Stephenson G, Grant DJW, and Gleason WB, Solid-State Pharmaceutical Chemistry, *Chem. Mater.*, 1994, 6(8), 1148 – 1158

3.   Othman A, Evans JSO, Evans IR, Harris RK, Hodgkinson P, Structural study of polymorphs and solvates of finasteride, *Journal of Pharmaceutical Sciences*, 96(5), 1380-1397

4.   Hodgkinson P, Solvates project, Unpublished

5.   Brittain HG, Polymorphism in Pharmaceutical Solids, Ed. Marcel Dekker, 1999, 95, 125-179.

6.   Dunitz JD, Bernstein J, Disappearing Polymorphs, *Acc. Chem. Res.* 1995, 28(4), 193-200

7.   Bauer J, Spanton S, Henry R, Quick J, Dziki W, Porter W, Morris J, Ritonavir: An Extraordinary Example of Conformational Polymorphism, *Pharm. Res.*, 2001, 18(6), 859

8.   Hodeau JL, Guinebretiere R, Crystallography past and present, *Applied Physics A Materials Science & Processing* 2007, 89(4), 813-823

9.   Hancock BC, Parks M, What is the True Solubility Advantages for Amorphous Pharmaceuticals, Pharm. Res., 2000, 17(4), 397-404

10. Jarring K, Larsson T, Stensland B, Ymen I. Thermodynamic Stability and Crystal Structure for Polymorphs and Solvates of Formoterol Fumarate, *Journal of Pharmaceutical Sciences*, 2005, 95(5), 1144-1161

Chapter 2 EXPERIMENTAL

2.1   *History*

The first successful demonstrations of NMR were published in 1946. Two independent groups discovered NMR almost simultaneously. Bloch[1], Hansen and Packard, working at Stanford University and Purcell[2], Torrey and Pound, working at Harvard University, published their results in consecutive issues of Physical Review. The importance of this discovery was recognised by the joint award of the 1952 Nobel Prize for Physics to the two group leaders Professor Felix Bloch and Professor Edward Purcell. Since then the applications of NMR have steadily widened[3]

2.2   *Fundamental concepts*

Zeeman Splitting and Spin States

Consider a sample containing only one type of nucleus with spin-$\frac{1}{2}$. The nuclear spin will have a nuclear magnetic dipole moment or just magnetic moment, μ.

Outside of the static magnet field the magnetic moments of the individual nuclei exist in all possible orientations (see Figure 2.1).

No Applied Magnetic Field
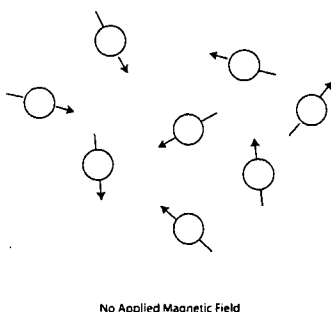
Figure 2.1 Individual nuclei randomly orientated when no magnetic field present.

In quantum mechanical terms[4] an atomic nucleus is characterized by a nuclear spin quantum number, I, referred to as *spin*. In general, the nuclear spin quantum number for a nucleus may be integer, half integer or zero.

The magnitude of the magnetic moment depends directly on the value of I. The magnetic moment has vector properties, that is, it has direction as well as magnitude.

But, quantum mechanically, only certain directions are allowed. These directions are expressed with respect to the z-axis of a Cartesian coordinate frame. The z-direction in NMR is conventionally taken to be that of the applied static magnetic field B_0. The component of the magnetic moment in z is given by

$$\mu_z = \gamma h m_I / 2\pi$$ where m_I = magnetic quantum number

γ = magnetogyric ratio

h = Planck's constant

In general there are $2I + 1$ possible values of m_I. Orientations characterised by a particular value of m_I are often refered to as *spin states*. So for a spin-½ proton there are two possible spin states. If we consider a spin-½ proton in a water sample when placed in a magnetic field B_0 certain things happen. The individual nuclei will align with or against the magnetic field. The magnetic moment will tend to precess around B_0 at a frequency known as the Larmor frequency, ω

$$\omega = -\gamma B_0$$ γ = magnetogyric ratio

The magnetic moment interacts with the B_0 field generating two possible energy levels (see figure 2.2). The two energy levels can be characterised by the nuclear spin quantum number m_I. Assuming γ is positive, then the state of the lower energy has the nuclear magnetic moment aligned with its z component parallel to B_0. It is characterised by $m_I = ^1/_2$. The state when $m_I = -^1/_2$ is the higher energy state and has the z component antiparallel to B_0. This energy level splitting is known as *Zeeman splitting*. If a large number of nuclei are considered there is a distribution between the two energy levels known as a Boltzmann distribution. Any peturbation of the system alters the populations of the energy levels .

This difference in energy between the two spins, ΔE, plays an important role in NMR, in particular the overall magnetisation and therefore the signal strength are

7

dependent on ΔE. The energy level splitting is directly proportional to the strength of the static field B_0.

$$\Delta E = h\gamma B_0/2\pi$$

Energy

$m_I = -1/2$

$\Delta E = h\gamma B_0/2\pi$

$B_0 = 0$

$m_I = +1/2$

$B_0 > 0$
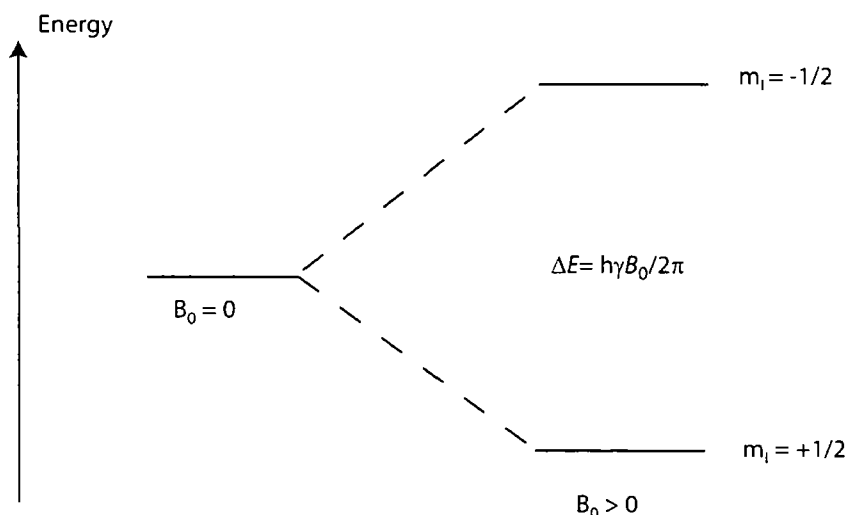
Figure 2.2 Energy levels of an isolated spin-½ nucleus in the absence ($B_0=0$) and presence ($B_0>0$) of an external field .

Rotating frame of reference[5]

A rotating frame of reference is used to apparently eliminate the precession around B_0. The coordinates are chosen such that the z′ axis is parallel to B_0 and x′ and y′ are in the same xy plane but rotating about z′ at the same frequency as the precession. The comparison to this is a person standing in a playground watching a child on a carosel. If he wants to interact with this child, for instance, to take payment for the ride, it would be very difficult to do so whilst the child is rotating on the carosel. If this person is standing on the carosel it would be possible for him to receive payment as the child would appear stationary. It means in effect that the B_0 field has disappeared.

Rotation of the Magnetisation (Effect of a pulse)

To rotate the magnetisation we need to apply a magnetic field in the xy-plane. The way this is achieved is by applying a small magnetic field along the x-axis and to make the field oscillate at or near the Larmor frequency. The coil used to detect the processing magnetic field can also be used to generate the oscillating magnetic field. A pulse of radio frequency (rf) power is fed to the coil and the resulting oscillating current will create the required oscillating magnetic field along the x direction. The oscillating magnetic field due to precession induces an oscillating current in a coil. This is the NMR signal.

Solid-State NMR Line Broadening

In the solid-state NMR of organic molecules there are four important interactions which may contribute to the line width:

i. Dipolar interaction

A direct interaction between magnetic dipoles of two nuclei. It can be either homonuclear between like spins or heteronuclear between two unlike spins I and S. In liquids, dipolar couplings are averaged out by molecular motion, but in solids they contribute to line broadening. It can be the dominant broadening factor.

ii. Shielding interaction (Chemical Shift Anisotropy)[6]

The shielding of the nucleus from the external field by surrounding electrons is orientation dependent. In a powder the molecules are orientated every which way and give a "powder pattern" of peaks that merge into a broad distribution. In a liquid, on the other hand, the dependence on orientation is averaged out by molecular tumbling, and thus the peaks are sharp.

iii.   Quadrupolar Interactions

These only occur for nuclei with spin greater than ½. It is the interaction between the nuclear electric quadrupolar moment and a non symmetric electric field gradient around the nucleus and if present is often dominating.

iv.   J Coupling (spin spin interactions)

This describes the interaction of nuclear spins through chemical bonds i.e. a pair of spins I and S. It is independent of the field and is usually small compared to dipolar interaction.

The differences between solution-state and solid-state NMR are that in the solution state:

a. The shielding interaction is averaged to a discrete value giving the isotropic chemical shift.

b. The dipolar and quadrupolar interactions are averaged to zero.

In the solid state there is a lot less motion and the interactions are not averaged. There is broadening of the NMR signal so that only a broad spectrum is obtained (see Figure 2.3). Here the solution state NMR spectrum of alanine is superimposed on top of the broad solid-state NMR spectrum.
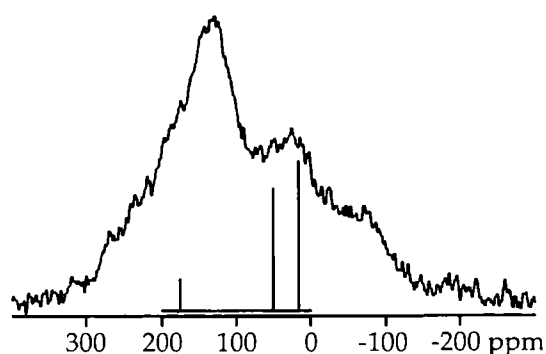
Figure 2.3 ^{13}C Solution-state versus static solid-state NMR spectra for alanine

Ways of removing line broadening

In order to obtain useful information from a solid sample it is necessary to remove the broadening mechanism using the following:

a. Magic-angle spinning[7] (MAS)

Spinning the sample at an angle of 54.7° relative to the static magnetic field (the magic-angle) results in the averaging of all anisotropic components so that a narrow line is observed at the isotropic chemical shift (see Figure 2.4). If the spin-rate is less than the width of the static line spinning sidebands can be observed. These occur symmetrically either side of a centreband (the isotropic shift) and are separated from it by a frequency equal to the spin rate.

b. High power proton decoupling

Dipolar interactions involving ^1H are particularly strong. For organic molecules C-H nuclear spin interactions (dipolar interactions) need to be removed (decoupled) in order to increase the resolution of ^{13}C spectra. By applying a continuous proton
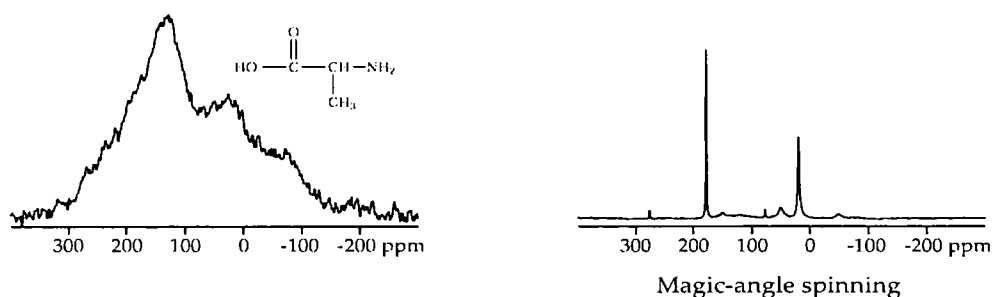
Figure 2.4 Static versus MAS solid-state NMR spectra for alanine

radio frequency (rf) field this heteronuclear coupling to protons can be removed, giving better resolution in the spectrum when combined with MAS (see Figure 2.5). Typically the ^{1}H rf nutation rate exceeds 50 kHz. Resolution can often be increased further by using modulated decoupling schemes such as two pulse, phase modulated (tppm) decoupling.

Relaxation

T_1 spin–lattice relaxation[8]

The relaxation time T_1 represents the rate constant of the first order process that returns the magnetisation to the Boltzman equilibrium along the z axis after a 90° pulse. Following the 90° pulse the magnetisation grows exponentially in the z direction according to the following equation:

$$M_z(t) = M_0(1-e^{-t/T_1}) \qquad \text{where } M_0 = \text{equilibrium magnetisation}$$

^{13}C T_1 measurements were used to get a better understanding of the mobility of the carbon atoms in the drug molecule. Long T_1 times usually correspond to slow molecular motion and short T_1 times to fast motion.

Figure 2.5 MAS and ^{1}H proton decoupled spectra for alanine

Chapter 2   EXPERIMENTAL

2.3   *The spectrometers*

The results were obtained using either a Varian Unity Inova spectrometer, operating at 299.82 MHz for ^{1}H, 75.40 MHz for ^{13}C, 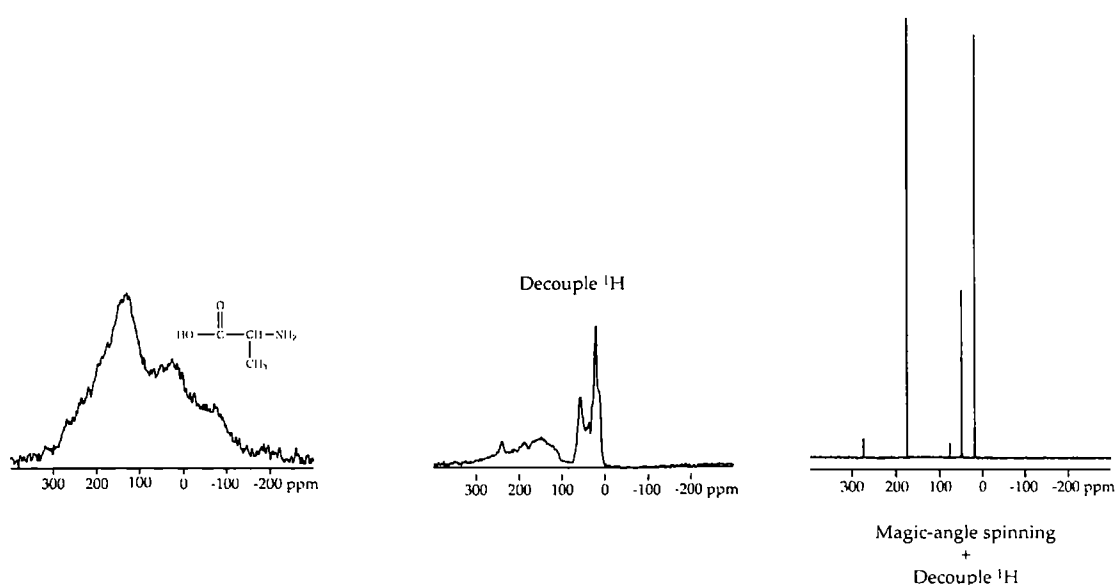30.39 MHz for ^{15}N and 46.07 MHz for ^{2}H, or a Varian VNMRS 400 spectrometer operating at 100.56 MHz for ^{13}C and 61.42 MHz for ^{2}H. The work on the Inova instrument used either a 7.5 mm (rotor o.d.) or a 5 mm probe. For the VNMRS instrument spectra were recorded using a 4 mm T3 HXY probe. Spectra were recorded on the Unity Inova unless otherwise stated. High-resolution spectra were obtained under magic-angle spinning (MAS) conditions using either a cross-polarisation (CP) or direct-polarisation (DP) experiment. The CP conditions used were: recycle rate of 5 s, contact time of 1 ms, acquisition time of 50 ms and a magic-angle spin rate of 5 kHz unless otherwise stated in the figure captions.

Dipolar dephased CP spectra were obtained with a 40 μs dephasing delay, other acquisition conditions are included in the figure captions. Spectra are referenced to tetramethylsilane (TMS) or nitromethane by setting the high-frequency signal from adamantane to 38.4 ppm and the nitrate signal from solid ammonium nitrate to -5.1 ppm.

The angle was set by monitoring the response of ^{79}Br from the spectrometer in a repeat single pulse mode.

2.4   *Setting the magic angle*[9]

Setting the magic angle is a very important task as, if the sample is not on angle, the chemical shift anisotropy and heteronuclear dipolar interactions are not fully averaged.

2.5   *^{13}C CPMAS*[10]

The cross polarisation (CP) experiment[11] provides a means for transfer of magnetisation from the more abundant ^{1}H spins to the less abundant spins ^{13}C (see Figure 2.6).

13

The main advantage to this is that the recycle delay then depends on the T_1 (H) and not T_1(X) and the former is usually much shorter.

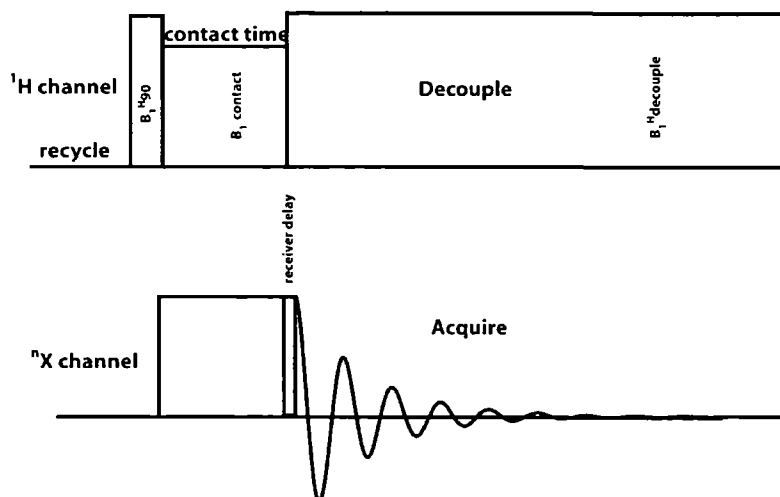The main disadvantage to CP work is that the signal intensities cease to be quantitative.

Fig 2.6 CP pulse sequence (not to scale, see text below)

A 90° pulse (typically 4 μs) is applied to the ^{1}H channel along the x axis which causes the magnetisation to rotate from the z axis into the y axis (see Figure 2.6). If the ^{1}H rf field is then phase shifted by 90° into the y axis it will be acting in the same direction as the magnetisation. The spins are now said to be spin locked. This is achieved using a pulse on the ^{1}H channel which is 90° out of phase with the first pulse. At the same time a pulse is applied on the X channel (where X can be any NMR active nucleus). The duration of the simultaneous pulses is called the contact time and is of the order of 1-10 ms.

If the two r.f. magnetic fields (amplitude of the pulses) B_{1H} and B_{1X}, are chosen to fulfil the Hartmann-Hahn[12] match condition then polarisation transfer can occur from ^{1}H to X. The amplitude of the fields is of the order of mT. The B_{1X} field is then switched off and the FID is recorded over the acquisition time (AT), typically 50 ms with proton decoupling. The B_{1H} field is then switched off and the system is allowed to relax for a recycle delay before the whole sequence is repeated.

$\gamma_H B_{1H} = \gamma_X B_{1X}$ where B_{1H} and B_{1X} are the strengths of the ^{1}H and X rf fields.

2.6   *Direct polarisation MAS*

Direct polarisation was carried out on a number of samples to show the more mobile components/groups.

It consists of a simple 90 ° pulse followed by the detection of a signal. A long recycle delay will detect all the species in a sample whereas with a short recycle delay, the DP spectrum shows those species with short T_1 values, that is, the mobile parts of the compound such as methyl groups.

2.7   *Dipolar Dephasing*[13]
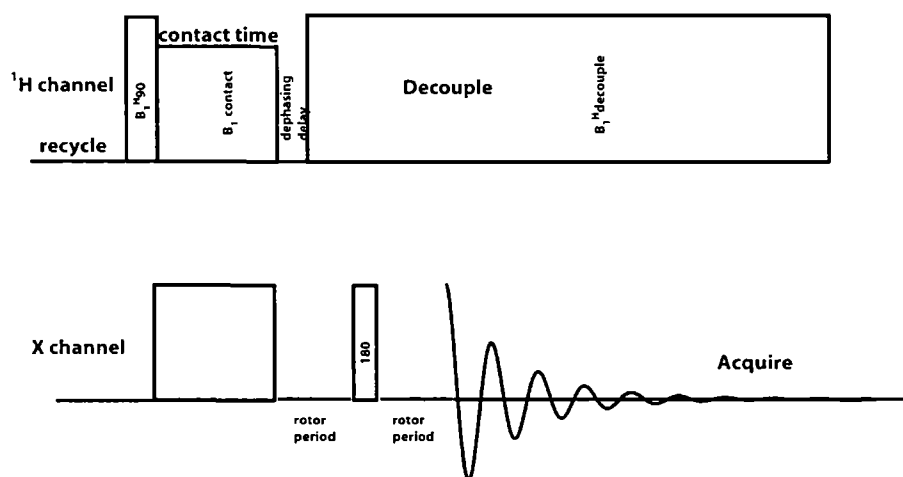
Fig 2.7 Dipolar dephasing pulse sequence

A dipolar dephasing experiment (Figure 2.7) is normally used to distinguish the quaternary and methyl ^{13}C atoms in a sample from the CH or CH_2s. The pulse sequence is similar to the CP sequence but has a delay time before acquisition. This time (a dipolar dephasing delay time) was set at 40 us. There is also a rotor synchronised 180° pulse on the X channel which refocuses the signal making it easier to process. The decoupling is turned off during this delay time and then turned on again afterward. Whilst the decoupling is turned off any signal originating from

species strongly dipolar coupled to hydrogen (CHs CH$_2$s) will decay faster than species weakly coupled to hydrogen.

2.8   Referencing

One of the most important parts of the sample set up is the referencing of the spectrometer. The standard references for ^{13}C, ^{15}N, ^{1}H and ^{2}H are tetramethylsilane (TMS) for ^{13}C and nitromethane for ^{15}N. However, in practice, secondary refencences were used because standard references are volatile liquids at room temperature and therefore cannot be used to set up the cross-polarisation experiment Hartmann-Hahn match conditions. The secondary references used have been discussed earlier in Section 2.3.

2.9 ^{1}H MAS NMR

Proton MAS spectra were obtained on a Varian Infinity Plus spectrometer which operates at 499.70 MHz and also a Varian Unity Inova spectrometer operating at 299.82 MHz.

2.10   Variable temperature work

Some of the experimental work was performed at temperatures other than ambient. Above ambient was achieved by heating the air passing into the NMR probe to the required temperature. Below ambient temperature nitrogen gas was passed through a heat exchanger placed in a 50 litre liquid nitrogen dewar. The nitrogen gas was then passed into the NMR stack and heated to the required temperature.

2.11   Carbon T_1

^{13}C T_1 measurements were obtained using the method of Torchia.[14]

2.12 Deuterium T_1 inversion recovery

This method involves the inversion of the magnetisation using a 180-τ-90-FID sequence. The magnetisation is placed into the $-z$ axis with a 180° pulse and allowed to recover longitudinally for a time τ and then monitored with the 90° pulse. The signal as a function of τ is given by

$$S(\tau) = S_{eq} (1-2e^{-\tau/T_1})$$ where S_{eq} is the signal obtained after full relaxation.

T_1 measurements were made using an inversion-recovery pulse sequence with a shaped adiabatic inversion pulse to improve the efficiency of the inversion over a square 180° pulse.

2.13 Saturation Recovery

Proton spin-lattice relaxation times (T_1) were obtained using the saturation-recovery method at various temperatures.
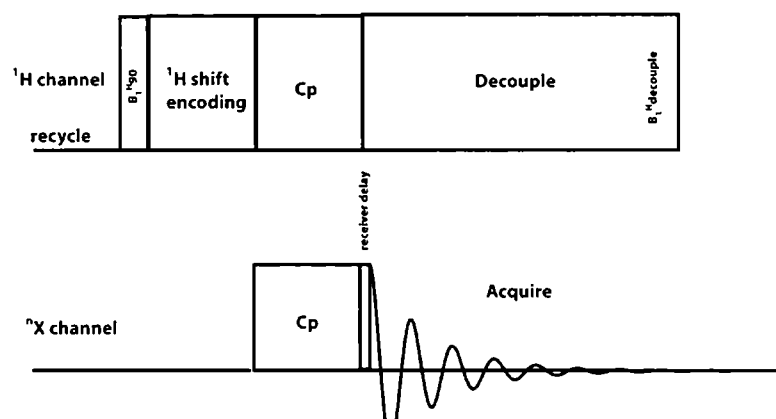
2.14 Heteronuclear Correlation (Hetcor)[15, 16, 17]

Fig 2.8 Hetcor pulse sequence

Solid-state cross polarization magic-angle-spinning (CP/MAS) Frequency Switched Lee Goldburg (FS-LG) decoupled dipolar-correlation spectra were obtained in a magnetic field of 400 MHz with the pulse sequence above (see Figure 2.8), using a solid-state Varian VNMRS 400 spectrometer operating at 100.56 MHz for ^{13}C with a 4 mm T3 HXY probe. The experiment correlates the carbon spectrum with the high resolution proton spectrum. The correlation is obtained when ^{1}H and ^{13}C nuclei are dipolar coupled, it is therefore a through space correlation. During the carbon acquisition the protons are decoupled from the carbons by using a TPPM decoupling scheme, which improved the resolution of the low frequency ^{13}C (methylene region) considerably.

2.15   *Thermal Gravimetric Analysis (TGA)*

TGA is carried out to quantify the mass loss from a sample whist being heated. It can give information about the amount of solvent present within a solvate as well as the amount of water present.

2.16   *Water Determination*

This was carried out using a Karl Fischer titration. There are two types of Karl Fischer titrators: volumetric and coulometric. The main difference between the two is that with the volumetric method, the titrant is added directly to the sample by a burette. Conversely, with the coulometric method, the titrant is generated electrochemically in the titration cell. The coulometric method detects much lower water levels than the volumetric method. The following reaction scheme has been proposed for the Karl Fischer titration:

1. $ROH + SO_2 + RN \rightarrow (RNH) \cdot SO_3R$

2. $(RNH) \cdot SO_3R + 2 RN + I_2 + H_2O \rightarrow$
    $(RNH) \cdot SO_4R + 2(RNH)I$

ROH represents an alcohol like methanol or ethanol.

In the coulometric method, the titration cell consists of two parts: an anodic and a cathodic compartment. The anodic compartment contains the analyte solution which includes sulfur dioxide (SO_2), iodide (I-) and imidazole needed in the chemical reaction. Methanol or ethanol (ROH) is usually used as a solvent. In coulometric Karl Ficher titration, iodine (I_2) is generated electrochemically from iodide (I-). When iodine (I_2) comes in contact with the water in the sample, water is titrated according

to the above mentioned reaction scheme (equations No. 1 and No. 2). The amount of water in the sample is calculated by measuring the current needed for the electrochemical generation of iodine (I_2) from iodide (I-) according to the following reaction (equation No. 3):

3. $2I^- \rightarrow I_2 + 2e^-$
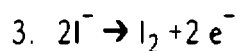
2.17   Preparative Work

The following samples were studied:

1. **Formoterol fumarate (F.F.) diethanol solvate:**

Supplied by AstraZeneca.

2. **Formoterol fumarate diisopropanol solvate**

Supplied by AstraZeneca.

3. **Formoterol fumarate dibenzyl alcohol solvate (contaminated with dihydrate)**

Supplied by AstraZeneca.

4.   Formoterol fumarate dibenzyl alcohol solvate

Supplied by AstraZeneca.

5.   Formoterol fumarate dihydrate prepared from 1

Formoterol fumarate dihydrate was obtained by placing the diethanol solvate in a relative humidity of about 90% for 1 day. Full conversion to the dihydrate was seen to take place by recording the ^{13}C spectrum (see Section 3.1.6).

6.   Formoterol fumarate anhydrate A prepared from 5

Anhydrate A was obtained by drying the previously made FF dihydrate at 85 °C under a vacuum. Full conversion was seen to take place by recording the ^{13}C spectrum.

7.   Formoterol fumarate anhydrate B prepared from 8

Anhydrate B was obtained by slurrying formoterol fumarate anhydrate C in dry ethyl acetate and then allowing to dry on the bench.

8.   Formoterol fumarate anhydrate C prepared from 1

Anhydrate C was obtained by allowing FF diethanol solvate to dry in air for 2 days.

9.   Formoterol fumarate anhydrate C prepared from 2

Anhydrate C was obtained by allowing FF diisopropanol solvate to dry in air for 2 days.

10. Ethyl acetate solvate

Ethyl acetate solvate was obtained by slurrying formoterol fumarate anhydrate C in "wet" ethyl acetate.

11. Preparation of deuterated anhydrate (deuterated on u and u' carbon atoms see Chapter 3, scheme 1)

Formoterol base (0.3 g) was dissolved in a mixture of water (1.02 ml) and isopropanol (4.98 ml) at 41°C (45°C) was not exceeded as formoterol base is not fully stable in solution). Fumaric acid (0.05 g) was added to the clear solution and after being dissolved the solution was allowed to cool down to about 20°C for 30 minutes. The product partially crystallised during this period. The obtained slurry was then cooled for 30 minutes to about 0 °C and left for 1.5 hours before being filtered off, washed with cooled isopropanol and dried (vacuum at 35°C) for 1 hour. The sample was then dried at 80 °C for a further 3 ½ hours. ^{13}C CPMAS spectra were recorded at intervals through this drying procedure.

Chapter 2 EXPERIMENTAL

2.18 *References*

1.   Bloch F, Hansen WW, Packard ME, Nuclear Induction, *Phys. Rev.*, 1946, 69,127

2.   Purcell EM, Torrey HC, Pound RV, Resonance absorption by nuclear moments in a solid, *Phys. Rev.*, 1946, 69, 37-39

3.   Andrew ER, A Historical review of NMR, British Medical Bulletin, 1984, 40(2), 115-119

4.   Nuclear Magnetic Resonance Spectroscopy in Chemistry And The Life Sciences, Sharp D, The Open University 1995

5.   Davies N, NMR study of Solid Organometalic Polymers, MSc Thesis, Durham University, 1992

6.   Duer MJ, Solid State NMR Spectroscopy, Blackwell, 2004, p125

7.   Pines A, Gibby MG, Waugh JS, *J. Chem. Phys.*, 1973, 59(2), 569-590

8.   Claridge TDW, High Resolution NMR technology in organic Chemistry, Perganon, 1999

9.   Dybowski C, Solid State NMR of Polymers, Plenum Press, 1991

10.   Duer MJ, Solid State NMR Spectroscopy, Blackwell, 2004, p96

11.   Pines A, Gibby MG and Waugh JS, *J. Chem. Phys.*, 59(2), 569-590

12.   Hartmann SR and Hahn EL, *Phy. Rev.*, 1962, 128(5), 2042-2053

13.   Harris RK, Nuclear Magnetic Resonance Spectroscopy Longman Scientific and Tech., 1986, p170

14.   Torchia DA, The measurement of proton-enhanced carbon-13 T_1 values by a method which suppresses artefacts, *J. Magn. Reson.*, 1978, 30, 613

15.   Lee M, Goldburg WI, *Phys. Rev. A*, 1965, 140, 1261

16.   Van Rossum BJ, Forster H, De Groot HJM, High Field and High-Speed CP-

        MAS ^{13}C NMR Heteronuclear Dipolar-Correlation Spectroscopy of Solids

        with Frequency-Switched Lee-Goldburg Homonuclear Decoupling, *J. Mag.*

        Res., 1997, 124, 516-519

17.   Van Rossum BJ, De Groot CP, Ladizhansky V, Vega S, De Groot HJM, A

        Method for Measuring Heteronuclear ([1]H-^{13}C) Distances in High Speed MAS

        NMR, *J Am. Chem. Soc.*, 2000, 122(14), 3465-3472.

Chapter 3 CHARACTERISATION

3.1   Introduction

Spectra have been obtained for each of the 3 formoterol fumarate solvates, carbon-13 spectral assignments have been made with the aid of solution-state data and dipolar dephasing experiments.

Anhydrates A, B and C of formoterol fumarate and also the dihydrate have been prepared and spectra obtained. Again with the aid of solution-state data and dipolar dephasing experiments carbon-13 spectral assignments have been made where possible. It was also shown that each sample was different. The work is summarised in this chapter.

Scheme 1. Formoterol fumarate
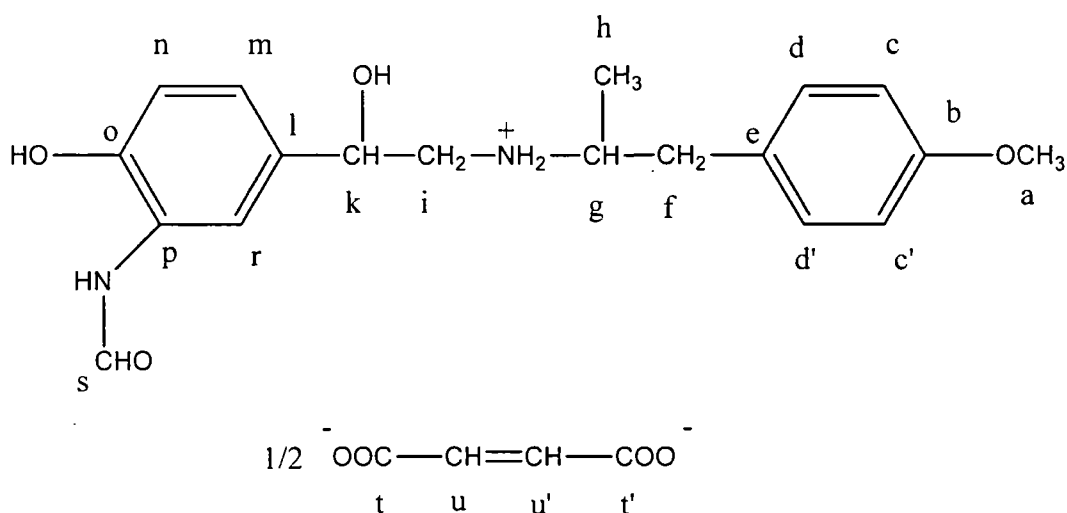
3.1.1   Formoterol fumarate diethanol solvate (1) characterisation

The carbon-13 CPMAS spectrum from **1** is shown in figure 3.1 along with signal assignments. Figure 3.2a is also the full CP spectrum. The spectrum from a dipolar dephasing experiment (Figure 3.2b) shows signals from quaternary carbons and from any cross polarisable mobile carbons such as methyl groups. Figure 3.2c is the spectrum from the DP experiment with a short (1 s) recycle delay. This spectrum contains a background signal from Teflon used as rotor caps which accounts for the

broad signal at 110 ppm. With a short recycle delay, the DP spectrum shows those species with short carbon T_1 values, that is, the mobile parts of the compound such as methyl groups and also any solvent either partially bound or free. From the DP experiment the carbon (h) in scheme 1 is seen at 13.3 ppm and the methoxy (a) at 53.3 ppm. Lines at 57.4 and 17.9 ppm (CH_2 and CH_3 respectively) arise from excess ethanol and the line at 19.5 ppm arises from the methyl group in the solvent molecule from 1 which is partially bound to the drug molecule. Note that it is shifted by 1.6 ppm relative to the free solvent.

Table 1 lists the chemical shifts that have been identified for the solvate. Signals from carbon atoms c, c', d and d' were not resolved from the CP experiment for either 1 or 2 due to motional broadening caused by rotation of this aromatic ring.
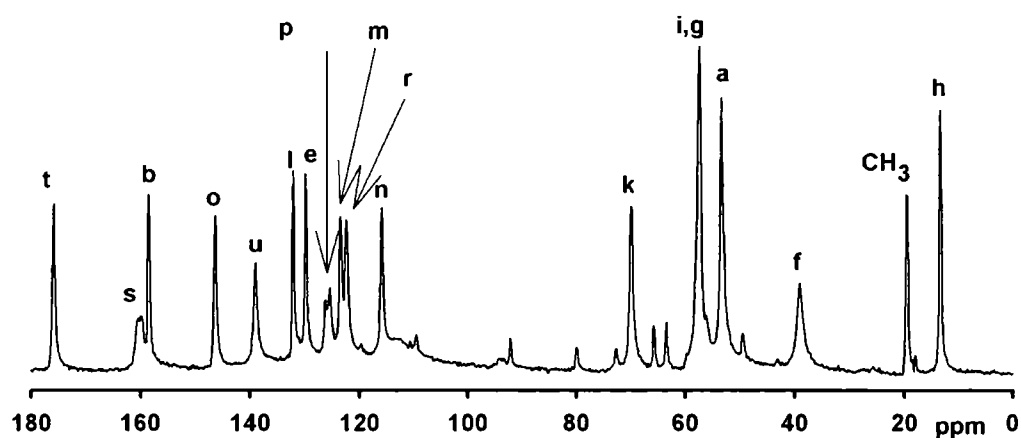

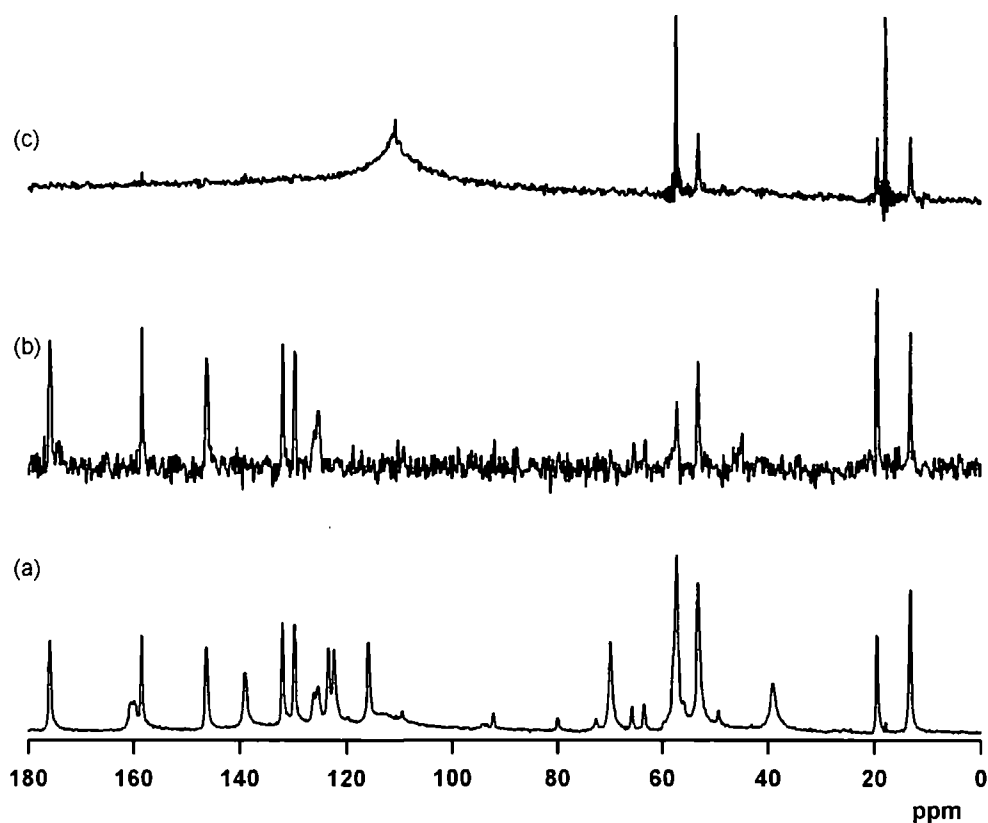Figure 3.1 Formoterol fumarate diethanol solvate ^{13}C CPMAS spectrum.

Figure 3.2   Formoterol fumarate diethanol solvate ^{13}C CPMAS (a), dipolar dephased (b) and DPMAS spectra (c)

3.1.2   *Formoterol fumarate diisopropanol solvate (2) characterisation*

The carbon-13 CPMAS spectrum from **2** is shown in Figure 3.3 with assignments according to scheme 1. Figure 3.4a shows the full CP spectrum, the spectrum from a dipolar dephasing experiment (Figure 3.4b) and Figure 3.4c is the spectrum from the short recycle delay DP experiment. Chemical shift values are listed in Table 1.

Carbon (h) is seen at 13.8 ppm and the methoxy (a) at 53.7 ppm. Signals at 63.6 and 25.3 ppm (CH and CH₃ respectively) are those of the free solvents. It was observed that the lines at 24.4 and 27.4 ppm from **2** were those of the two methyl groups from

a partially bonded solvent molecule. This indicates they are inequivalent and experiencing different shielding effects when the solvent interacts with the drug molecule. There are a number of possible explanations for this. One of which is that each fumarate ion is hydrogen bonded to two equivalent isopropanol molecules but the methyl groups within each solvent molecule are inequivalent. Alternatively the two solvent molecules are inequivalent but there is no evidence for multiple COO signals (carbon t). Lastly there could be two types of solvent, mobile solvent residing in the channels of the structure and also hydrogen bonded solvent. A doublet would be seen for the CH in the solvent, which is not present.
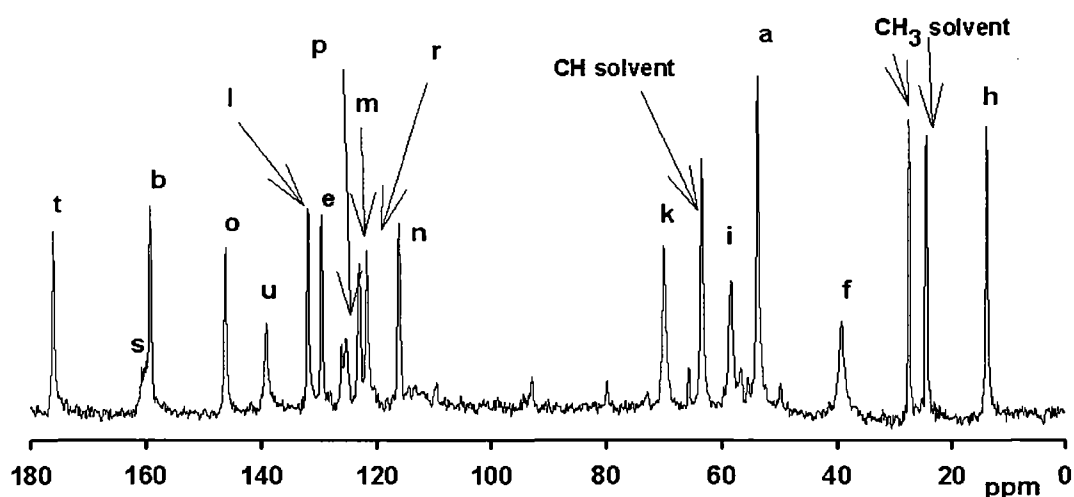

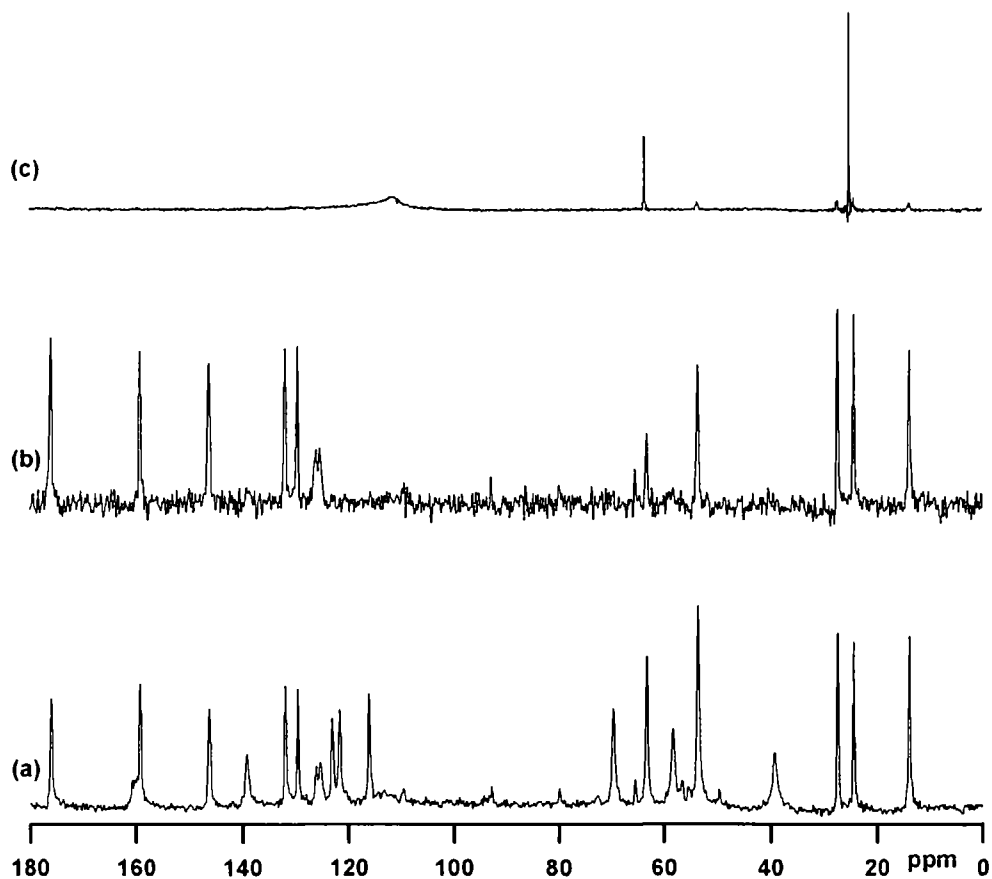Figure 3.3 Formoterol fumarate diisopropanol solvate ^{13}C CPMAS spectrum.

Figure 3.4 Formoterol fumarate diisopropanol solvate ^{13}C CPMAS (a), dipolar dephased (b) and DPMAS spectra (c)

3.1.3   Formoterol fumarate dibenzyl alcohol solvate (3) characterisation

The carbon-13 MAS spectrum from **3** is shown in Figure 3.5. Figure 3.6a is the full CP spectrum. Figure 3.6b is from a reanalysis of the sample two months after the first measurement and Figure 3.6c is that of the FF dihydrate. On closer examination of the spectra it was apparent that there was a large amount of FF dihydrate present as an impurity (see h carbon atom marked at 16.2 ppm). In this case only a small number of the carbon atoms belonging to the solvate were identified due to the problem of contamination. The sample was initially analysed on the 6th October 2006 and on reanalysis on the 8th January 2007 the solvate had degraded further to the dihydrate, so no more work was performed on this sample.
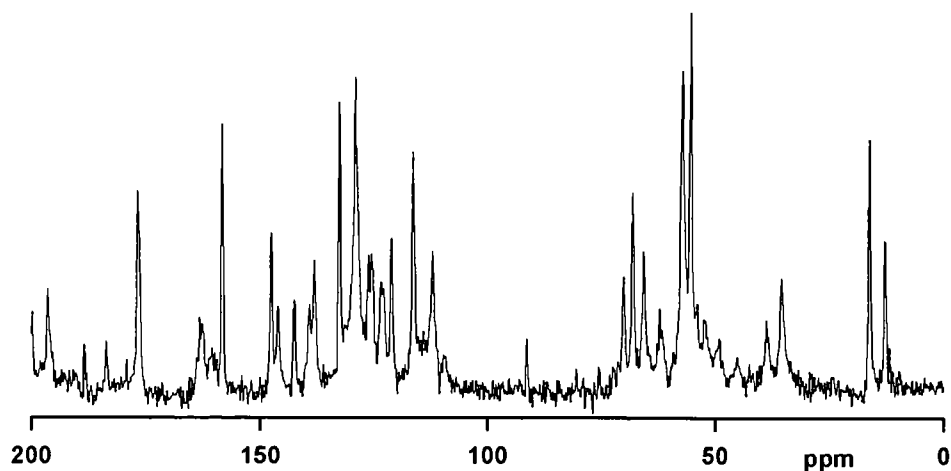
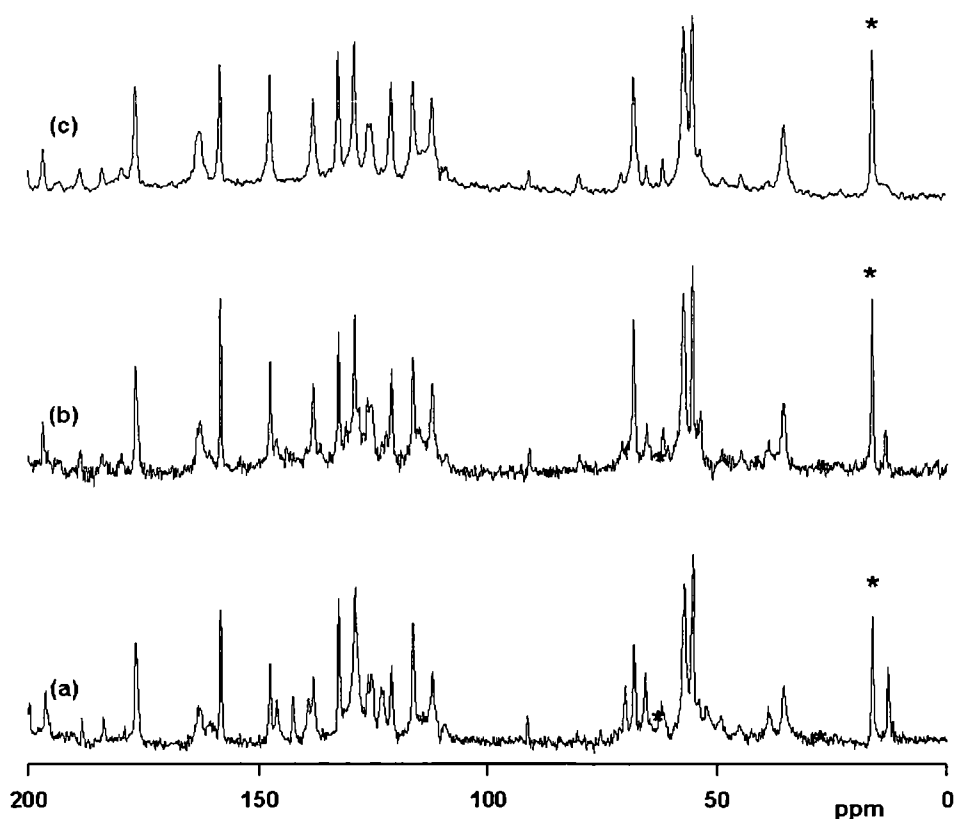Figure 3.5 Formoterol fumarate dibenzyl alcohol solvate ^{13}C CPMAS spectrum, contaminated with dihydrate

Figure 3.6 Formoterol fumarate dibenzyl alcohol solvate ^{13}C CPMAS (a), repeat after 2 months (b), ^{13}C CPMAS formoterol fumarate dihydrate spectra (c)

3.1.4 Formoterol fumarate dibenzyl alcohol solvate (4) characterisation

The carbon-13 CPMAS spectrum from **4** is shown in Figure 3.7 with signal assignments according to scheme 1. Figure 3.8a shows the full CP spectrum, the spectrum from a dipolar dephasing experiment (Figure 3.8b) and Figure 3.8c is the spectrum from a short recycle delay DP experiment.
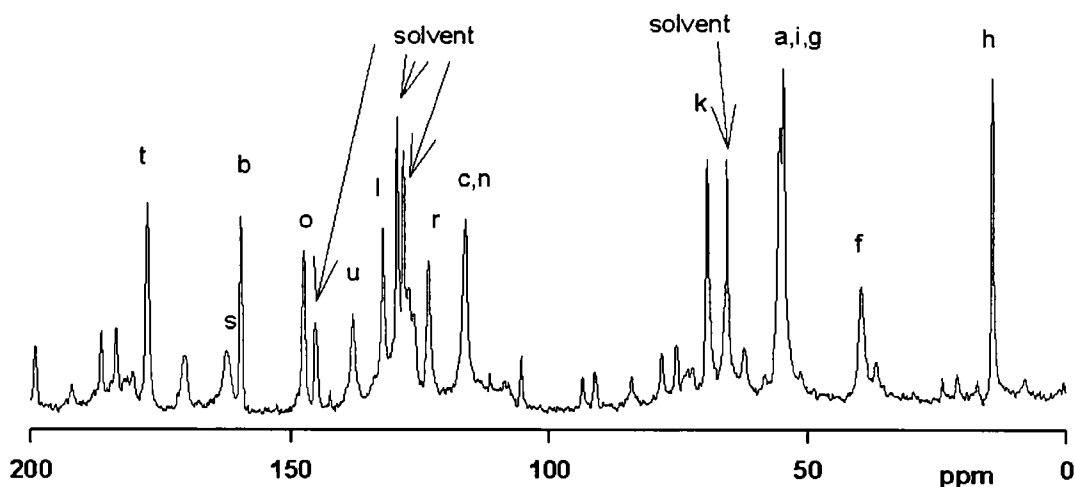

Figure 3.7 Formoterol fumarate dibenzyl alcohol solvate ^{13}C CPMAS spectrum.

From the DP experiment the carbon (h) in scheme 1 is seen at 13.4 ppm and the methoxy (a) at 53.6 ppm. Lines at 64.5 (CH_2), 127.3, 128.6 and 141.4 ppm (aromatic CH's) in the spectrum are those of the free solvent. The solvent lines at 127.3 and 128.6 ppm overlap the aromatic carbon atoms in the formoterol resulting in carbon atom m not being resolved from the spectrum. The amount of FF contained in the rotor was quite small compared to other samples because of a large excess of solvent which could not be easily removed. This has resulted in a lower signal-to-noise ratio than for previous spectra.

Table 1 shows the individual carbon atoms that have been identified from the solvate. Signals from carbon atoms c, c', d and d' were not resolved from the CP experiment for this solvate due to motional broadening caused by rotation of this aromatic ring.
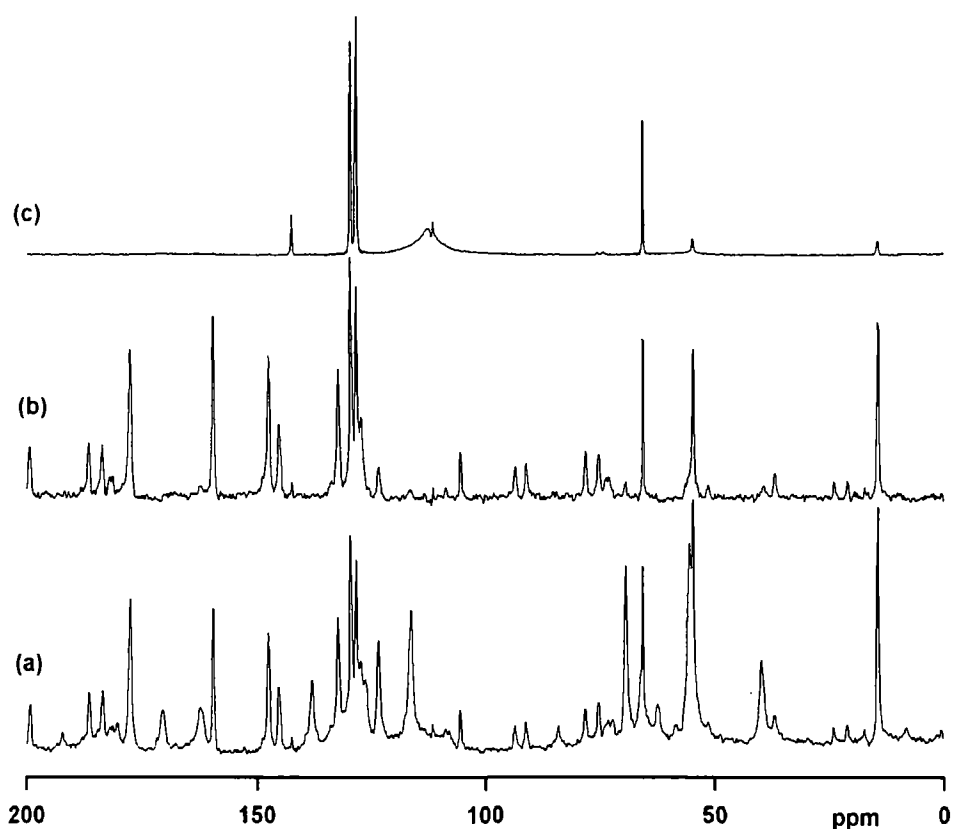
Figure 3.8 Formoterol fumarate dibenzyl alcohol solvate ^{13}C CPMAS (a), dipolar dephased (b) and DPMAS (c) spectra

3.1.5 Formoterol fumarate solvates comparison

(i)   Carbon atoms c, c', d and d' appear to be unresolved in each of the solvates, again due to motional broadening caused by rotation of this aromatic ring (see Figure 3.9).

(ii)   Solvent is detectable in all three solvates as shown by the DP experiments.

(iii)   Two methyl signals were observed for the isopropanol in **2**.

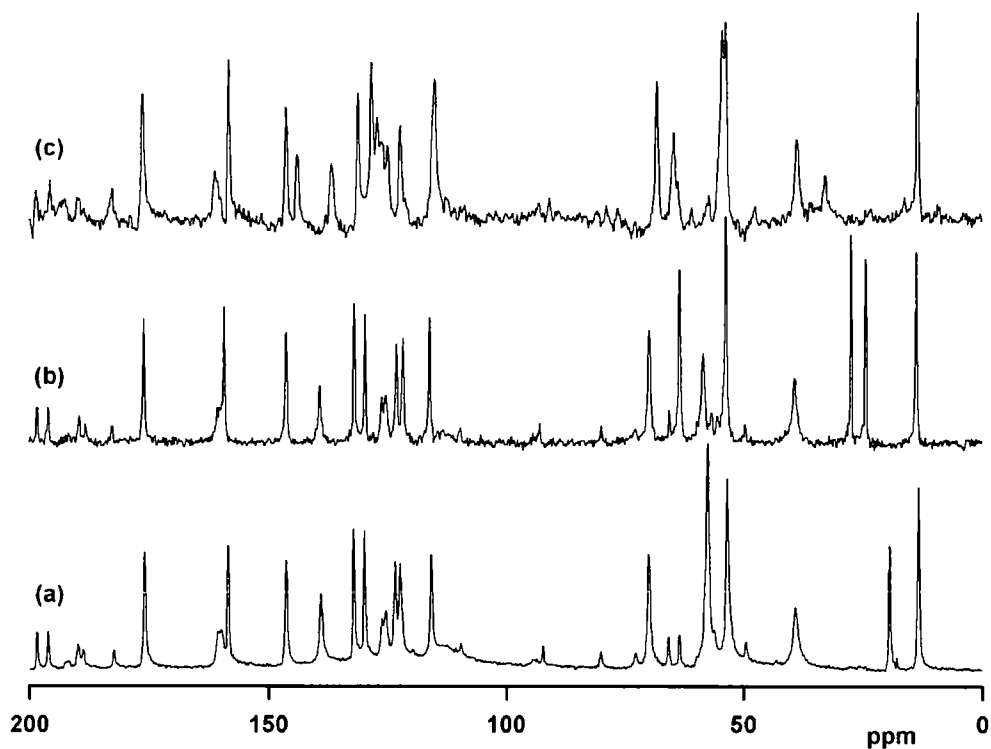(iv)   The greatest differences in the spectra occur in the aliphatic region.

Figure 3.9. Formoterol fumarate solvates ^{13}C CPMAS spectra
(a) diethanol (b) diisopropanol (c) dibenzyl alcohol.

3.1.6   Formoterol fumarate dihydrate characterisation

The dihydrate made from the diethanol solvate sample was found to be identical to one previously analysed [1] (Figure 3.10).
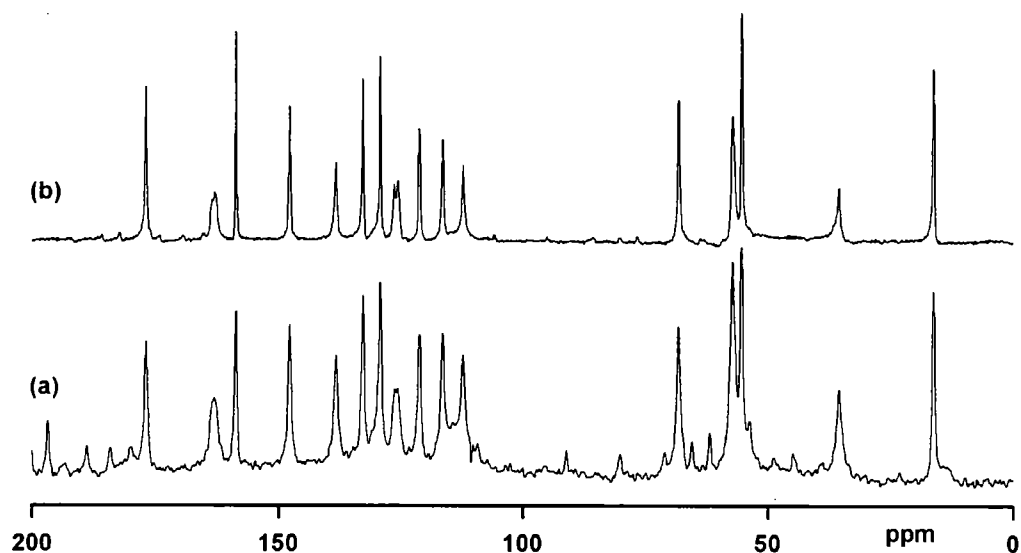
Figure 3.10. Formoterol fumarate dihydrates ^{13}C CPMAS 2007 spectrum (a), ^{13}C CPMAS 2003[1] spectrum (b). (Note the additional signals in (a) are from spinning side bands)

3.1.7 Formoterol fumarate anhydrates[2] comparison

Carbon-13 MAS spectra from anhydrates A (6), B (7) and C (8) are shown in Figures 3.11, 3.12, 3.13 and 3.14. The ^{13}C chemical shift data are also shown in Table 3. The spectrum is different for each anhydrate. 7 gives rather broad lines and was identical to one previously analysed [1]. It was also noted that 8 made from either 1 or 2 gave the same spectrum, these data are not included in this report. The anhydrates are compared against each other in Figure 3.15.

8 gives the narrowest lines of the three anhydrates (50 Hz on average) which implies this is likely to be the most ordered. 6 also shows doublets in many but not all of the carbon atoms which might imply two molecules in the asymmetric unit. 7 gives broader lines (120 Hz) compared with 8 potentially indicating a degree of disorder in the structure.
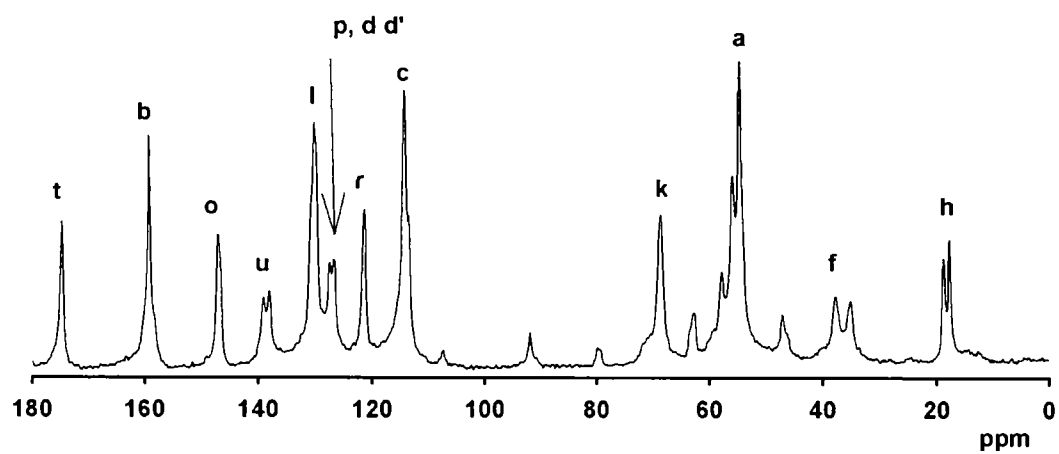
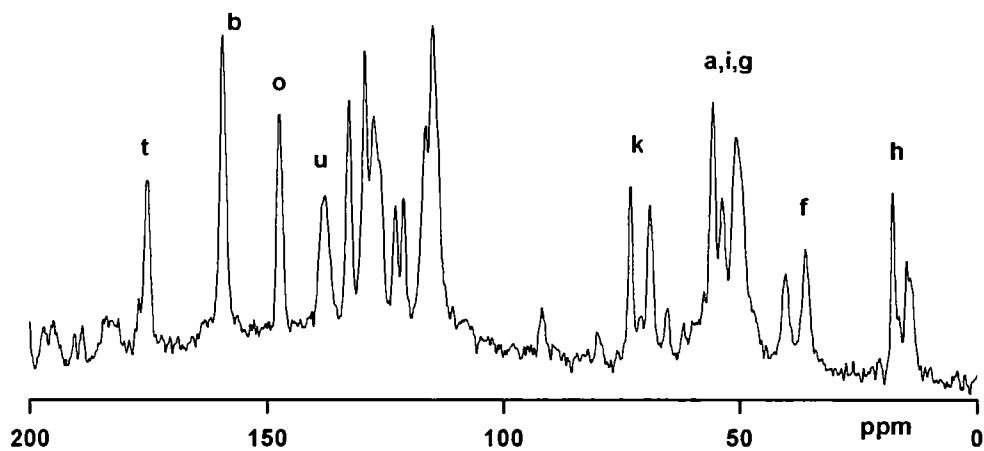Figure 3.11 Formoterol fumarate anhydrate A ¹³C CPMAS spectrum

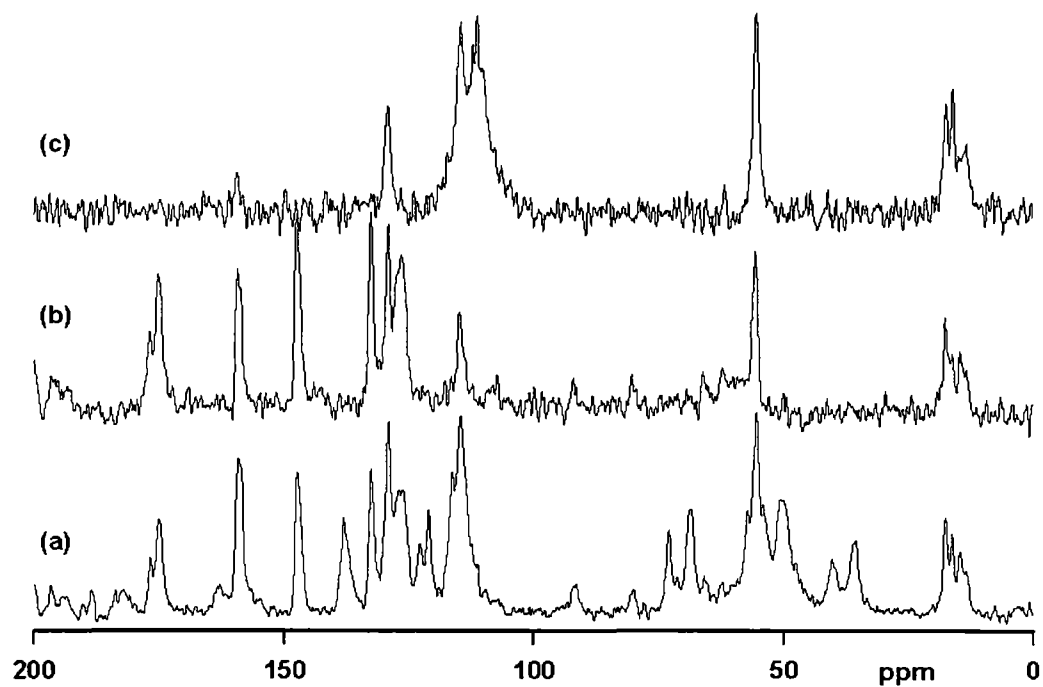Figure 3.12 Formoterol fumarate anhydrate B ¹³C CPMAS spectrum.

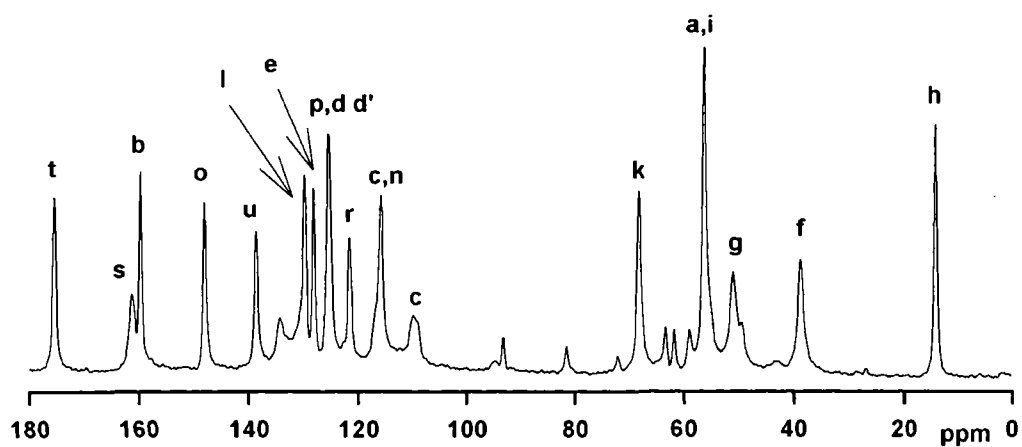Figure 3.13 Formoterol fumarate anhydrate B ^{13}C CPMAS (a), dipolar dephased (b) and DPMAS (c) spectra.

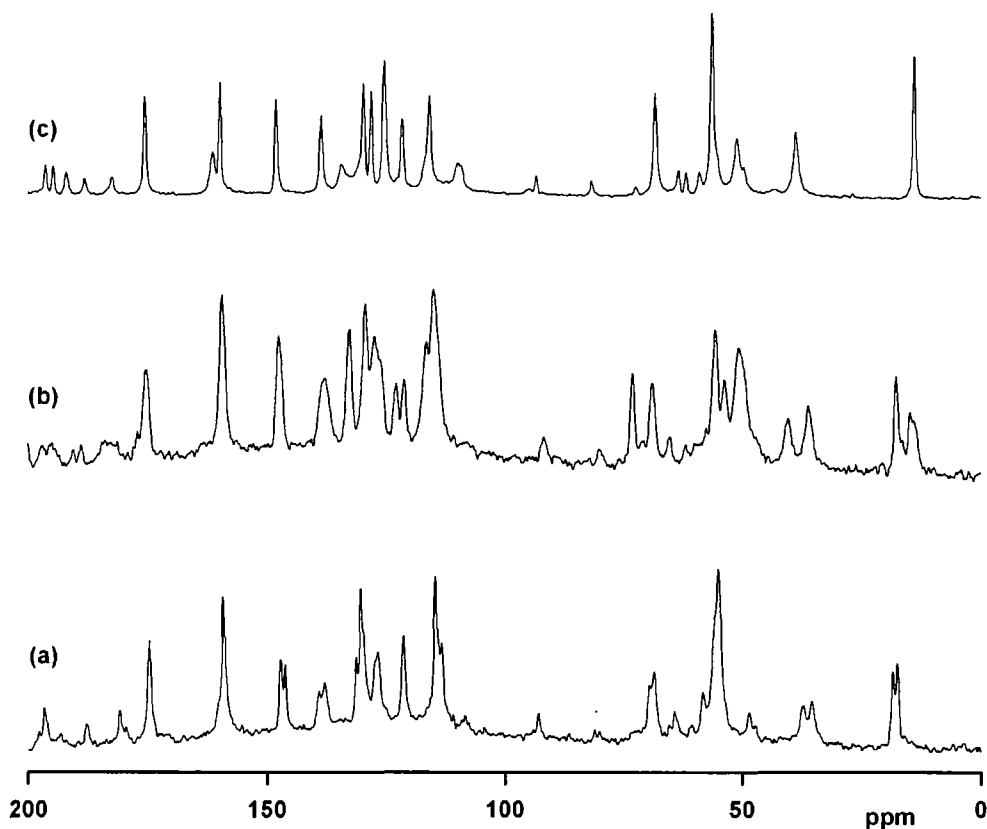Figure 3.14 Formoterol fumarate anhydrate C ^{13}C CPMAS spectrum.

Figure 3.15 Formoterol fumarate anhydrates ^{13}C CPMAS spectra
(a) anhydrate A (b) anhydrate B (c) anhydrate C.

3.2   Proton MAS analysis of solvates

Proton MAS spectra from **2** and **1** are shown in Figures 3.16 and 3.17. Figure 3.16 shows the isopropanol lines at 4.9, 3.9 and 1.1 ppm which are the OH, CH and CH_3 protons respectively and Figure 3.17 shows the ethanol lines at 3.8 and 1.3 ppm which are the CH_2 and CH_3 respectively. These lines were seen to reduce in intensity in a subsequent spectrum (not shown) and it was concluded that this was due to the loss of solvent through spinning-induced heating. Unfortunately, the solvent signal dominates these spectra and no information can be obtained on the FF from them. Since the ethanol was lost on spinning at 25 kHz it will require a low-temperature

run to study the solvates intact. Because of the problem of solvent saturating the proton signal a Hetcor experiment (see Section 2.14) was used to investigate further the protons within formoterol fumarate. These results are summarised in Section 3.8.
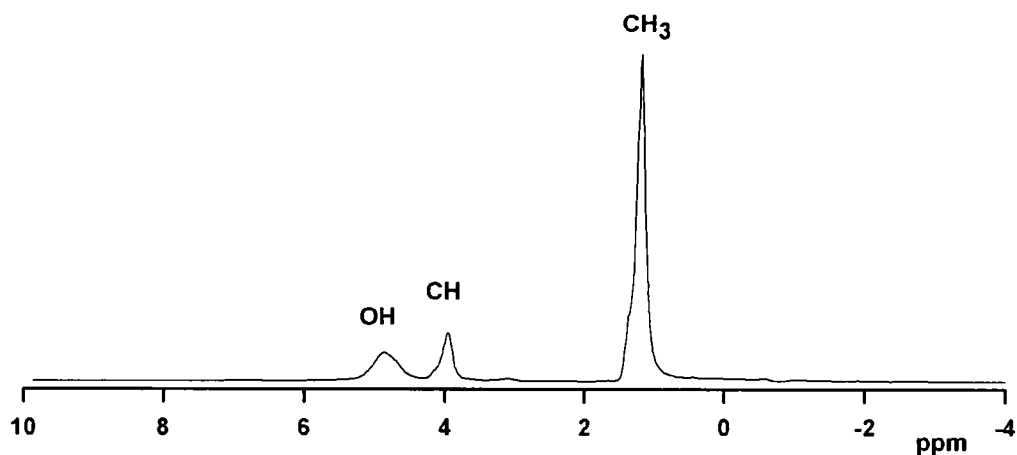

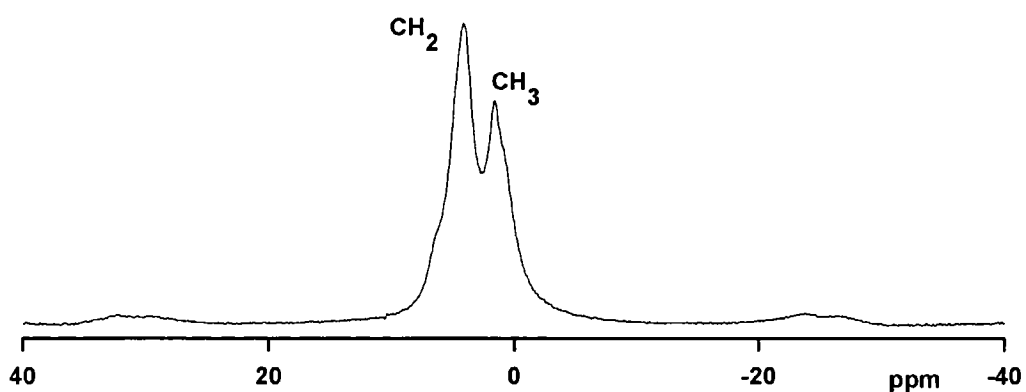Figure 3.16 Formoterol fumarate diisopropanol solvate ¹H MAS spectrum spin rate 14 kHz.

Figure 3.17 Formoterol fumarate diethanol solvate ¹H MAS spectrum spin rate 14 kHz.

3.3 Nitrogen-15 CPMAS analysis

Nitrogen-15 CPMAS spectra from **1**, **5** and **8** are shown in Figure 3.18. The NH_2 shift, at 300 MHz, is between -325 to -326 ppm in all three samples and the lines are relatively broad which is usually the case for NH_2's using a continuous wave decoupling field with a nutation rate of 45 kHz. The NH shift for the ethanol solvate and the anhydrate C is -252 ppm and for the dihydrate -247 ppm.

Nitrogen-15 CPMAS spectra from **1**, **2** and **8** are shown in Figure 3.19 at 400 MHz. TPPM decoupling with a nutation rate of 65 kHz was used in this case and the NH_2 lines between -325 and -326 have narrowed slightly.

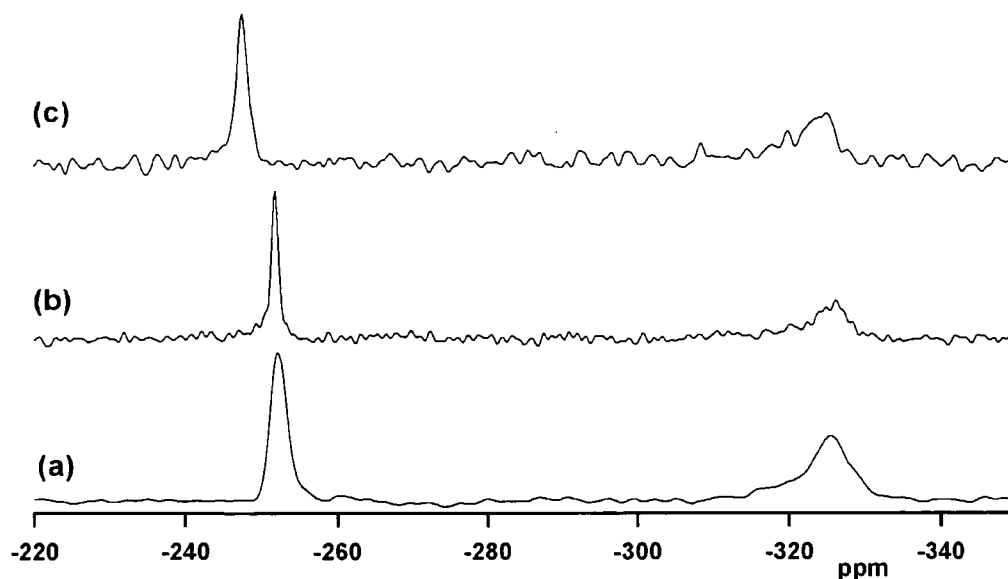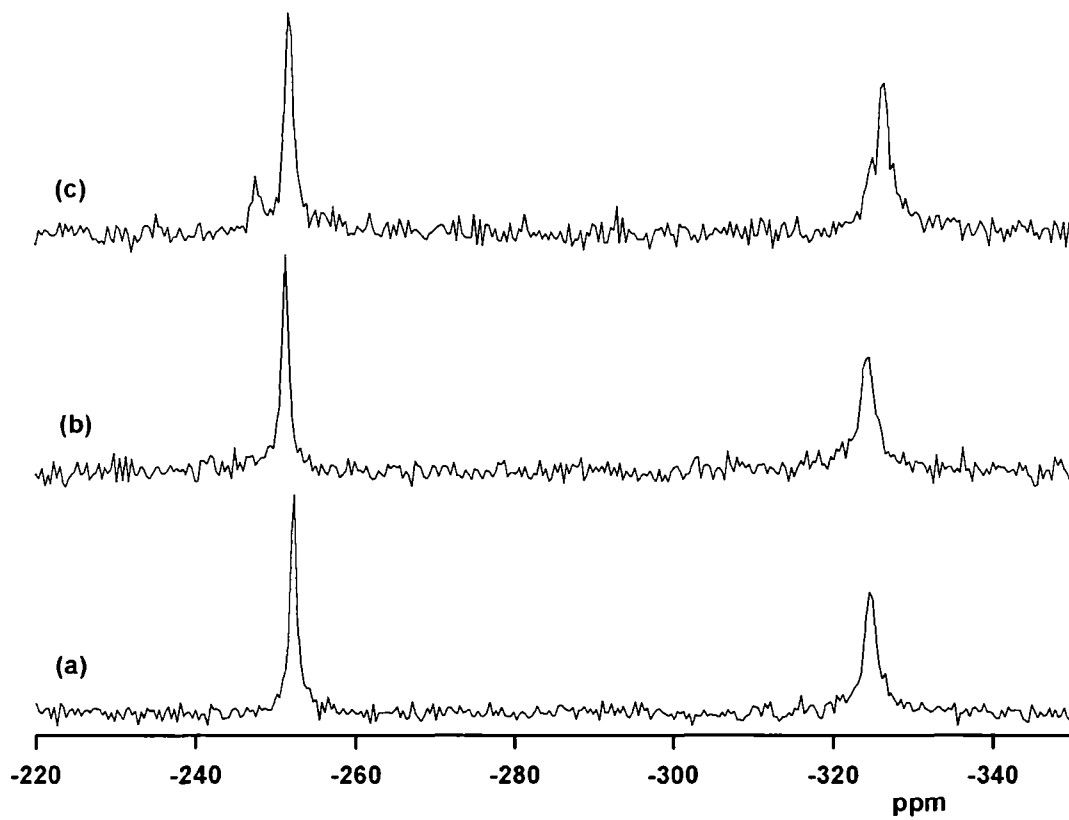**Figure 3.18 Formoterol fumarate ^{15}N CPMAS spectra (a) diethanol solvate (b) anhydrate C (c) dihydrate.**

Figure 3.19 Formoterol fumarate ^{15}N CPMAS spectra (a) diethanol solvate (b) diisopropanol solvate (c) anhydrate C (Varian VNMRS 400).

Table 1. ^{13}C Carbon Chemical Shifts for FF anhydrate in solution and samples **1, 2, 4** and **5** in the Solid-state

Atom Letter	Solution ^{13}C shift/ppm	Solid ^{13}C shift/ppm for dihydrate (5)	Solid ^{13}C shift/ppm for diethanol solvate (1)	Solid ^{13}C shift/ppm for diisopropanol solvate (2)	Solid ^{13}C shift/ppm for dibenzyl alcohol solvate (4)
a	56.1	55.2	53.3	53.6[b]	53.7
b	160.7	158.4	158.5	159.2	158.5
c	115.6				
c′	115.6				
d	131.8				
d′	131.8				
e	130	129.2	129.8	129.6	131.2
f	40.3	35.4	39.1	39.1	38.9
g	57.3	57.0	57.4	63.3[b]	54.3
h	16.4	16.2	13.4	13.8	13.5
i	53.1	57.0	57.4	58.3[b]	53.7
k	70.8	67.9	69.8	69.8	68.2
l	133.9	132.8	132.1	132.0	131.2
m	124.3	121.1[a]	123.4[a]	123.1[a]	
n	116.6	112.2[a]	115.8[a]	116.1[a]	115.1[a]
o	148.9	147.5	146.4	146.3	146.4
p	127.3	126	125.4	125.4	125.2
r	120.7	116.4[a]	122.3[a]	121.8[a]	122.4[a]
s	162.4	162.9	160.0	160.7	161.3
t, t′	174.7	176.7	175.9	176.0	176.4
u, u′	137.5	138.2	139.1	139.2	136.9
CH3			19.5		
CH3				24.4	
CH3				27.4	
CH2			57.4		64.5
CH				63.3	127-141[c]

[a] Assignments not certain
[b] Assignment of g at one of these positions
[c] Assignment not certain due to large excess of solvent

Table 2. Signals present in the dipolar dephased spectra

Atom Letter	diethanol solvate (1)	diisopropanol solvate (2)	anhydrate C (8)
a	✓	✓	✓
b	✓	✓	✓
c	x	x	x
c'	x	x	x
d	x	x	x
d'	x	x	x
e	✓	✓	✓
f	x	x	x
g	x	x	x
h	✓	✓	✓
i	x	x	x
k	x	x	x
l	✓	✓	✓
m	x	x	
n	x	x	x
o	✓	✓	✓
p	✓	✓	✓
r	x	x	x
s	x	x	x
t, t'	✓	✓	✓
u, u'	x	x	x
CH_3	✓	✓	
CH_2	x		
CH_3		✓	
CH		x	

✓- quaternary, methyl and solvent carbons remaining in the spectrum
x- CH and CH_2 carbons removed

Table 3. ^{13}C Chemical shifts

Atom Letter	Solution ^{13}C shift/ppm	Solid ^{13}C shift/ppm for FFA[1]	Solid ^{13}C shift/ppm for anhydrate A (6)	Solid ^{13}C shift/ppm for anhydrate B (7)	Solid ^{13}C shift/ppm for anhydrate C (8)
a	56.1	55.2	54.8	55.6	56.2
b	160.7	159.2	159.1	159.5	159.7
c	115.6				110.1
c′	115.6				116.1
d	131.8				
d′	131.8				134.2
e	130	129.4			128.1
f	40.3	40.0 and 36.1	37.1 and 35.4	40.3 and 36.3	38.7
g	57.3	53.6 and 49.9	54.8	53.7 and 50.6	56
h	16.4	17.2 and 14.5	18.5 and 17.5	17.9 and 14.9	13.9
i	53.1	53.6 and 49.9	54.8	53.7 and 50.6	50.9
k	70.8	72.6 and 68.3	68.4	73.0 and 68.9	68.1
l	133.9	132.3	130.3 and 131.4	132.2	129.7
m	124.3	122.9[a]		122.9[a]	
n	116.6	114[a]		115.2[a]	115.8[a]
o	148.9	147.1	146.1 and 147.1	147.5	148.0
p	127.3	127.0	126.8	127.5	125.4
r	120.7	120.8[a]	121.4[a]	121.3[a]	121.6[a]
s	162.4	159.0	159.1	159.5	161.2
t, t′	174.7	175.1	174.6	175.1	175.4
u, u′	137.5	137.7	138.0 and 139.1	137.9	138.6

[a]Assignments not certain

3.4 Stability of F.F. diethanol (1) and diisopropanol (2) solvates

The stability of **1** and **2** was tested by spinning each sample at 5.0 kHz and recording a CPMAS and DPMAS spectrum every hour for 26 hours. Figures 3.20 and 3.23 shows the effect of MAS on **1** over this period. Figures 3.21 and 3.22 are expansions of Figure 3.20 to show the desolvation more clearly. It can be seen that after 26 hours the solvate has converted to **8**. It was noted that no intermediate product was seen to be formed during this conversion. A small amount of dihydrate was produced during this experiment which can be seen by the line marked at 16.2 ppm (Figure 3.20). It is suggested that the dihydrate was formed when the experiment was initially started using sealed rotor end caps. This rotor configuration does not allow solvent to exit or water to enter the rotor. The most stable solvate[2], the dihydrate, was formed probably from rearrangement of the residual water molecules within the system. When the experiment was restarted, using end caps which allowed the solvent to escape, the desolvation to **8** continued with no further increase in formation of the dihydrate.

The stability of **2** was tested in the same fashion (Figure 3.24 with expansions for Figures 3.25 and 3.26) and again the solvate formed **8** over a similar period (25 hrs).

3.5 Stability of F.F. dibenzyl alcohol solvate(4)

Solvate (4) was allowed to stand for 21 days with spectra taken at intervals to see the effect of drying (see Figure 3.27). It was shown that on standing in air the solvent is replaced by water molecules and converts to the dihydrate. No indication of the formation of an anhydrate was observed. It is proposed that water in the solvent aids the formation of **8** by stabilising the crystal structure as the solvent is released. **4** probably has the least water in the solvent as benzyl alcohol has the lowest miscibility with water (4 g/100 ml)[3] and it also has a high boiling point (205 °C). The boiling point slows the desolvation by evaporation and the low miscibility restricts the amount of water available to form **8**.
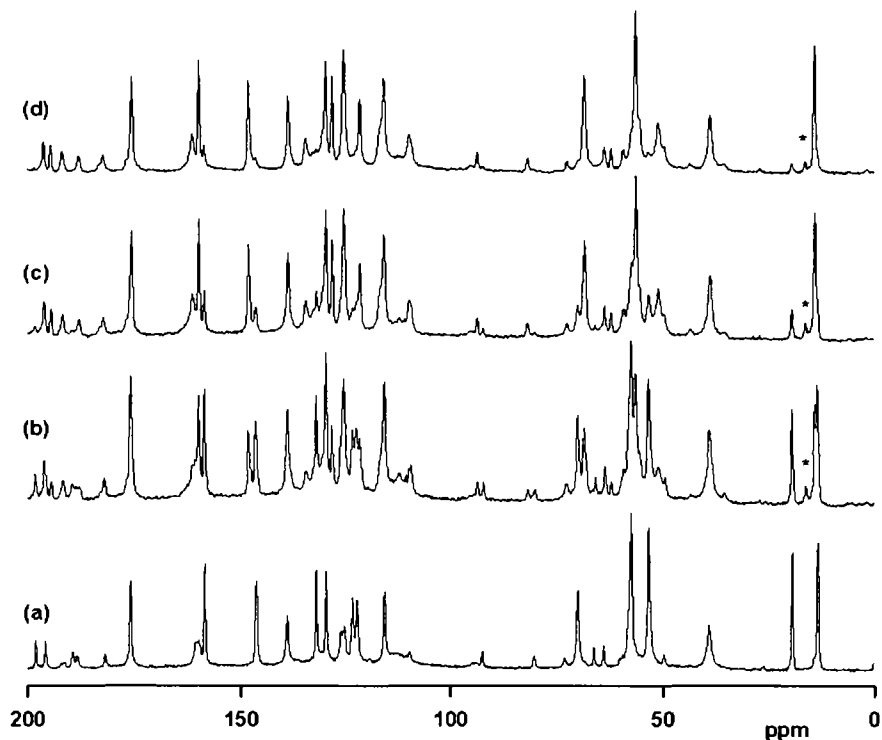
Figure 3.20. Formoterol fumarate diethanol solvate ^{13}C CPMAS spectra versus time (a) 1 hr, (b) 9 hrs, (c) 17 hrs (d) 25 hrs.
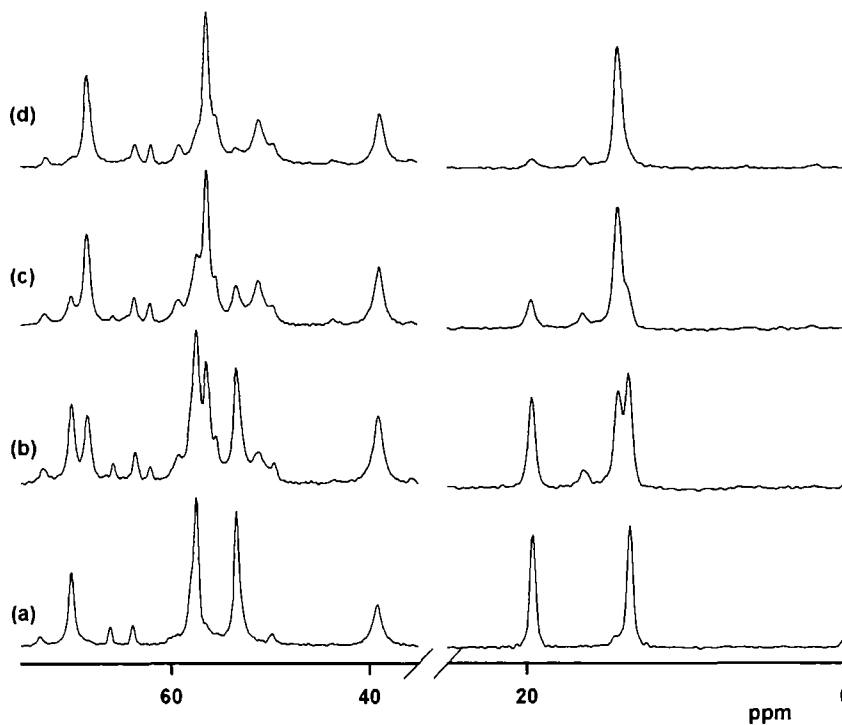

Figure 3.21. Formoterol fumarate diethanol solvate ^{13}C CPMAS spectra (a) 1 hr, (b) 9 hrs, (c) 17 hrs (d) 25 hrs. Note this is an expansion of Figure 3.20.
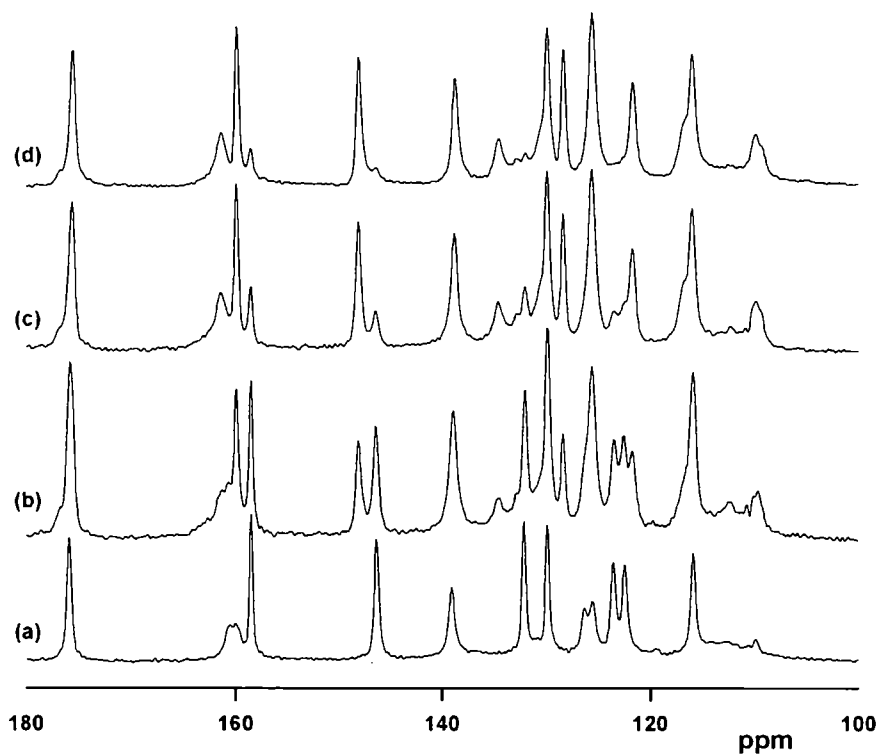
Figure 3.22. Formoterol fumarate diethanol solvate ^{13}C CPMAS spectra (a) 1 hr, (b) 9 hrs, (c) 17 hrs (d) 25 hrs. Note this is an expansion of Figure 3.20.
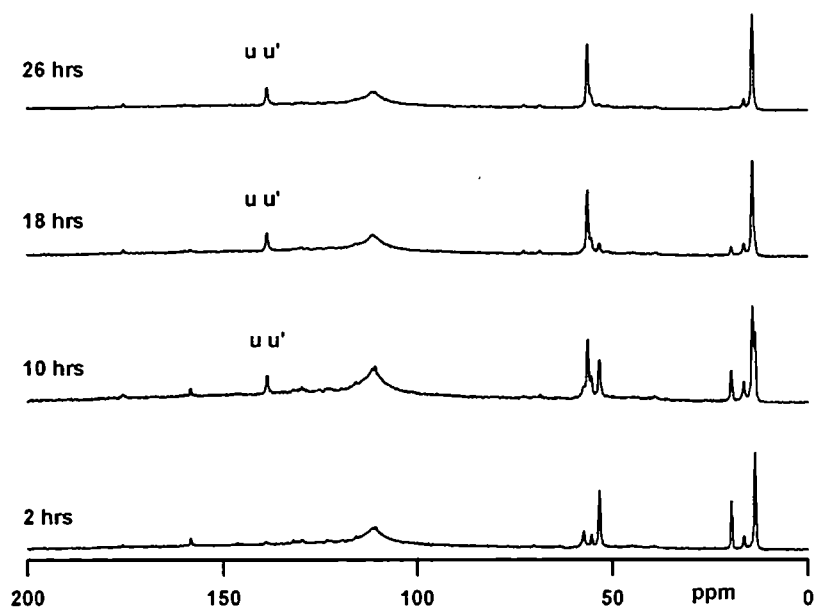

Figure 3.23. Formoterol fumarate diethanol solvate ^{13}C DPMAS spectrum.

Figure 3.24. Formoterol fumarate diisopropanol solvate ^{13}C CPMAS spectra (a) 1 hr, (b) 5 hrs, (c) 9 hrs (d) 15 hrs (e) 20 hrs (f) 25 hrs.

Figure 3.25. Formoterol fumarate diisopropanol solvate ^{13}C CPMAS spectra (a) 1 hr, (b) 5 hrs, (c) 9 hrs (d) 15 hrs (e) 20 hrs (f) 25 hrs. Note this is an expansion of Figure 3.24
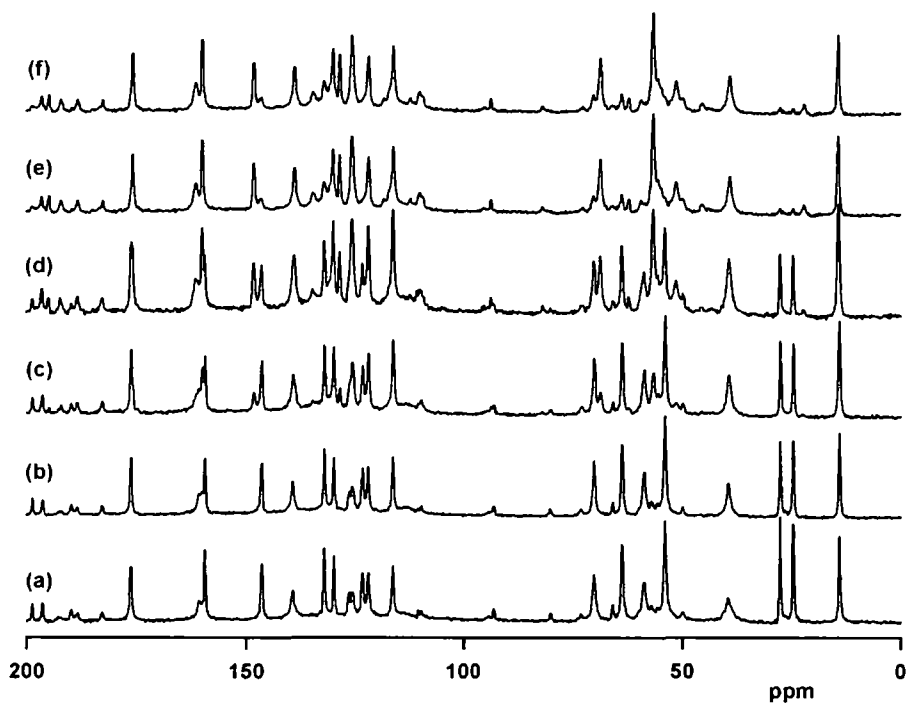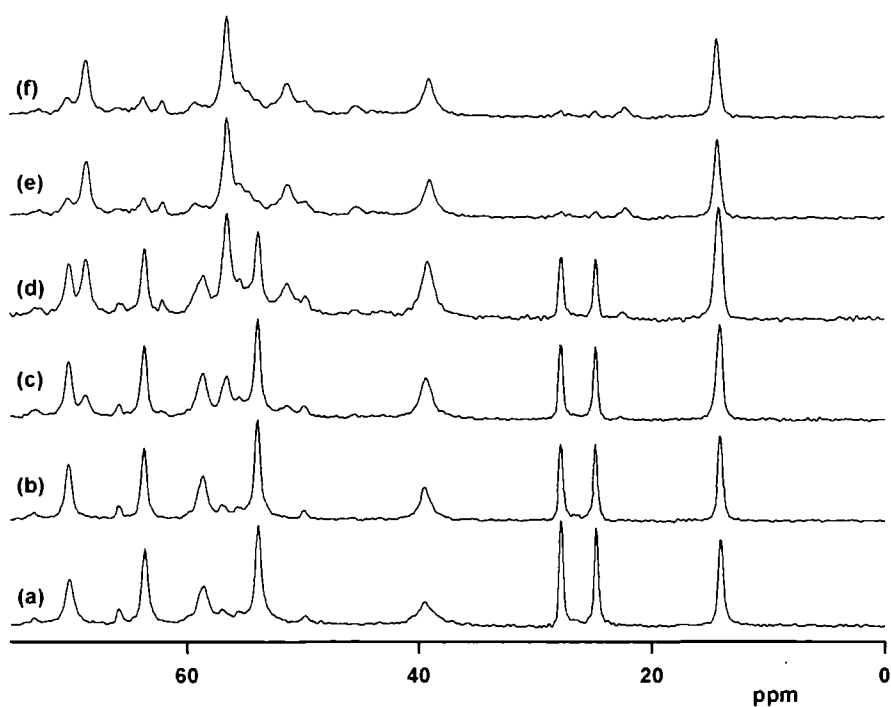
Figure 3.26. Formoterol fumarate diisopropanol solvate ^{13}C CPMAS spectra (a) 1 hr, (b) 5 hrs, (c) 9 hrs (d) 15 hrs (e) 20 hrs (f) 25 hrs. Note this is an expansion of Figure 3.24
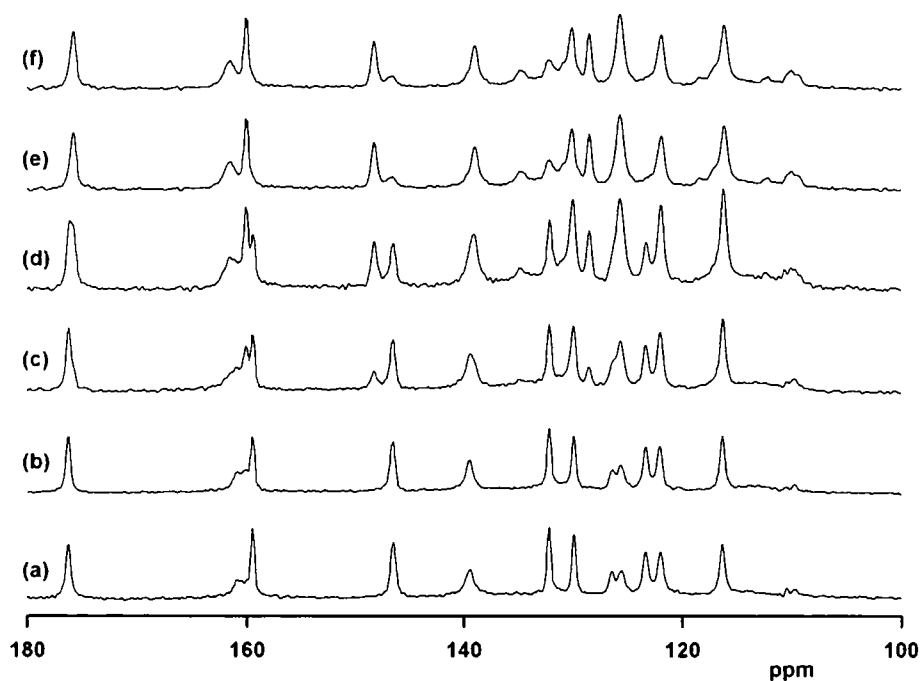
3.6 Stability of anhydrates A and B

Anhydrates A and B appear to be relatively unstable and were converted to the dihydrate on standing overnight in the laboratory in a relative humidity of 30-40%.

3.7 Stability of anhydrate C

8 was left in a relative humidity of 70% for 3 weeks and was unchanged after this time. It was only converted to the dihydrate after addition of 0.1 ml of water to 0.25 g of 8. These spectra are not shown. It is believed that hydrophobic areas are formed in the structure, which restrict water uptake[2].
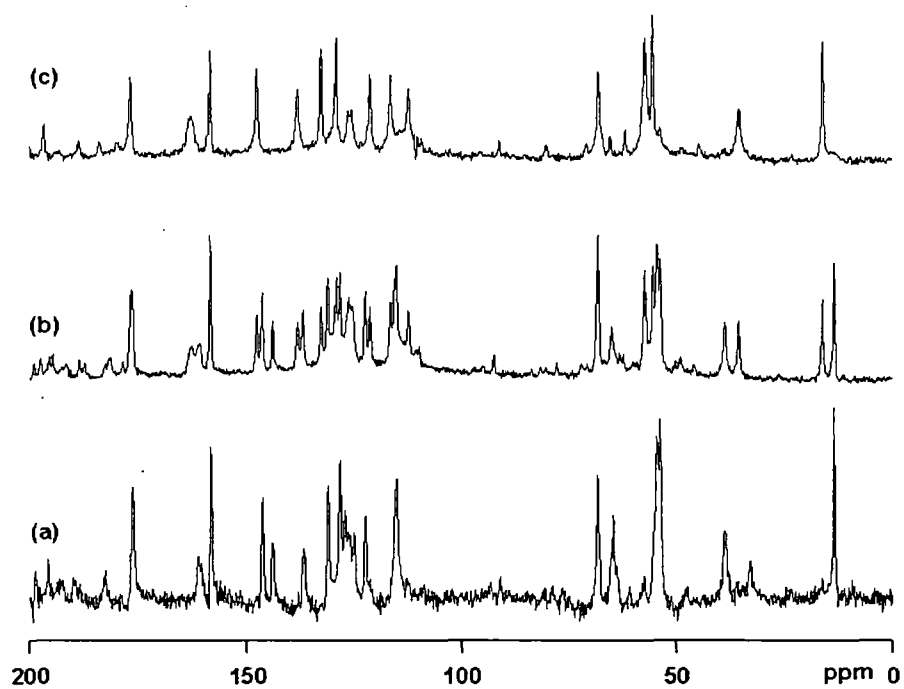
Figure 3.27. Formoterol fumarate dibenzyl alcohol solvate ^{13}C CPMAS spectra showing the desolvation to the dihydrate.
(a) 0 days, (b) 21 days , (c) formoterol fumarate dihydrate

3.8 Frequency Switched Lee-Goldburg Heteronuclear Correlation (FSLG-HETCOR) experiment

It has been demonstrated that 2D ^{1}H-^{13}C HETCOR NMR methods using a frequency switched Lee-Goldburg (FSLG) ^{1}H decoupling sequence at high MAS rates can provide intermolecular and spatial distance information[4]. The HETCOR spectrum often gives multiple proton cross peaks for each carbon, and these cross peaks can be extremely helpful in the spectrum assignment. Because, in this sequence, the mixing is accomplished during the Hartmann-Hahn contact time, with short mixing times (<100 µs), only strong correlations for directly bonded ^{1}H and ^{13}C atoms (^{1}H-^{13}C bond) can be obtained. On the other hand, when experiments are performed with a longer mixing time (500-1000 µs) long range ^{1}H-^{13}C spatial correlations can be obtained.[5]

The HETCOR experiments presented here were carried out to determine whether useful ^{1}H chemical shift information could be obtained from samples of this type. Observations from three measurements are listed in this chapter. The spectra illustrate that these techniques are potentially useful and that the measurements suggest potential future experiments.
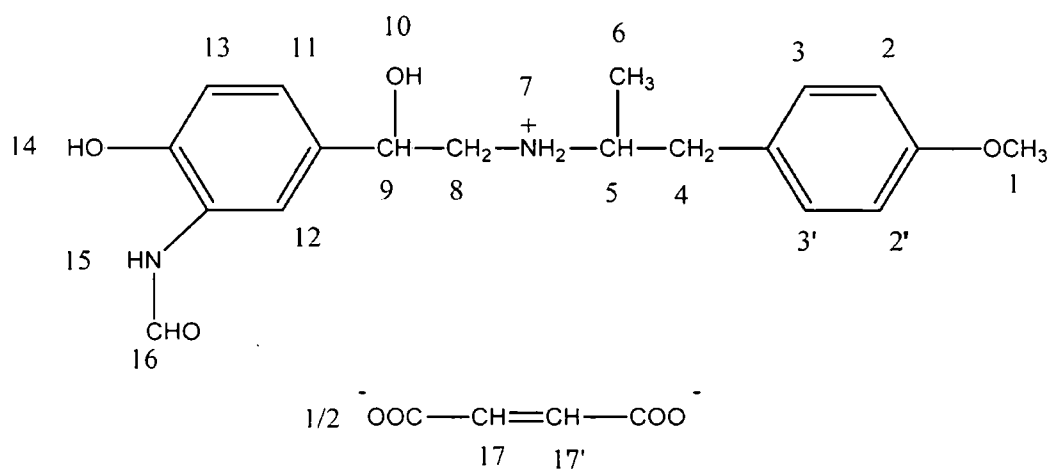
Scheme 2

3.9 *Formoterol fumarate anhydrate B (7)*

The resolution of the FSLG Hetcor experiment is a large improvement on the DPMAS ^{1}H spectra for the solvates/anhydrates (see Section 3.2). Using a contact time of 1 ms enables identification of most of the sample. From the spectra (see Figures 3.28, 3.29 and 3.30) the following information was obtained for anhydrate B. The methyl protons, **6** from scheme 2 are resolved at 0 ppm as are the methoxy protons **(1)** at 2-3 ppm. These protons **(1)** correlate with the carbon **(a)** at 56 ppm as do the aromatic protons **2** and **2'** at 6 ppm. The methylene protons **(4)** are seen at 2-3 ppm as well as the CH **(9)** proton at 4 ppm. Repeating the experiment with a longer contact time may determine the chemical shifts for i and g carbon atoms as a correlation with the methyl protons **(6)** for g carbon atom should be possible. The n carbon atom correlates to the aromatic proton **(13)** at 6 ppm. The c carbon atom correlates with its own proton **(2)**. The m carbon atom correlates with its own proton **(11)** at 6 ppm. The quaternary carbon atoms p, e, l, b and o all show correlations.

(a) The p carbon atom to NH **(15)** at 7-8 ppm *shown as a doublet* (due to residual dipolar coupling to the ^{14}N).

(b) The e carbon atom to methylene **(4)** at 2-3 ppm and aromatic CH's **3** and **3'** at 6 ppm.

(c) The l carbon atom to the aromatic CH **(12)** and also the CH **(9)**.

(d) The b carbon atom to the methoxy protons **(1)** at 1-2 ppm and aromatic CH's **(2 and 2')** at 6 ppm.

(e) The o carbon atom to OH **(14)** at 12 ppm which appears to be hydrogen bonded and the aromatic CH **(13)**.

The u and u' carbon atoms correlate to their own protons **(17 and 17')** at 6 ppm. The t carbon atom at 175 ppm correlates to the OH **(14)** at 12 ppm indicating it to be hydrogen bonded.
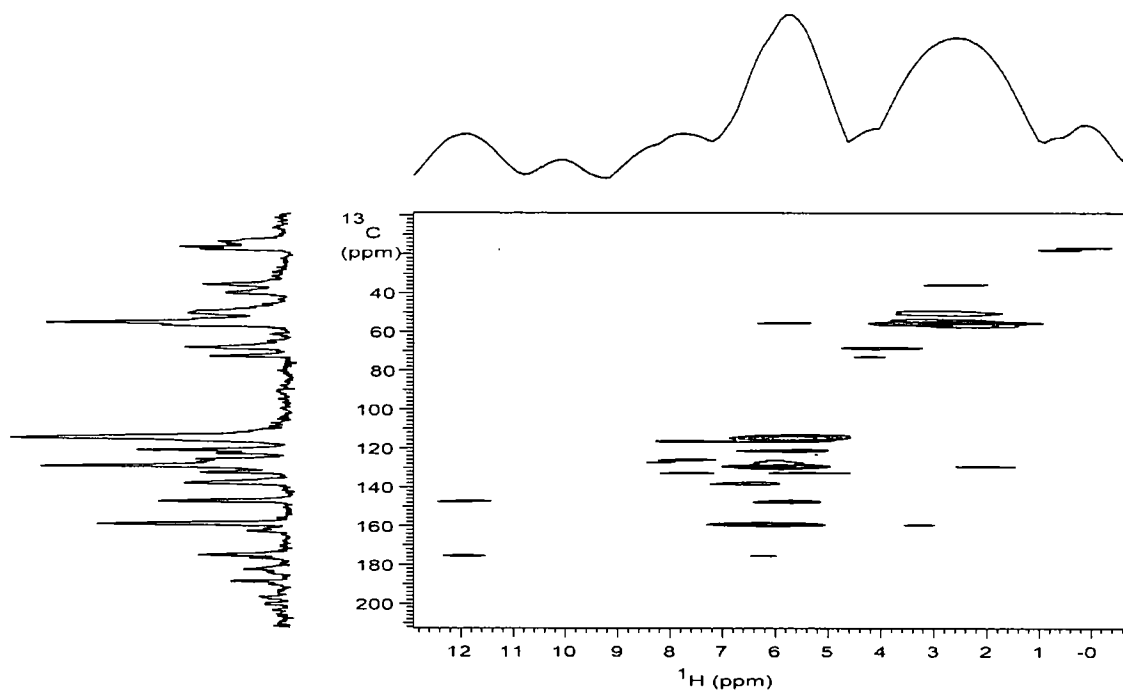
Figure 3.28. Formoterol fumarate anhydrate B, 2D ^{1}H-^{13}C HETCOR, contact time 1 ms
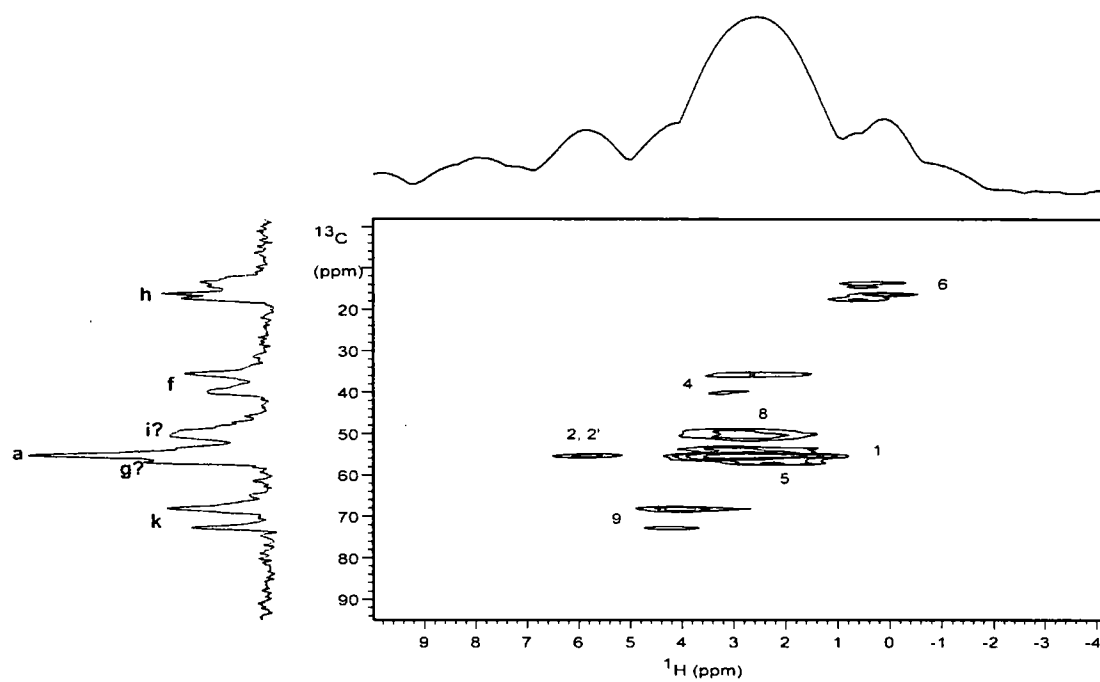

Figure 3.29. Formoterol fumarate anhydrate B 2D ^{1}H-^{13}C HETCOR, contact time 1 ms
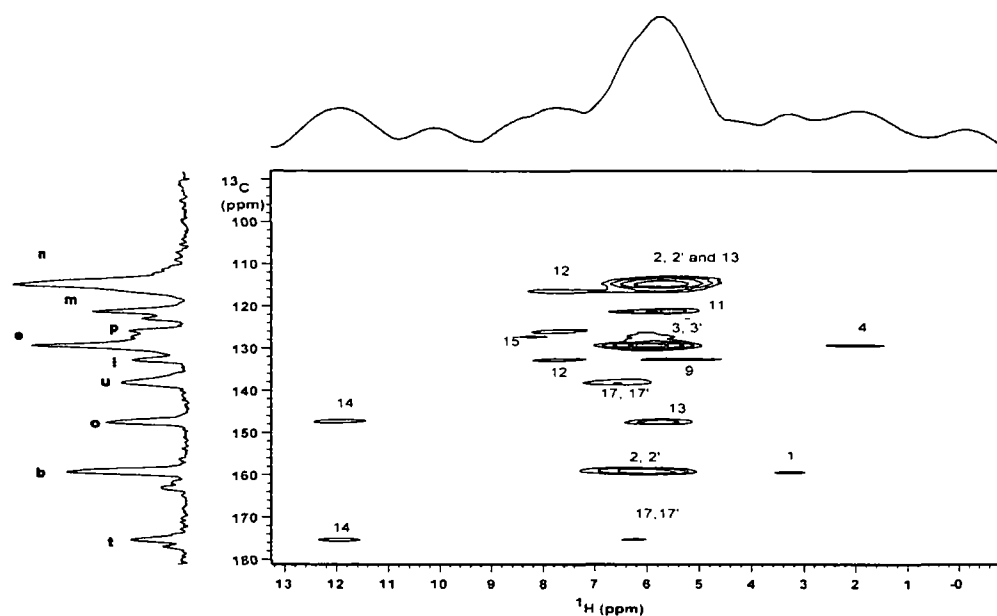
Figure 3.30. Formoterol fumarate anhydrate B 2D ^{1}H-^{13}C HETCOR, contact time 1 ms

3.10   Formoterol fumarate dihydrate (5)

The contact time for this experiment was shortened to 0.1 ms and only directly bonded protons were detected (see Figures 3.31, 3.32 and 3.33). The methyl protons (6) are resolved at -1 ppm as are the methoxy protons (1) at 0-2 ppm.* The methylene protons (4) are seen at 0-2 ppm as well as the CH protons (9) at 3-4 ppm. The quaternary carbon atoms having no directly bonded protons show no correlations. The aromatic carbons m, r and n show correlations to their own aromatic CH's (11, 12 and 13) at 4-7 ppm. The u and u' carbon atoms correlate to their own protons (17 and 17') at 6-8 ppm. The s carbon atom at 163 ppm correlates with the NH (15) at 7-8.5 ppm. There is no correlation for the t carbon atom at 175 ppm

* In this experiment the ^{1}H shift axis is scaled using glycine. It is difficult to determine precisely the scaling factor and absolute referencing in this indirect dimension.
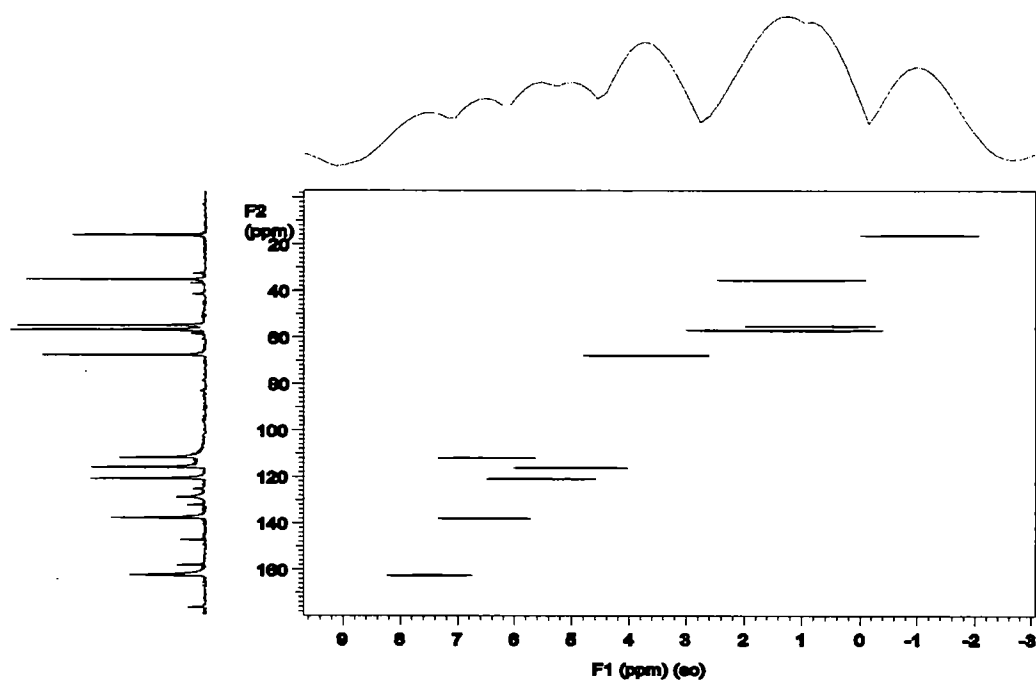
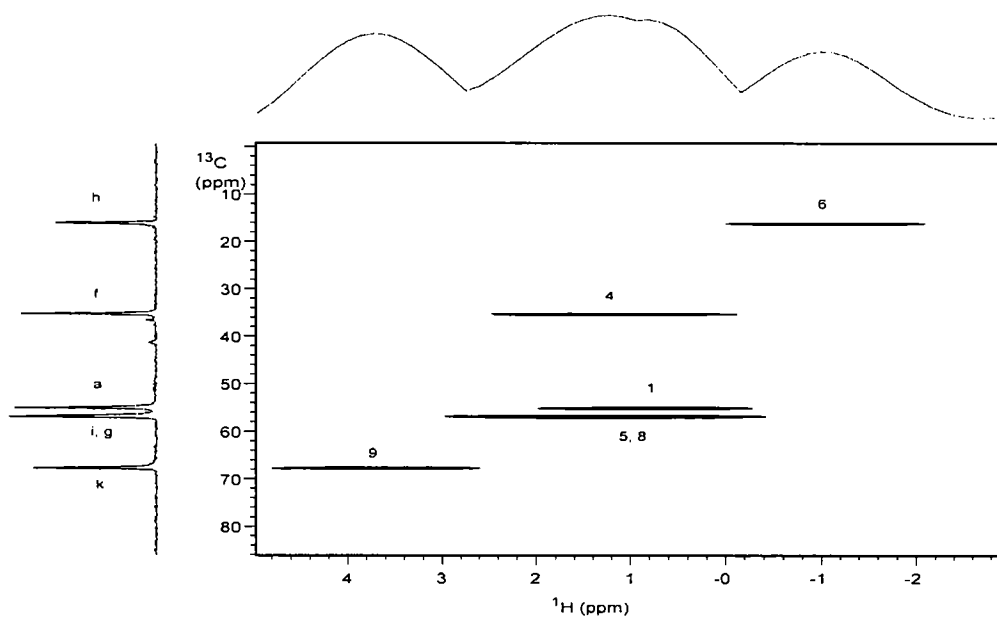Figure 3.31. Formoterol fumarate dihydrate 2D ¹H-¹³C HETCOR, contact time 0.1 ms

Figure 3.32. Formoterol fumarate dihydrate 2D ¹H-¹³C HETCOR, contact time 0.1 ms
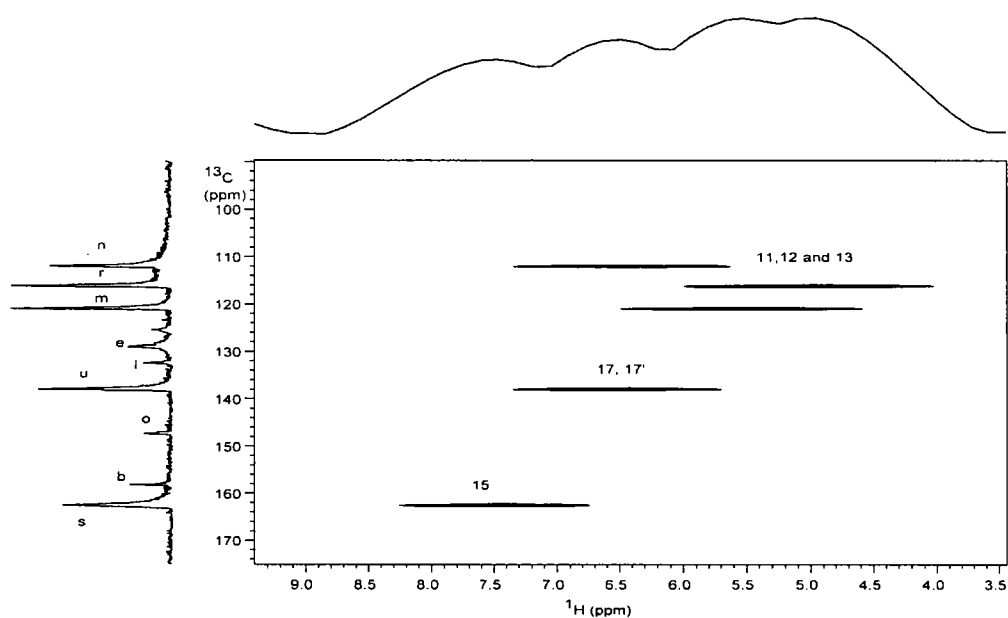
Figure 3.33. Formoterol fumarate dihydrate 2D ^{1}H-^{13}C HETCOR, contact time 0.1 ms

3.11   Formoterol fumarate anhydrate C (8)

The methyl protons (6) are resolved at 2 ppm (see Figures 3.34, 3.35 and 3.36) as are the methoxy protons (1) at 2-4 ppm. The methylene protons (4) are seen at 2-4 ppm. The CH (5) at 4 ppm and aromatic CH's 3 and 3' at 7 ppm correlate with the carbon f at 38 ppm. The CH proton (9) at 5-6 ppm and the OH (10) at 7-8 ppm correlate with the carbon atom k at 48 ppm. The unresolved i and g carbon atoms show a correlation to NH$_2^+$ (7 ppm) and the methyl (6) at 2 ppm. It can be seen that the aromatic CH's 2 and 2' and 3 and 3' are resolved at 6 and 7 ppm and 6.5 and 7.5 ppm respectively.

The quaternary carbon atoms p, l and b all show correlations.

    (a) The p carbon atom to NH (15) at 7-8 ppm.

    (b) The l carbon atom to the aromatic CH's (11) and (12) at 7 ppm.

    (c) The b carbon atom to the aromatic CH's (2 and 2') at 7 ppm.

The aromatic CH (13) is seen at 7 ppm as is (12) also at 7 ppm. The s carbon atom at 160 ppm correlates with the formamide proton (16) at 3 ppm.

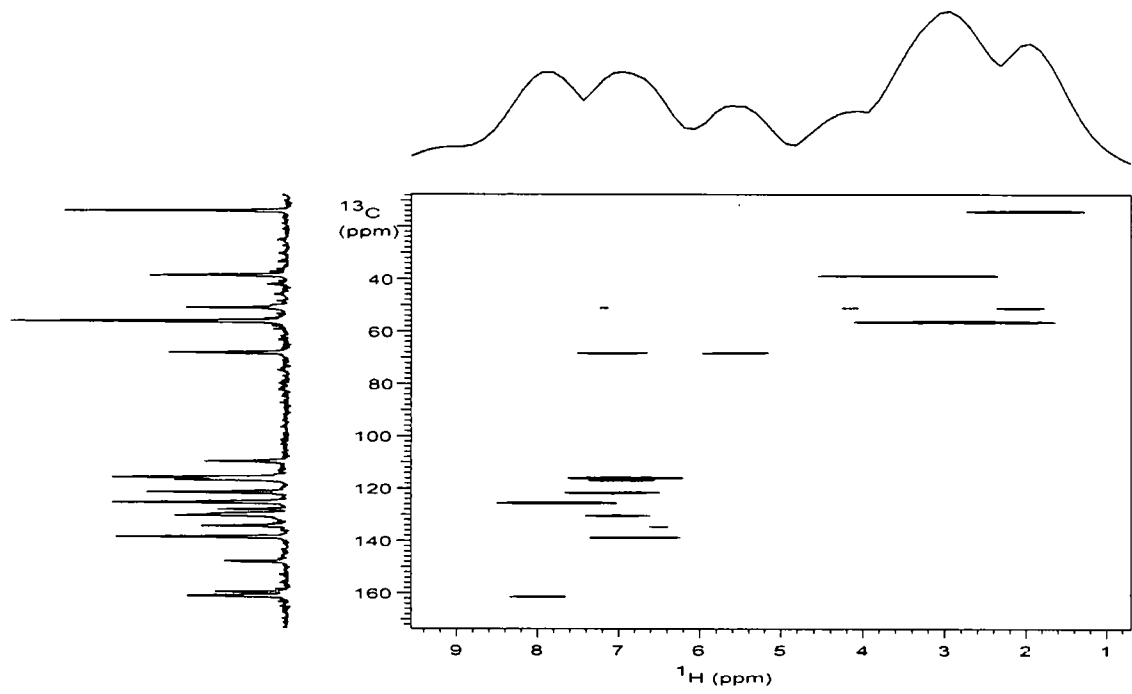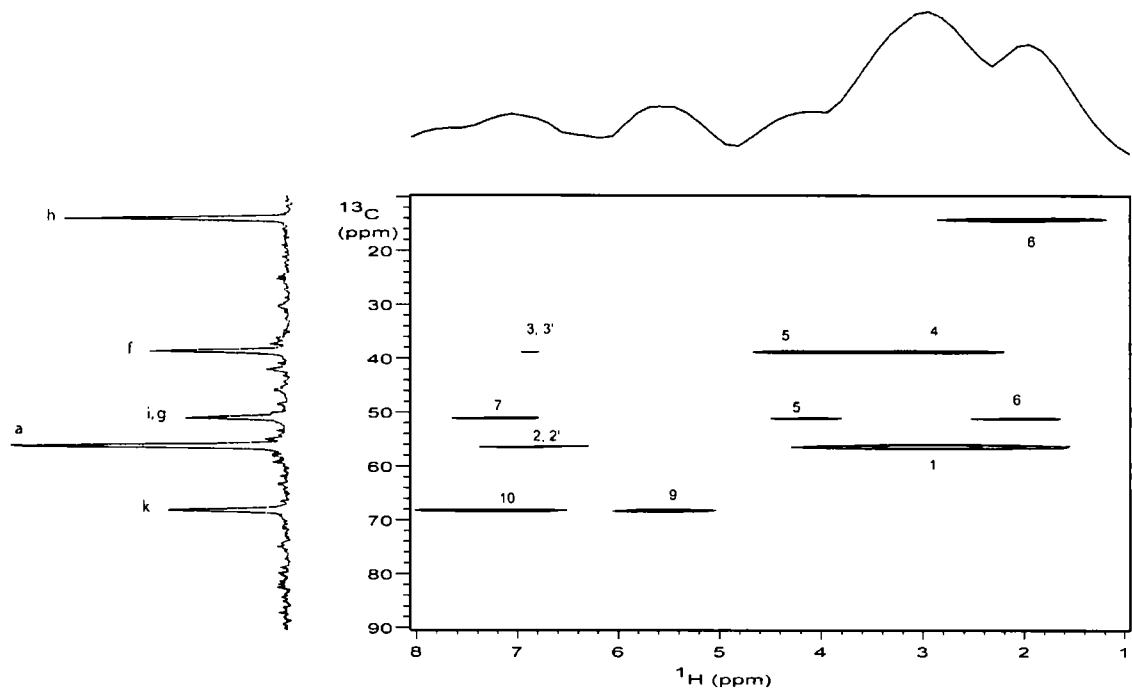**Figure 3.34. Formoterol fumarate anhydrate C 2D ¹H-¹³C HETCOR, contact time 1 ms**

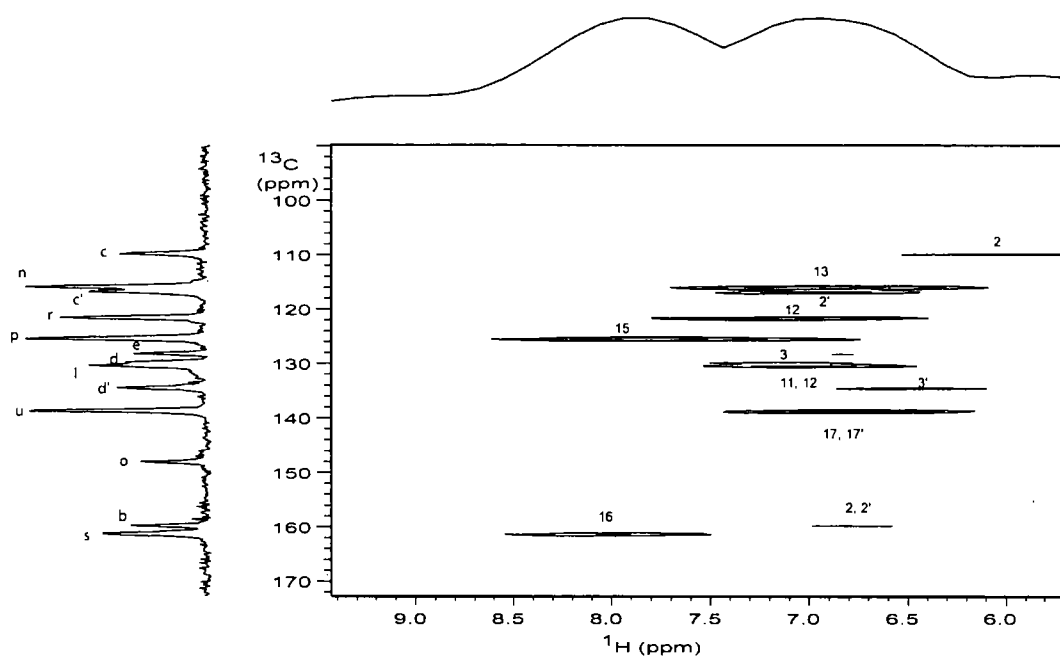**Figure 3.35. Formoterol fumarate anhydrate C 2D ¹H-¹³C HETCOR, contact time 1**

Figure 3.36. Formoterol fumarate anhydrate C 2D ¹H-¹³C HETCOR, contact time 1 ms

3.12   *Conclusions*

(a) Solvates

Spectra have been obtained for each of the three solvates diethanol (**1**), diisopropanol (**2**) and dibenzyl alcohol (**4**) and, with the aid of solution-state data and dipolar dephasing experiments, carbon-13 spectral assignments have been made. It was observed that the lines at 24.4 and 27.4 ppm from **2** were those of the two methyl groups from a partially bonded solvent molecule. This indicates they are inequivalent and experiencing different shielding effects when the solvent interacts with the drug molecule.

It was shown that **1** and **2**, are relatively stable to MAS but do gradually convert to anhydrate C (**8**). **4** is more stable than the other two solvates, eventually desolvating to the dihydrate on standing, probably due to the higher boiling point of benzyl alcohol and lower solubility in water.

So far, one-dimensional ^{1}H spectra have not proved useful but Frequency Switched Lee-Goldburg Heteronuclear Correlation (FSLG-HETCOR) experiments show better resolution and with longer contact times the i and g carbon atoms should be identified in anhydrate B (**7**). It was shown using a short contact time (0.1 ms) only ^{1}H-^{13}C correlations between directly bonded protons were observed in **5**. Longer range correlations were seen for **7** and **8** using a 1 ms contact time.

^{15}N CPMAS on the **1**, **5** and **8** have shown some differences in NH chemical shifts.

(b) Anhydrates/dihydrates

The dihydrate (**5**), anhydrate A (**6**), anhydrate B (**7**) and anhydrate C (**8**) have been prepared and spectra obtained, again with the aid of solution-state data and dipolar dephasing experiments carbon-13 spectral assignments have been made where possible.

It was also shown that each sample was different. The relative line widths of the anhydrates suggest that there is a degree of disorder in anhydrate B (7). The ^{13}C CPMAS dipolar dephasing experiment (see Figure 5.5, Chapter 5) was performed from -80 °C upto 100 °C with no apparent change in line widths. This suggests the disorder is static but further ^{13}C CPMAS experiments at variable temperature should confirm this.

Anhydrate C (8) can only be formed by desolvating 1 and 2.

Future work

(a) An FSLG-HETCOR experiment with a long (>1 ms) contact time could characterise carbon atoms i and g for 7.

(b) ^{13}C CPMAS VT experiments may determine if the disorder in 7 is static or dynamic.

(c) Desolvating the solvates under pressure may give information on the effect this may have on the formation of 8.

3.13 References

1. Apperley DC, Harris RK, Larsson T, Malmstrom T, Quantitative Nuclear Magnetic Resonance Analysis of Solid Formoterol Fumarate and Its Dihydrate, *Journal of Pharmaceutical Sciences*, 2003, 92(12), 2496-2503

2. Jarring K, Larsson T, Stensland B, Ymen I, Thermodynamic Stability and Crystal Structures for Polymorphs and Solvates of Formoterol Fumarate, *Journal of Pharmaceutical Sciences*, 2005, 95(5), 1144-1161

3. CRC handbook of Chemistry and Physics, ed Weast RC, Chemical Rubber Publishing Company, 1984, C168-C169

4. Lee M, Goldburg WI, *Phys. Rev. A*, 1965, 140 1261

5. Van Rossum BJ, De Groot CP, Ladizhansky V, Vega S, De Groot HJM, A Method for Measuring Heteronuclear (^{1}H-^{13}C) Distances in High Speed MAS NMR, *J Am. Chem. Soc.*, 2000, 122(14), 3465-3472

4.1   *Methoxy benzene ring-flips in the solvates*

Formoterol fumarate contains a methoxybenzene ring as well as a methyl group. In solids, motion still takes place and rotational diffusion of the methyl group and π rotation of the methoxybenzene ring is possible. The appearance of the spectrum depends on the rate of rotation relative to the frequency difference of the appropriate signals in the absence of rotation. At higher temperatures methoxy ring rotation may occur quickly, in the order of μs, and in this case only two lines may be observed in the spectrum from carbon atoms c, c' and separately d, d' (see scheme 1 in chapter 3). If the rotation rate is slowed down (< 10 ms) on cooling then four lines may be observed. A flat topped, unresolved spectrum of, say, c and c' may be observed at a temperature between 50 °C and 80 °C for anhydrate C (see Figure 4.1), and is called the coalescence temperature[1]. From the coalescence temperature (see equation page 62) an exchange rate can be calculated.
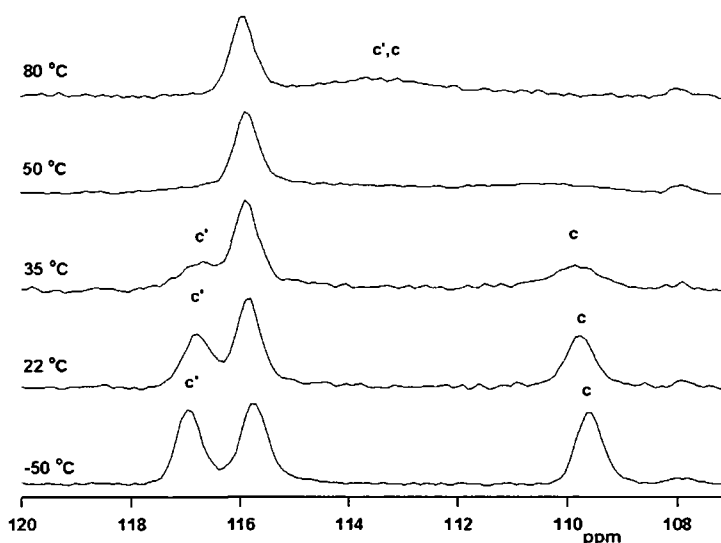
Figure 4.1 ^{13}C CPMAS spectra, coalescence temperature of formoterol fumarate anhydrate C between 50 °C and 80 °C

Diethanol solvate **(1)** was examined from -80 °C to 20 °C (see Figure 4.2). At low temperature a signal is observed at 108 ppm and this is assigned to carbon c or c', (c'/c) occurs under the signal at 115 ppm (see Table 1, Chapter 3). As the temperature

is increased the line broadens and eventually the c and c' signals coalesce[1]. The coalescence temperature was found to be between 0 and 20 °C. Knowledge of the coalescence temperature gives information on the exchange rate (see below). A detailed analysis of the band shape can yield exchange rates at other temperatures but does require a spectrum free from any interfering signals. Spectra were not obtained at higher temperatures due to desolvation.
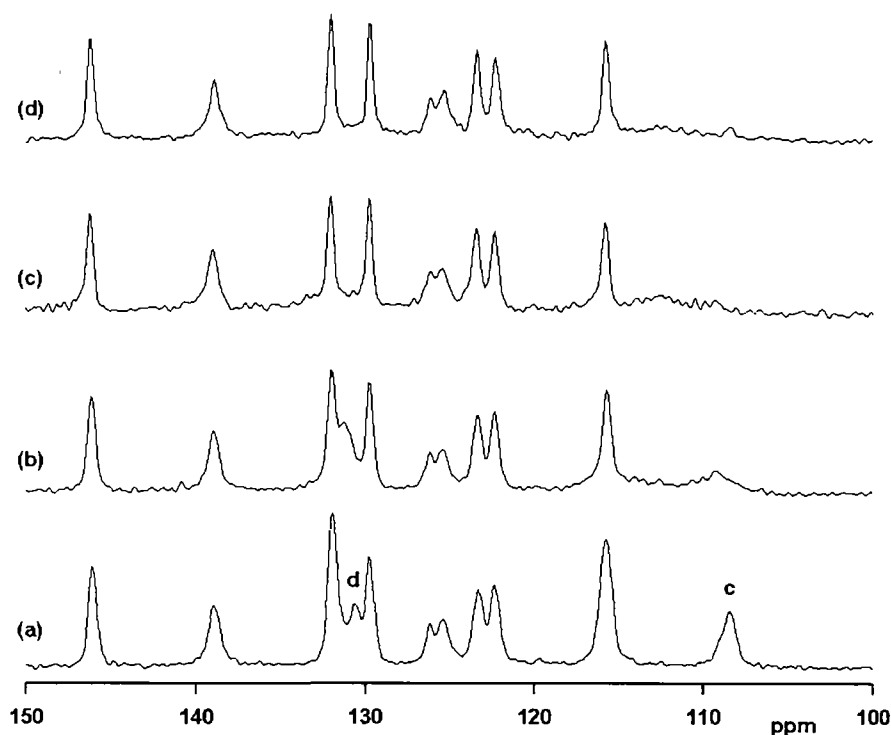

Figure 4.2. Formoterol fumarate diethanol solvate ^{13}C CPMAS spectra (a) -80°C, (b) -50°C , (c) 0 °C, (d) 20 °C

Diisopropanol solvate (2) was also examined from -80 °C to 10 °C and from these data it was shown that the coalescence temperature was between 0 °C and 10 °C for carbon atoms c and c' (see Figure 4.3). Unlike 1 the carbon atoms c and c' were

resolved at -80 °C. But carbon atoms d and d′ were not fully resolved so their coalescence temperature could not be determined. At -80 °C the separation between c and c′ is 848 Hz and from this the exchange rate was calculated (assuming a 180° ring flip) for the methoxy benzene ring-flip from the equation below:
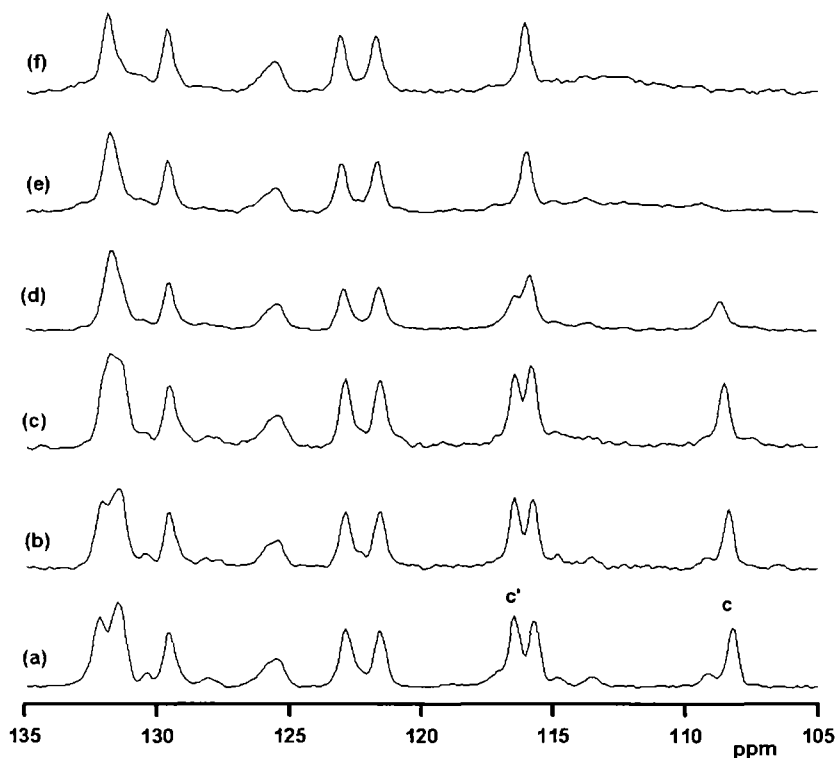
Figure 4.3. Formoterol fumarate diisopropanol solvate ^{13}C
CPMAS spectra (Varian VNMRS 400)
(a) -80°C, (b) -60°C , (c) -40 °C, (d) -30 °C, (e) 0 °C (f) 10 °C

$$\tau^c = \sqrt{2}/\pi \, | \nu_c\text{-}\nu_{c'} |$$

where τ^c is the lifetime of the ring in one environment at the coalescence temperature and $\nu_c\text{-}\nu_{c'}$ is the frequency difference (in Hz) of the lines corresponding to c and c′

τ^c = 0.53 ms (or an exchange rate of 1900 s^{-1}) at 0 °C to 10 °C

The two methyl groups in the propanol solvent were also resolved in the spectrum

for **2** (see Figure 4.4). The variable temperature work made it possible to calculate the

coalescence temperature (between 70 and 80 °C) of these methyl group signals. From

this the exchange rate was calculated and found to be 1050 s^{-1} at this temperature.
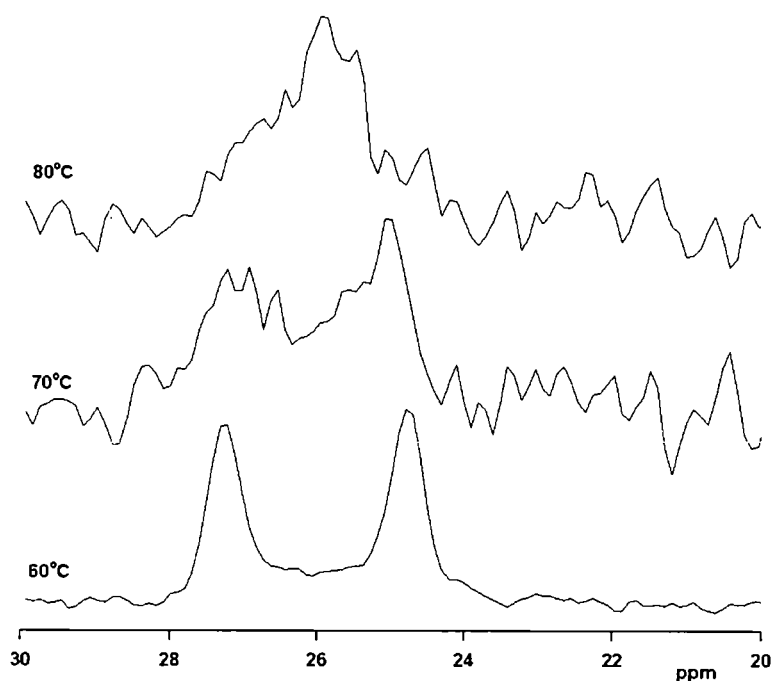
**Figure 4.4. Formoterol fumarate diisopropanol solvate ^{13}C
CPMAS spectra (Varian VNMRS 400) normalised spectra.
(a) 60 °C, (b) 70 °C , (c) 80 °C**

4.2 *Methoxy benzene ring-flips in the anhydrates*

Anhydrate B **(7)** was examined between -80 and 100 °C (see Figure 4.5). The general

behaviour of the line at 115 ppm is the same as that expected for a line above the

coalescence temperature. We know from a dipolar dephasing experiment that the

ring must be moving (carbon c/ c′ are not suppressed). However, we cannot obtain

Figure 4.5 Formoterol fumarate anhydrate B ^{13}C dipolar
dephased spectra.
Note change in behaviour of the line at 115 ppm.

spectra at a temperature below the coalescence so we cannot prove that this is a 180°

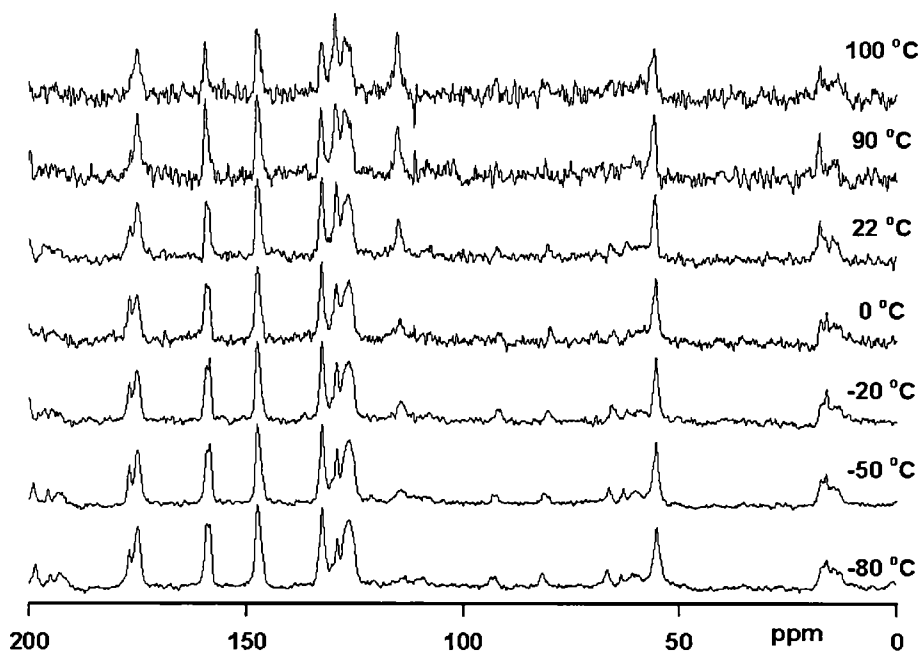ring flip. There are other reasons why lines might broaden although they all require

some dynamic process. An effect similar to *rotary resonance recoupling*[2] can occur if the

frequency of the molecular motion approaches that of the spinning speed of the

sample. This will interfere with the ability of MAS to remove CSA and line

broadening will occur. If the frequency of the molecular motion approaches that of

the nutation rate of the rf decoupling field then ^{1}H-^{13}C dipolar recoupling could occur

and result in line broadening. The apparent coalescence temperature for **7** was

shown to be around -80 °C. Comparing with anhydrate C (**8**), which has a

coalescence temperature of between 50 °C and 80 °C, it shows that if this is a real

coalescence temperature the methoxy ring rotation has increased in speed (at room

temperature) in **7**. This could be due to the fact that there is no solvent or water in the

crystal structure hindering the ring rotation.

Anhydrate C (**8**) was examined between -50 and 80 °C (see Figure 4.6). The spectra

show resolution of c and c' carbon atoms at room temperature. This, combined with

the coalescence temperature for **8** of between 50 °C and 80 °C, shows that the

methoxy ring rotation has slowed in comparison to the solvates **1** and **2** at room

temperature.

This could be caused by a small reduction in the size of the structure, sufficient to

restrict ring rotation. From variable temperature measurements the exchange rate

was calculated and found to be 1650 s^{-1} at between 50 °C and 80 °C.

A VT experiment on **8** showed a possible coalescence temperature of -95 °C for u and

u′ carbon atoms on the fumarate ion (see Figure 4.7). Because of the possibility of an

effect similar to rotary resonance recoupling taking place (see above) the decoupling

power and spin rates were changed and the data plotted against the line width for

the u and u′ carbon atom in the spectra (see Figures 4.8). No unexpected changes in

line widths were noted.
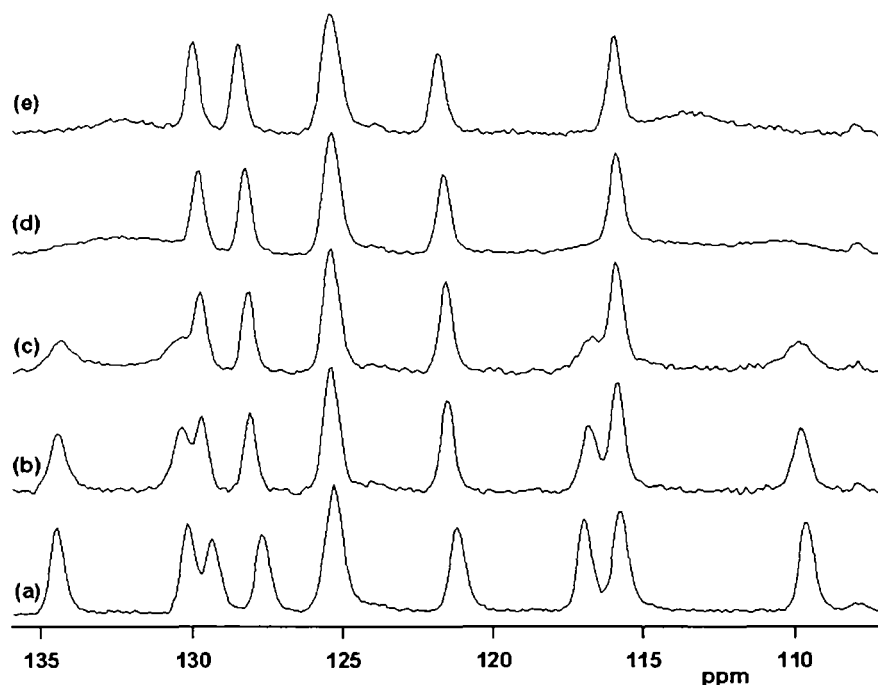
**Figure 4.6. Formoterol fumarate anhydrate C ^{13}C CPMAS
spectra (Varian VNMRS 400)**
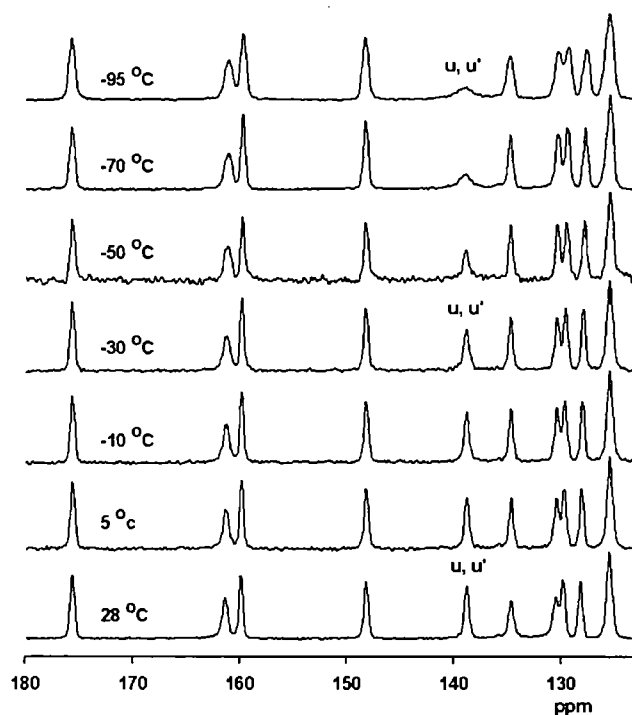**(a) -50 °C, (b) 22 °C, (c) 35 °C, (d) 50 °C , (e) 80 °C**

Figure 4.7. Formoterol fumarate anhydrate C ^{13}C CPMAS
spectra (Varian VNMRS 400) VT experiments from -95 °C to 28
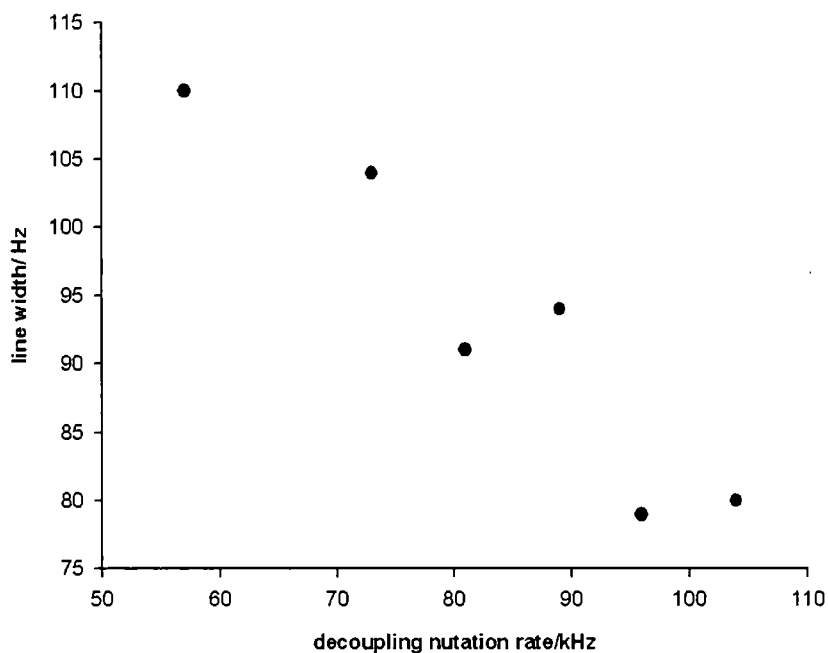°C showing broadening of the u, u' carbon signal

Figure 4.8 Formoterol fumarate anhydrate C (Varian VNMRS
400) line width (Hz) of u, u' carbon signal versus decoupling
strength

Chapter 4   MOLECULAR MOTION:RELAXATION AND EXCHANGE
MEASUREMENTS

4.3 ^{13}C T_1 *measurements*

In the DPMAS stability experiment (see Section 3.4) u ^{13}C atom was seen to become more mobile after 10 hours as the anhydrate C was formed (Figure 3.23) for both **1** and **2**. The outcome from this is that the u carbon atom relaxes more quickly in **8**. Providing the system is on the low temperature side of the T_1 minimum (see Section 4.5) then this implies that the mobility of this carbon atom on the fumarate ion increases as **8** is produced. This may indicate the loss of the hydrogen bonding between the solvent and the fumarate ion, allowing more freedom of movement for the fumarate ion once the solvent is removed. Because of this result it was decided to look at the ^{13}C T_1 measurements in detail to get a better understanding of the mobility of the carbon atoms in the drug molecule.

Thus ^{13}C T_1 measurements were obtained for **2, 4, 6** and **8** using the method of Torchia[3].

Tables 1 and 2 show the T_1 values obtained. The data shows that the T_1 for the u carbon atom in **8** decreases in magnitude, by a factor of approximately 15, relative to **2, 4** and **6**, suggesting an increase in the mobility of the fumarate ion. The experiment was repeated using different temperatures and the activation energy for the motion of the fumarate ion was calculated as 14 kJ mol^{-1} from an Arrhenius plot (see Figure 4.9). T_1 data for the t carbon atom also shows a similar trend in increased mobility with increased temperature. The a and h carbon atoms, being methoxy and methyl carbon atoms, are mobile and have low T_1 values. To further investigate this, deuterium-labelled formoterol fumarate was crystallised from deuterium-labelled fumaric acid and formoterol base.

Table 1 ^{13}C T_1 data for solvates and anhydrates

C atom	2 T_1 s^{-1}	4 T_1 s^{-1}	6 T_1 s^{-1}	8 T_1 s^{-1}
t	94	65	79	21
b	77	101	56	67
o	93	112	47	76
u	17	23	29	1.4
l	60	111	32	43
e	70		33	40
p d,d	56			49
r	39	64	57	38
c,n	69			34
c	43	74	32	29
k	43		38	18
a	4.3	2.6	2.7	1.3
f	37	23	25	18
h	0.9	4.3	0.7	0.5

Table 2 ^{13}C T_1 data for anhydrate C (8)

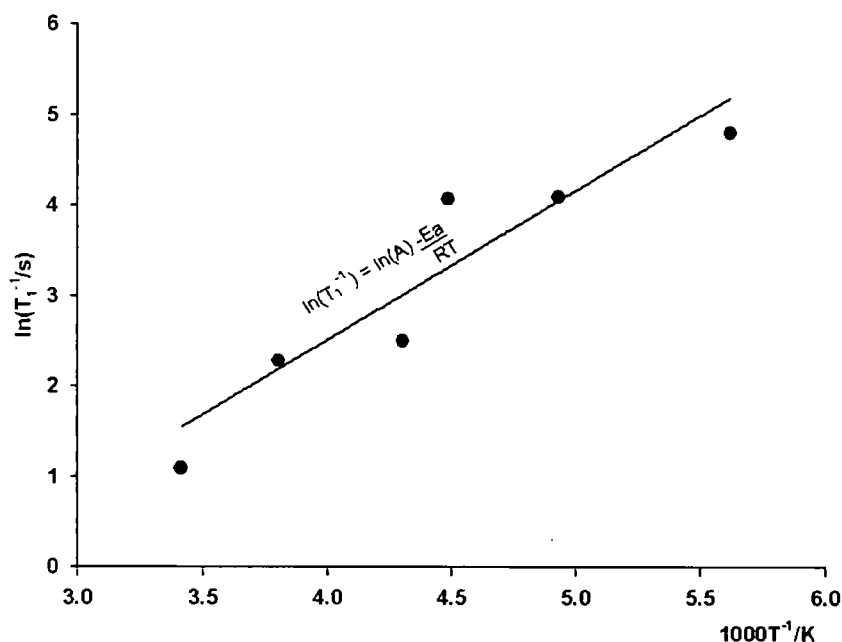| C atom	-95 °C T_1 s^{-1}	-70 °C T_1 s^{-1}	-50 °C T_1 s^{-1}	-40 °C T_1 s^{-1}	-10 °C T_1 s^{-1}	20 °C T_1 s^{-1}
t	110	117	128	95	88	31
s	47	41	38	32	34	104
b	28	33	69	55	52	98
o	106	91	72	85	119	22
u	123	61	59	12	9.8	3.0
d'	55	47	37	44	45	58
c	71	54	39	37	65	40

Figure 4.9 Formoterol fumarate anhydrate C (Varian VNMRS 400). Arrhenius plot showing ^{13}C T_1 relaxation behaviour as a function of temperature. The solid line is a least squares fit for the equation shown where R- gas constant
T- temp
A- constant (the pre exponential factor)
Ea- Activation energy

4.4 $^2H\ T_1$ measurements and band shapes

Formoterol fumarate anhydrate A with the u carbon atoms labelled with deuterium (11) was prepared as described earlier (see Section 2.17). Direct measurement of T_1 was not possible for this compound as the signal-to-noise was too low using DP methods, suggesting that the T_1 is very long. The deuterium spectrum was recorded and shown in Figure 4.10b using a CPMAS experiment. This indicates it to be a fairly rigid solid[4] as the band shape is similar to fumaric acid which is typical of a rigid solid (Figure 4.11).
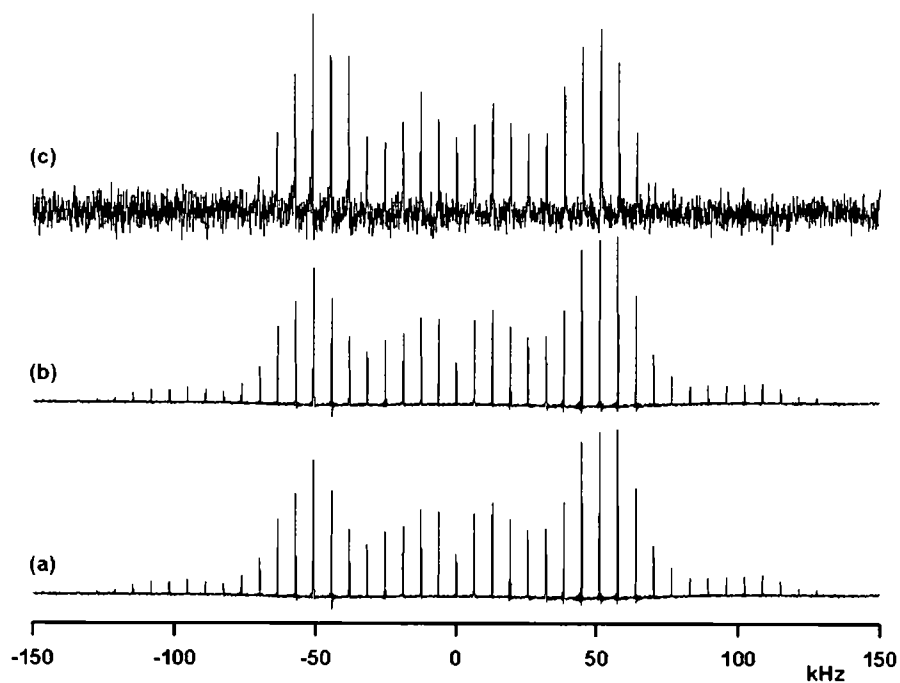
Figure 4.10 Formoterol fumarate anhydrate C (Varian VNMRS 400)
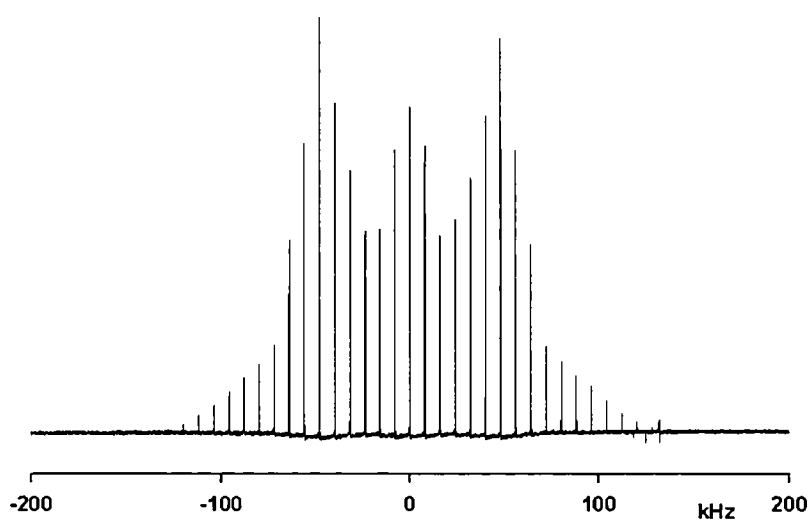(a) dihydrate ^{2}H CPMAS, (b) anhydrate A ^{2}H CPMAS,
(c) anhydrate C ^{2}H DPMAS

Figure 4.11 Fumaric acid ^{2}H CPMAS spectrum spin rate 8 kHz

Deuterated anhydrate (**11**) was converted on standing in the laboratory overnight to the dihydrate. The ^{2}H T_1 was measured for this compound and found to be 9 seconds. The deuterium spectrum, recorded using a CPMAS experiment, is shown in Figure 4.10a. The band shape is very similar to **11**, indicating it to be a rigid solid.

The dihydrate was then converted to the diethanol solvate by slurrying with ethanol. The resultant solvate was allowed to dry overnight to form the formoterol fumarate anhydrate C. It was possible to record a DPMAS spectrum with a short recycle delay (0.1 s) showing that the ^{2}H relaxation time had dropped dramatically from **11** (see Figure 4.10c). This spectrum was obtained *after several minutes* whereas the CP spectra were obtained over 16 hrs. Variable temperature DPMAS measurements of the deuterium spectrum for the formoterol fumarate anhydrate C showed no variation with temperature (see Figure 4.12). This indicates that the fumarate ion does not undergo fast, isotropic reorientation even though the relaxation time is short.

Inversion recovery T_1 measurements were made on anhydrate C using a shaped adiabatic inversion pulse to improve the efficiency of the inversion over a square 180° pulse. The experiment was repeated using different temperatures. From the Arrhenius plot an activation energy for the motion of the fumarate ion was calculated as 20 kJ mol^{-1} (see Figure 4.13).
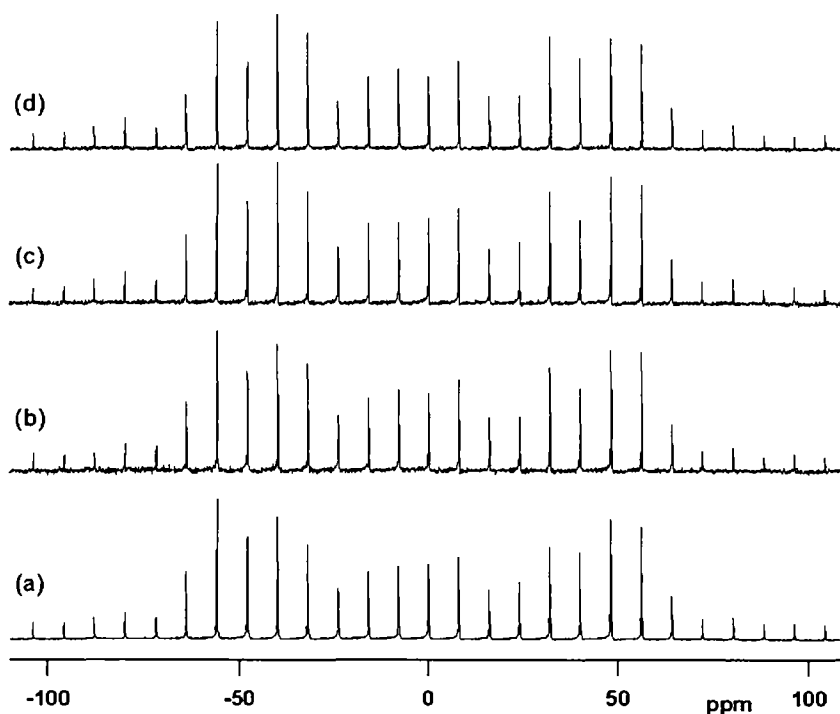
Figure 4.12 Formoterol fumarate anhydrate C ^{13}C DPMAS spectra (Varian VNMRS 400)
Acquisition conditions:
(a) -10 ºC, (b) 35 ºC , (c) 50 ºC, (d) 80 ºC

4.5 Static ^1H T_1 measurements

Static T_1 measurements were made using a saturation recovery sequence on 8 as a function of temperature. Proton relaxation information can reveal some complex behaviour but it should be noted that ^1H relaxation is likely to be a molecule wide average because the protons are strongly coupled. From the Arrhenius plot (Figure 4.14) it is evident that T_1 increases with temperature (above 253 K) indicating that the molecular motion falls within the extreme narrowing side of the minimum. At temperatures of 295 K and above the Arrhenius plot appears to be linear and from this an apparent activation energy of 19 kJ mol^{-1} was obtained. T_1 measures molecular motions in the MHz regime and the minimum on the Arrhenius plot is at the point where these molecular motions are taking place in the order of 300 MHz, the frequency of the magnetic field.

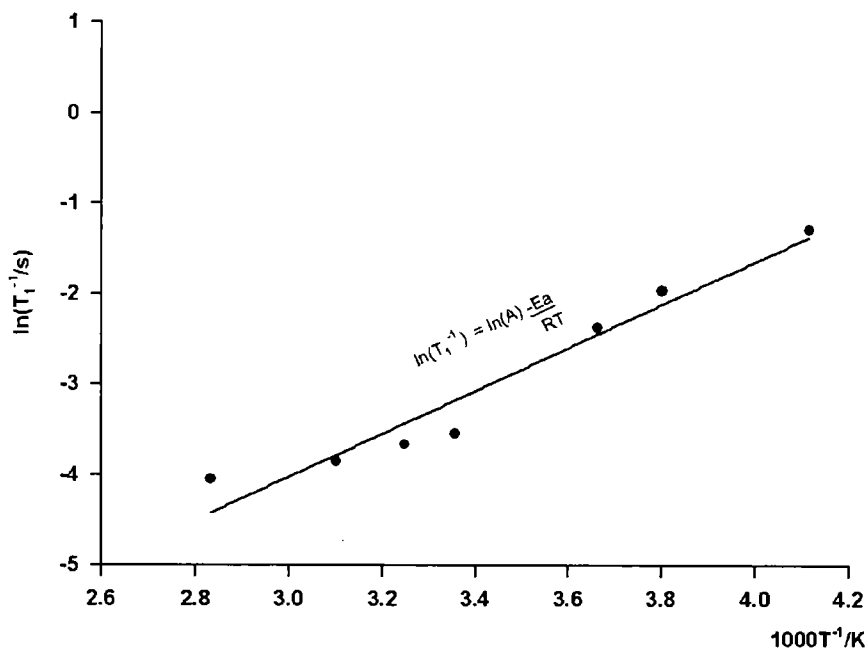Figure 4.13 Formoterol fumarate anhydrate C (Varian VNMRS
400) Arrhenius plot showing ^{2}H T_1 relaxation behaviour as a
function of temperature. The solid line is a least squares fit for
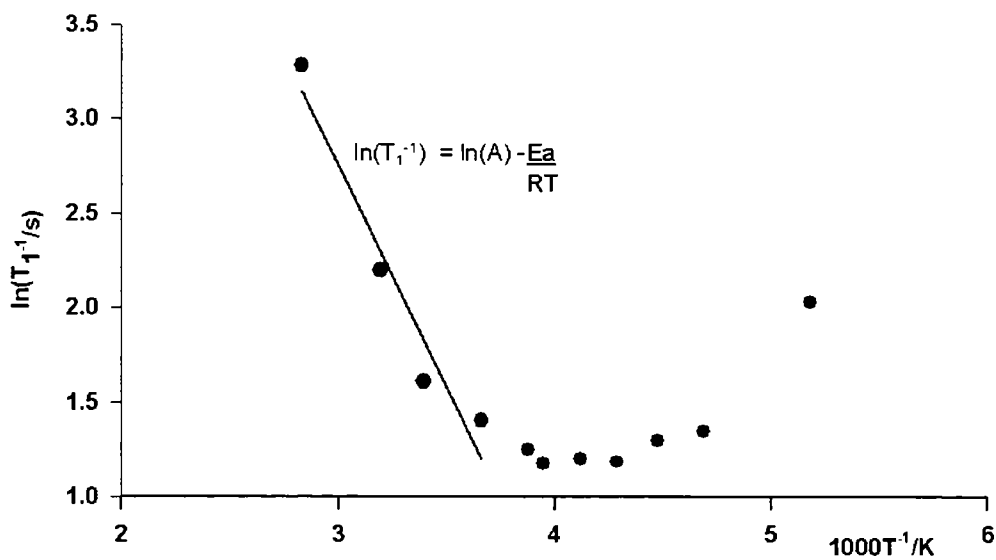the equation shown.

Figure 4.14 Formoterol fumarate anhydrate C Arrhenius plot
showing ^{1}H T_1 relaxation behaviour as a function of
temperature. The solid line is a least squares fit for the
equation shown.

4.6   Conclusions

The coalescence temperatures of **1** and **2** for carbon atoms c and c' were found to be between 0 and 20 °C with an exchange rate for the methoxy benzene ring-flip of 1900 s^{-1} at that temperature.

The coalescence temperature of anhydrate C (**8**) for carbon atoms c and c' was found to be between 50 and 80 °C with an exchange rate for the methoxy benzene ring-flip of 1650 s^{-1} at that temperature.

^{13}C CPMAS spectra indicate slower rotation of the methoxy benzene ring in **8** compared to solvates **1** and **2**. This slower rotation could be due to a partial shrinkage of the crystal structure.

^{13}C and ^{2}H T_1 measurements suggest that the fumarate ion is mobile in the anhydrate C (**8**) structure. The ^{2}H DPMAS spectrum, however does not indicate isotropic motion for the ion. A possible coalescence temperature below -100 °C was identified for the u and u' carbon atoms in **8** which again indicates a motional process is taking place. This process is not yet fully understood.

Future work

Molecular dynamics could be used to better understand the motion/exchange process involved with the fumarate ion in **8**.

4.7   *References*

1.   Harris RK, Nuclear Magnetic Resonance Spectroscopy, ed. Longman

Scientific and Technical , Harlow, Essex, 1986, 122-125

2.   Oas TG, Griffin RG, Levitt MH, Rotary resonance recoupling of dipolar

interactions in solid-state nuclear magnetic resonance spectroscopy, *The*

Journal of Chemical Physics, 1988, 89(2), 692-695

3.   Torchia DA, The measurement of proton-enhanced carbon-13 T1 values by a

method which suppresses artefacts, *J. Magn. Reson.*, 1978, 30, 613

4.   Bryce DL, Bernard GM, Gee M, Lumsden KE, Wasylishen RE, Practical

Aspects of Modern Routine Solid-State Multinuclear Magnetic Resonance

Spectroscopy: One Dimensional Experiments, *Canadian Journal of Analytical*

Sciences and Spectroscopy, 2001, 46, 46-82

5.1   *Formoterol Fumarate crystal structures*
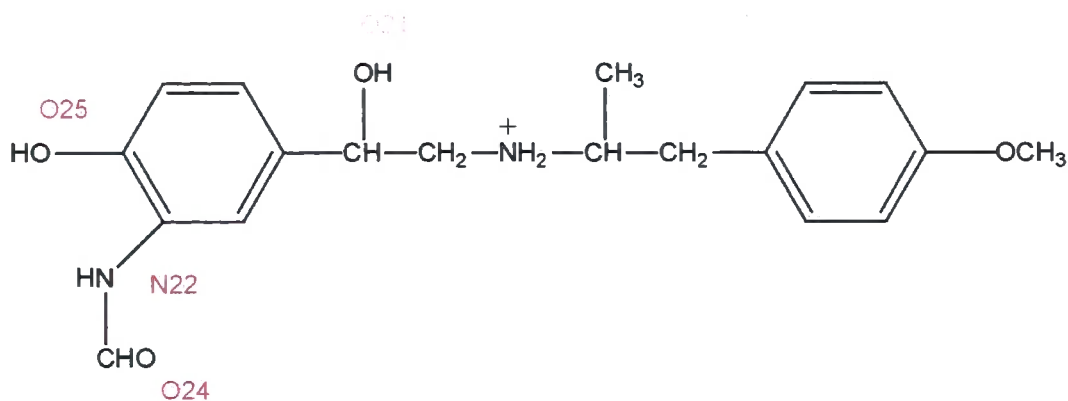
Scheme 5.1

Crystal structure of diethanol solvate (1)[1]

The crystal structure of **1** is dominated by hydrogen bonding (see Figures 5.1 and 5.2). The fumarate anions are surrounded by four formoterol molecules, which donate six hydrogen bonds to one full fumarate anion. Two further hydrogen bonds connect to two solvent molecules.

Two additional intermolecular hydrogen bonds, to the eight already mentioned (O21-H21...O25 and O25-H25.....O24) connect the formoterol molecules so that hydrogen bonded chains are formed (see Scheme 5.1).
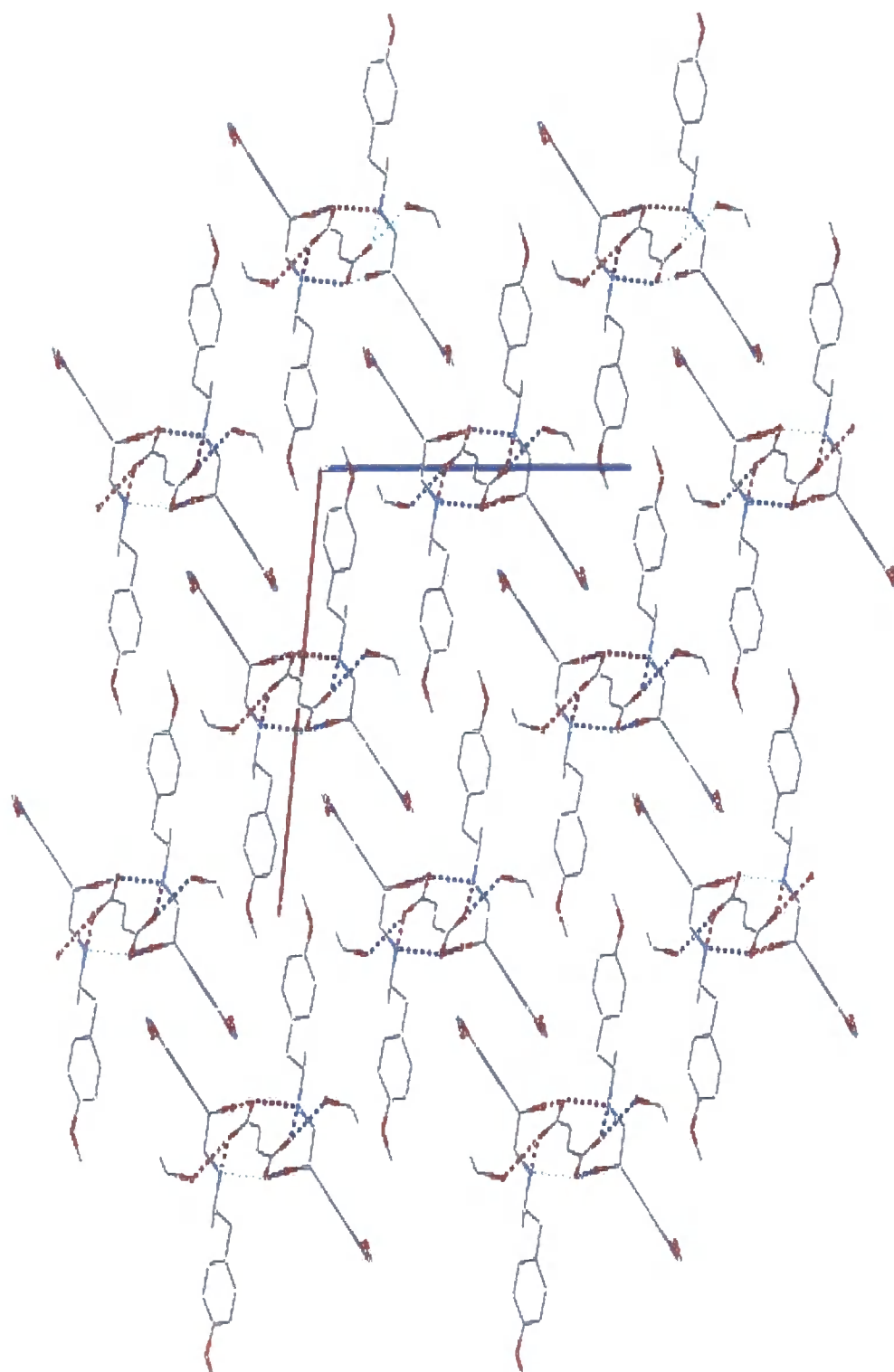
Figure 5.1. Formoterol fumarate diethanol solvate (a axis-red and the c axis-blue)
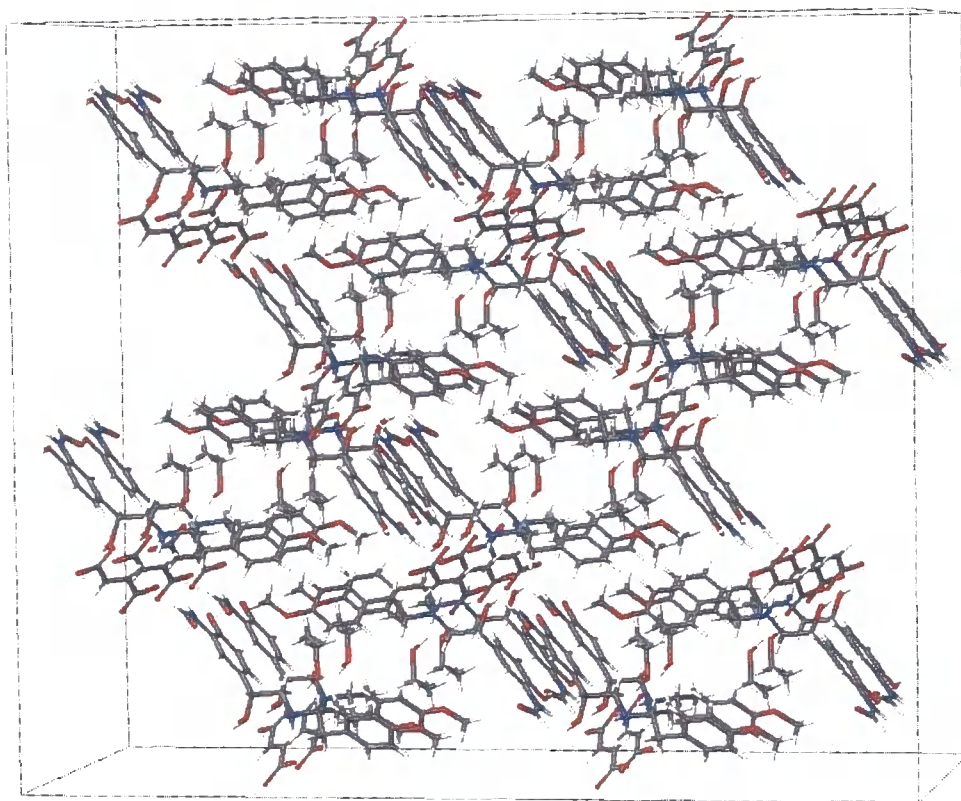
Figure 5.2. Formoterol fumarate diethanol solvate

Crystal structure of the dihydrate (5)[1]

The crystal structure of 5 is also dominated by hydrogen bonding (see Figure 5.3). The fumarate anions are surrounded by four formoterol molecules, which donate eight hydrogen bonds to one full fumarate ion. Two other hydrogen bonds connect to two water molecules.

There are no intermolecular hydrogen bonds between formoterol molecules but instead all hydrogen bonds stretch directly or indirectly to the fumarate anion.

Figure 5.3. Formoterol fumarate dihydrate, (c axis-blue and b axis-green)

Crystal structure of anhydrate B (7)[1]
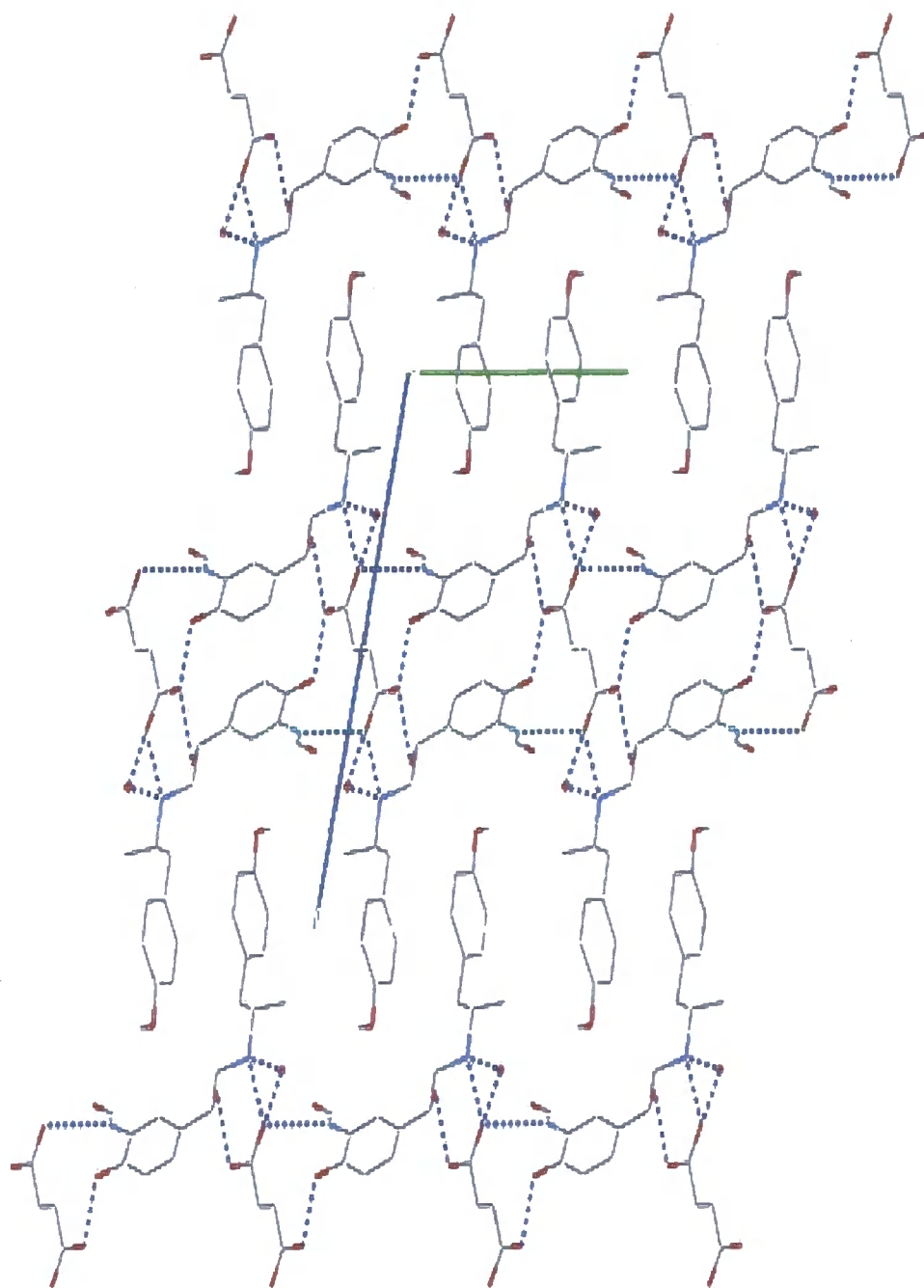
The crystal structure of **7** is similar to **5** (see Figure 5.4). The fumarate anions in one part of the structure are surrounded by four formoterol molecules, which donate eight hydrogen bonds to one full fumarate ion. In the other part of the structure the fumarate anion is again surrounded by four formoterol molecules, which donate four hydrogen bonds to one full fumarate anion. One intermolecular hydrogen bond (O21-H21...O24) connects the formoterol molecules (see Scheme 5.1).
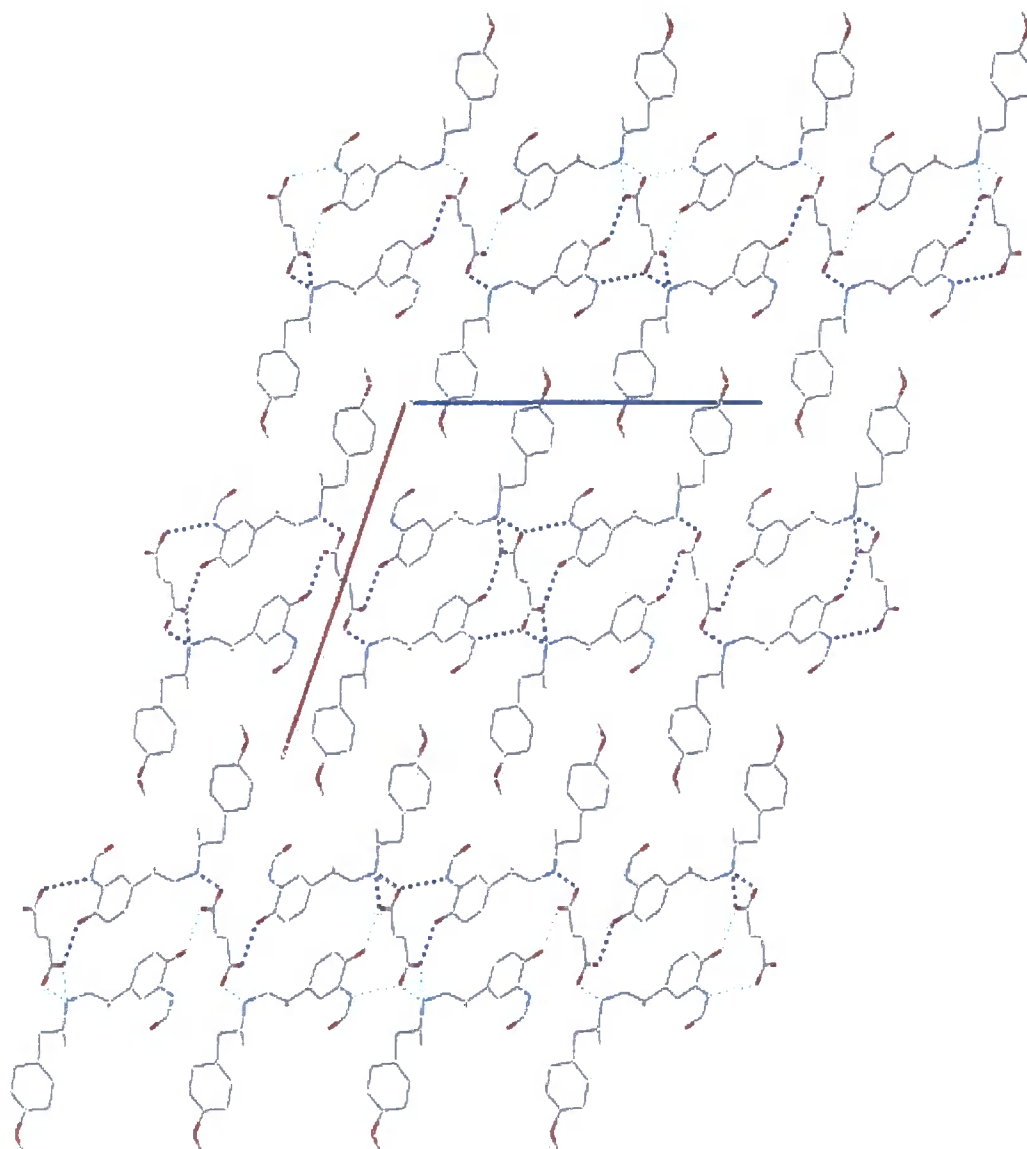

Figure 5.4. Formoterol fumarate anhydrate B (a axis-blue and c axis-red)

Crystal structure of anhydrate C (8)[1]

A single crystal XRD determination of the structure of **8** has not been undertaken as the crystals were too small. A comparison of the ^{13}C CPMAS spectra of **1, 2, 4** and **8** (see Figure 5.5) shows that there is very little difference between them. The c and c′ carbon atoms in **8** (marked at 116 ppm on the spectrum) are better resolved indicating the methoxy ring rotation has slowed relative to the diethanol and diisopropanol solvates at 25 °C. This indicates that the crystal structure has changed sufficiently to restrict this rotation, possibly by a partial shrinkage (see Section 4.2). In the spectra of the solvates the solvent peaks are highlighted in red. The similarities in the spectra suggest that the crystal structures are also similar, implying that the solvent can evaporate from the solvate (either **1** or **2**) leaving the crystal structures intact. This may explain why **8** cannot be formed via **5, 6** or **7**.
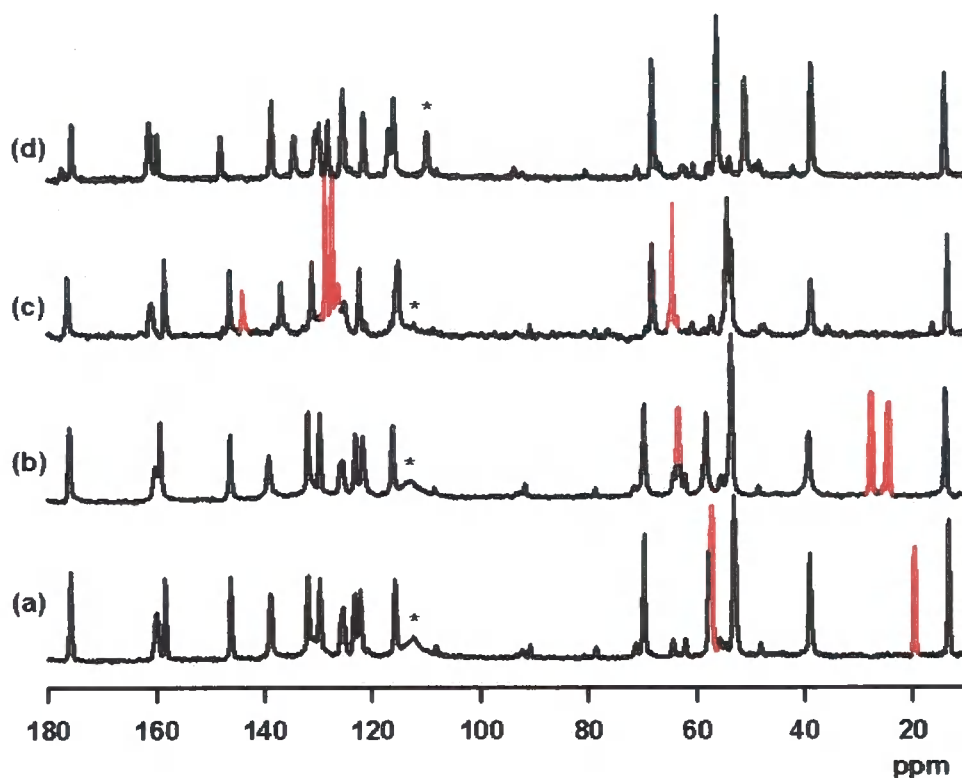

Figure 5.5. Formoterol fumarate ^{13}C CPMAS spectra,
(a) diethanol solvate, (b) diisopropanol solvate, (c) dibenzyl
alcohol solvate, (d) anhydrate C

5.2   *Anhydrates Water Content*

The anhydrates A (6), B (7) and C (8) give different solid-state NMR spectra so must have different crystal structures (see Figure 3.15). The following observations have been made:

(i).   The T_1 of the u carbon atom in anhydrate C implies it to be mobile.

(ii).   Dry ethyl acetate appears to remove water from 6 and 8 (see Section 1.5).

Because of these observations it was decided to examine the water content in the anhydrates.

Anhydrate A is formed by drying the dihydrate under vacuum at 85 °C. Anhydrate C is formed by allowing solvates 1 and 2 to desolvate and anhydrate B is formed by slurrying anhydrates A or C in **dry** ethyl acetate or **dry** acetone (see Figure 1.2). It is believed anhydrate C could contain more water than anhydrates A and B as the solvents being used to form the solvates are likely to contain water.

Moisture determination of anhydrates A (6), B (7) and C (8)

The melting points of 6 and 8 (130 and 122 °C) meant TGA analysis could decompose the samples and release water. Because of this, moisture determination on dry ethyl acetate before and after slurrying with an anhydrate was chosen as a way of measuring the water content in the anhydrates.

Ethyl acetate (0.2779 g) containing 0.08 % w/w water was added to 8 (0.0605 g). The sample was allowed to mix for several minutes and then the ethyl acetate was reanalysed for water. The solvent water content had increased to 0.16 % w/w showing that the solvent had removed 0.08 % w/w water from 8. This equates to 0.14 moles of water or 1 mole of water for every 7 moles of formoterol fumarate in the crystal structure. This procedure was repeated for both 6 and 7 giving 0.06% w/w water for 6 and no water detected for 7.

Moisture determination using a Metrohm moisture meter indicated that anhydrate A (6) and anhydrate C (8) both contain water. Anhydrate B (7) is free from water and is a true anhydrate.

The anhydrates[1] A (6) and C (8) contain water which is probably hydrogen bonded into the crystal structure. This water cannot be removed by heating in a vacuum oven at 85 °C in forming 6 and is not evaporated with the solvent when 8 is formed. It is believed/suggested this water helps to maintain the crystal structure of 8 by stabilising the hydrogen bonding in the crystal. If completely dry solvents were used in the formation of the solvates from 6, and the samples were kept in a dry environment, then anhydrate B (7) would be formed since water from 6 would be removed by the solvent. If this process was performed under atmospheric conditions then a solvate would be formed as water would be absorbed from the atmosphere helping the solvate formation.

5.3   *The role of water in the crystal structures*

The following observations for anhydrates A (6) and B (7) may be linked to the lack of water in the crystal:

(i).   7 has two molecules in the asymmetric unit with more disorder in the structure than 6 (in one NH_2^+ ion it has one hydrogen bond and in the other it has two-see page 80).

(ii).   6 also has two molecules in the asymmetric unit.

(iii).   The disorder in 7 is in the chain linking the two aromatic rings[1].

From these observations it is proposed that the water in 6 (and also 8) helps to maintain the hydrogen bonding, in particular around the NH_2^+ ion. When there are sufficient protons available as in 1, 2, 4, 5 and 8 then the NH_2^+ ion uses up all its available protons to form two hydrogen bonds. But when the proton count in the crystal is restricted, due to lack of water, as in 7, the NH_2^+ ion can only use one of its available protons for hydrogen bonding in part of the crystal. 7 appears to be more disordered (see Section 3.1.7) probably due to static disorder within the region with only one hydrogen bond on the NH_2^+ ion. 8 requires water for its formation from the

desolvation of **1** and **2**. The water helps stabilise the crystal structure and without its presence **7** will be formed.

Comparison of dihydrate/anhydrates (5), A (6), and 7 (B)

The s carbon atom in **5** has a chemical shift of 162 ppm (see Figure 5.6). In **6** and **7** this has shifted to lower frequency suggesting **5** is experiencing more hydrogen bonding
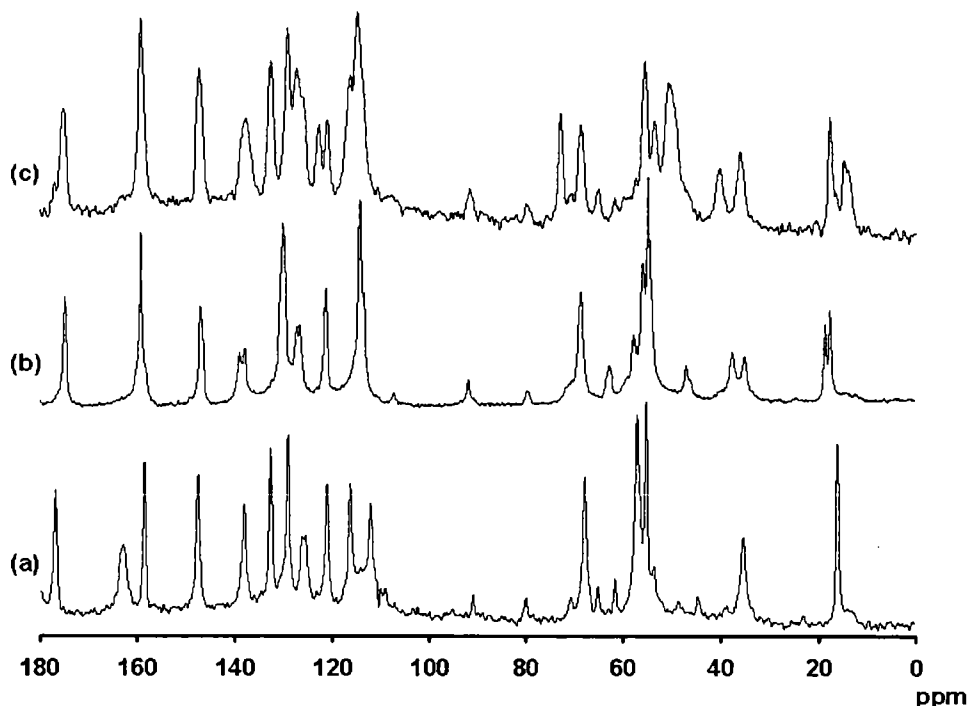

Figure 5.6. Formoterol fumarate ^{13}C CPMAS spectra, (a) dihydrate, (b) anhydrate A, (c) anhydrate B

around the s carbon atom. Likewise k and f carbon atoms in **5** are singlets, but are doublets to low-frequency in **7** suggesting an increase in hydrogen bonding in **5**.

5.4   Hydration of anhydrate A (6)

Since **6** is formed by drying **5** in a vacuum oven it was believed to have less water in the structure than **8** (see Section 5.2). To determine if **8** could be formed by hydration of **6**, **6** was placed into a relative humidity chamber where the atmosphere had been maintained at 100% RH using water. The sample was analysed at time zero and then after 15 and 25 minutes. The results showed that **6** is hydrolysed to **5** and **8** is not an intermediate in this conversion (see Figures 5.7 and 5.8).

5.5 *Ethyl acetate reaction with formoterol fumarate anhydrate C (8)*

Ethyl acetate was shown to form a possible solvate with **8** (see Figure 5.9). The ^{13}C CPMAS spectrum was unlike any of the other formoterol fumarate spectra. The line widths were quite narrow indicating the sample was crystalline. The lines at 19.8 and 171.17 ppm were those of the solvent molecule. There appear to be no doublets in the spectrum unlike **6** and **7** indicating there is only one molecule in the asymmetric unit. On heating the sample the ethyl acetate was removed and **8** was reformed (see Figure 5.10). These observations suggest the sample may be an ethyl acetate solvate. The TGA analysis of this sample showed a weight loss of 8.3 % w/w (see Figure 5.11).
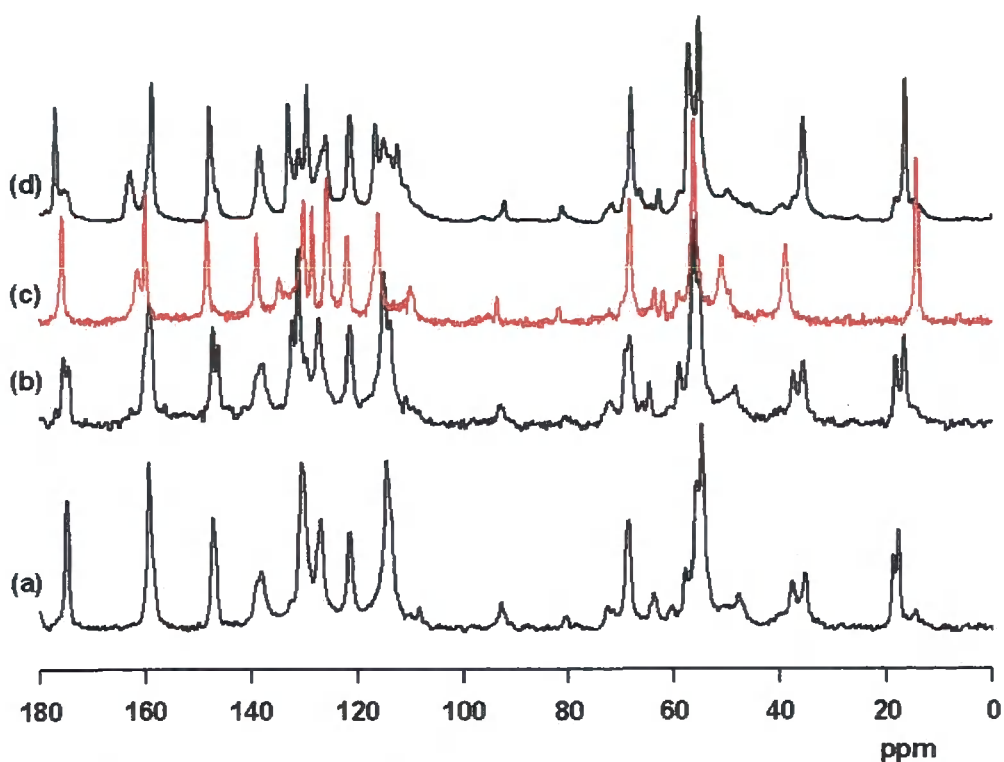

Figure 5.7. Formoterol fumarate anhydrate A ^{13}C CPMAS spectra, (a) 0 mins, (b) 15 mins, (c) anhydrate C, (d) 25 mins

Note: Spectrum (c) is an Anhydrate C reference spectrum.
The spectra show Anhydrate C is not formed in the hydration of anhydrate A to the dihydrate.
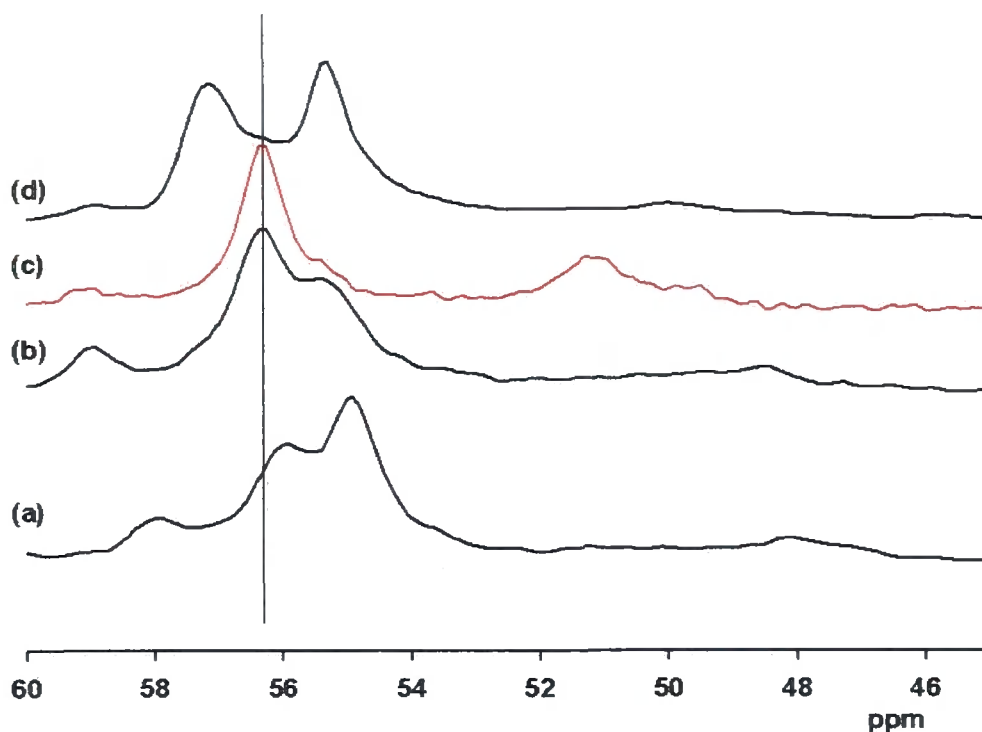
Figure 5.8. Formoterol fumarate anhydrate A ^{13}C CPMAS spectra, (a) 0 mins, (b) 15 mins, (c) anhydrate C, (d) 25 mins

This is slightly lower than the weight required for one molecule of ethyl acetate per molecule of formoterol fumarate (9.9 % w/w). The dehydration proceeded to 7 when the water content in the ethyl acetate was <0.03 % w/w and to the "solvate" when the water content was 0.18 % w/w (see Figure 5.12). The water content was measured using a Metrohm moisture meter. The reaction route to 7 is favoured when the ethyl acetate is dry because the water in 8 is removed by the ethyl acetate. When the water content is higher the water removal by the ethyl acetate is not possible and the reaction proceeds to the solvate.
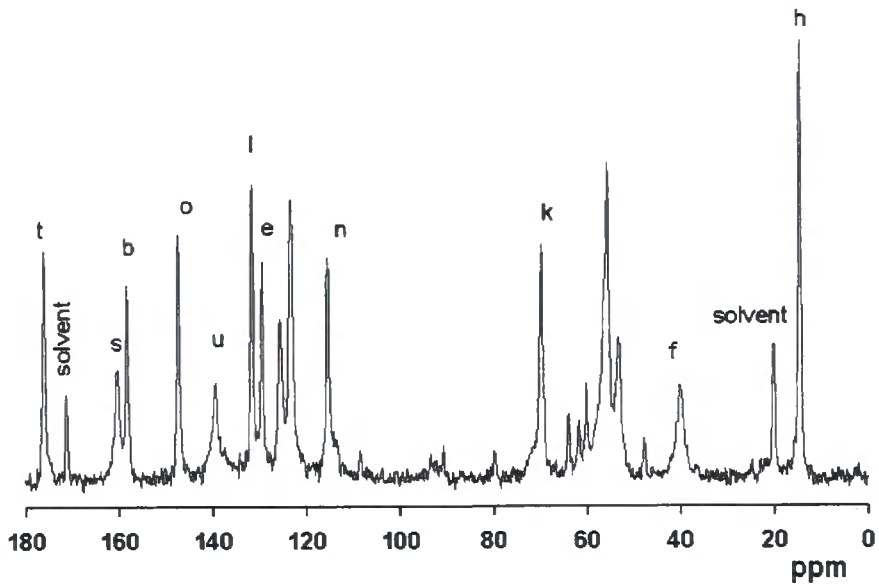
Figure 5.9. Formoterol fumarate ethyl acetate solvate ^{13}C CPMAS spectrum
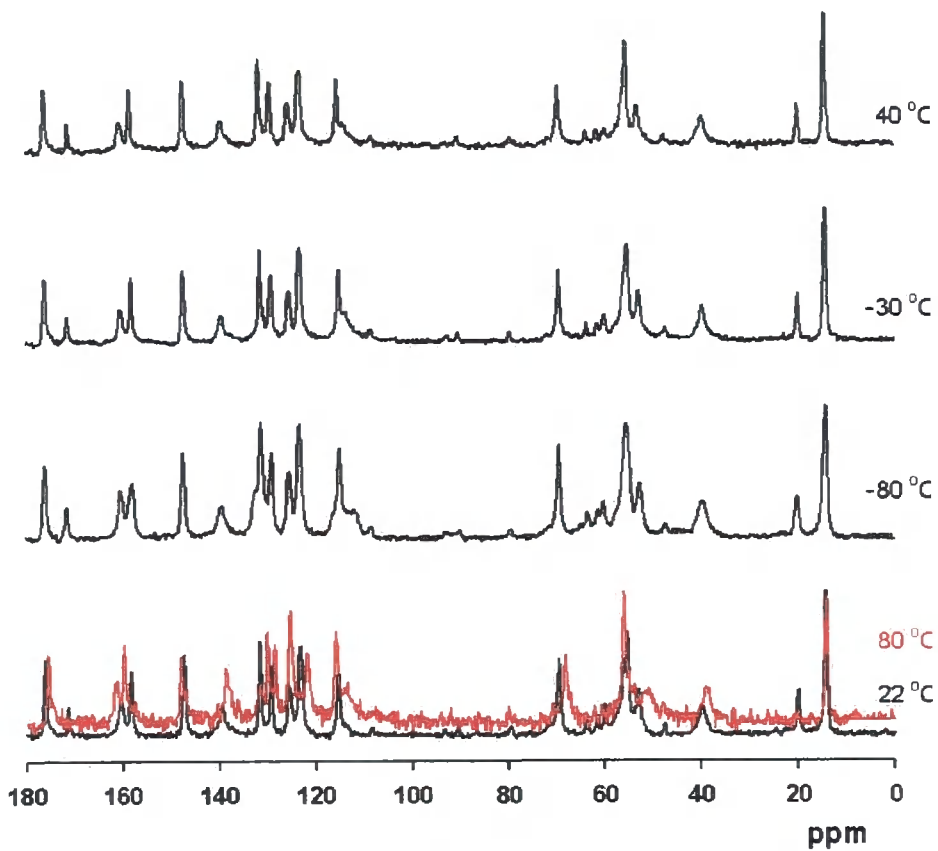

Figure 5.10. Formoterol fumarate ethyl acetate solvate ^{13}C CPMAS spectra

Note the spectrum at 80 °C shows it has converted to anhydrate C and is different to the starting material at 22 °C.

5.6   Dehydration of formoterol fumarate dihyrate using ethanol

A mixture of **5** and **8** (see Figure 5.13a) was combined with absolute ethanol with a water content <200 ppm w/w. The sample was dried in an oven at 50 ℃ until most of the ethanol was removed. On reanalysis the mixture had been converted to **1** (see Figure 5.13b). Dihydrate also combined with absolute ethanol to form **1** (see Figure 5.13c). The hydrogen bonded water molecules in the dihydrate were possibly removed forming **6** or **7** and then the mixture of anhydrates was then converted to the solvate. Conversion to the solvate was probably helped as the dry ethanol will have picked up water in the atmosphere during the preparation.
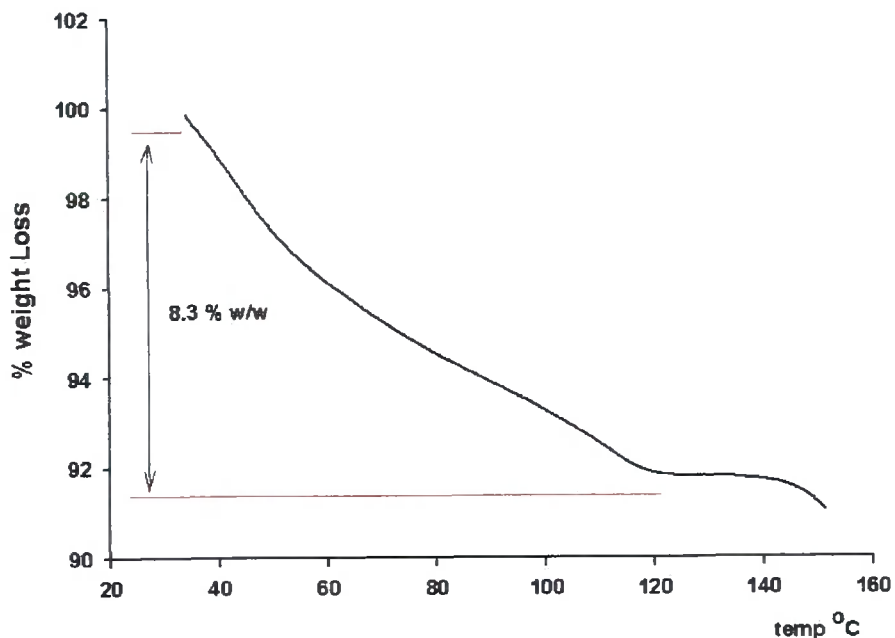

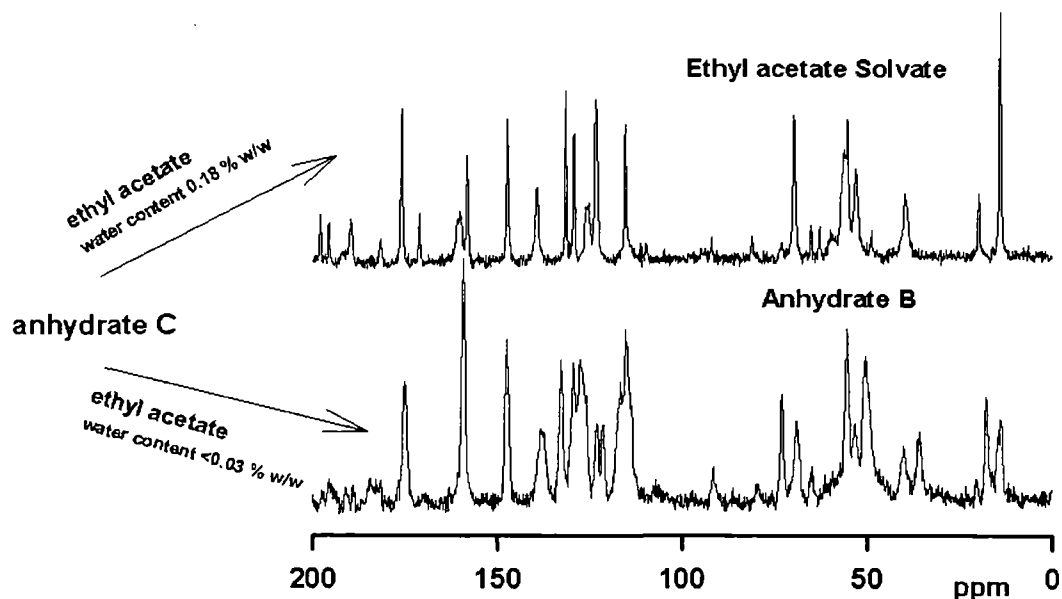**Figure 5.11 Formoterol fumarate ethyl acetate solvate**

ethyl acetate
water content 0.18 % w/w

Ethyl acetate Solvate

anhydrate C

ethyl acetate
water content <0.03 % w/w

Anhydrate B

200   150   100   50   ppm   0

Figure 5.12. Formoterol fumarate ^{13}C CPMAS spectra
Note: Ethyl acetate either removes water to form Anhydrate B or forms an
ethyl acetate solvate.

(c)
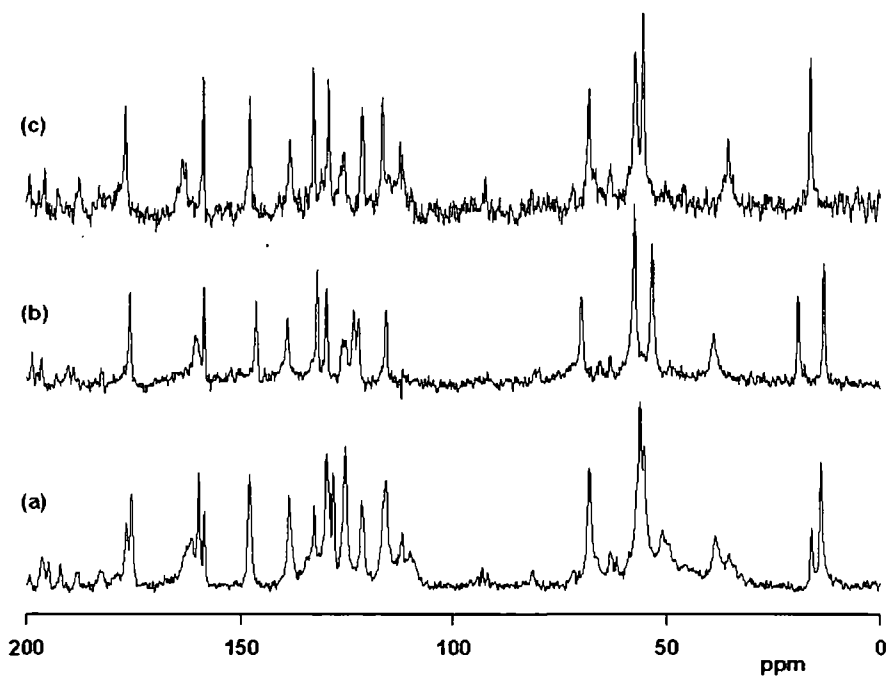
(b)

(a)

200   150   100   50   ppm   0

**Figure 5.13. Formoterol fumarate anhydrate C ^{13}C CPMAS
spectra, (a) anhydrate C, (b) diethanol solvate, (c) dihydrate**

Note: (a) and (c) were combined separately with dry ethanol to form (b).

89

5.7   Conclusions

Water measurements of anhydrate A (**6**) and anhydrate C (**8**) indicate it to contain water 0.06 and 0.08 % w/w. It is believed that this water is hydrogen bonded to the NH_2^+ ion and is difficult to remove by heating. It is also believed water is fundamental to the stability of the solvates and anhydrates A and C. Anhydrate B was the only material that demonstrably contained no water.

An ethyl acetate solvate of formoterol fumarate was produced by slurrying **8** with "wet" ethyl acetate (0.18 % w/w water). This solvate desolvates to **8** on standing or under MAS.

The dihydrate (**5**) and anhydrate B (**7**) prepared were shown to be identical to samples previously analysed. A route for preparing the solvates by bypassing the need to dry the dihydrate has been found. It involves slurrying **5** with dry ethanol (<200 ppm w/w water). The ethanol solvate is then produced.

Future work

(a) The structure of **8** is, as yet, not defined. Powder XRD combined with CASTEP calculations could help in determining the crystal structure.

(b) Using water labelled, with ^{17}O, could help to identify the nature of the water in **8**. It is unclear if the water present is mobile in the channels or hydrogen bonded and aiding in the salt formation.

(c) A ^{15}N CPMAS experiment on anhydrate B will determine if there are two nitrogen environments for the NH_2^+ ion.

5.8   *References*

1.   Jarring K, Larsson T, Stensland B, Ymen I, Thermodynamic Stability and Crystal Structures for Polymorphs and Solvates of Formoterol Fumarate, Journal of Pharmaceutical Sciences 95(5): 1144-1161